

7020 Portwest Drive, Suite 150, Houston, Texas 77024
Telephone: (713) 869-0000 • Telex: 499-3065

December 24, 1986

Sandia National Laboratories
P. O. Box 5800
Albuquerque, NM 87185

Attention: Mr. Dennis Engi

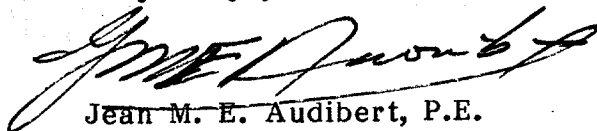
Re: "Some Aspects of the Fundamental Behavior of Axially Loaded
Piles In Clay Soils" - Final Report

Gentlemen:

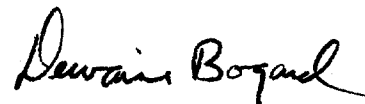
As per your Document No. 32-8727, Contract #SF 6432-STD (4-83), we are pleased to submit three (3) copies of our report, entitled "Some Aspects of the Fundamental Behavior of Axially Loaded Piles in Clay Soils".

We appreciate your contribution to the project, and hope that we can be of further service to you in the future.

Very truly yours,



Jean M. E. Audibert, P.E.
Associate Principal
General Manager, Gulf States Division



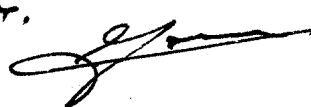
Dewaine Bogard
Senior Engineer

JMEA/JDB/plm

Enclosures

P.S. Charles:

*I thought you might like to get a copy
of your own ahead of time.*



PREFACE

The work reported herein is a part of a continuing research effort at The Earth Technology Corporation which is directed toward increasing the understanding of the mechanics of the behavior of axially loaded piles. In particular, the research involves a study of the relationships among the shear transfer and the displacement during static and cyclic loading. In addition, the research includes observation of the evolution in the radial soil and pore pressures during consolidation and static and cyclic loading, and the effects of the changes in the radial pressures on the shear transfer capacity of clay soils.

The research was performed in one continuous period of field activity, although the sponsorship of the work was divided into the public and private domains. The original sponsorship of the research was by the National Science Foundation, which sponsored three field experiments, with two additional experiments being privately funded. This report contains the results of the three experiments performed under NSF Grant Number 818122 as well as the additional data for which funding was made available by the following corporations: Chevron, Conoco, Marathon, Mobil, Sandia National Laboratories/Minerals Management Services and The Earth Technology Corporation.

The project team for The Earth Technology Corporation consisted of Dewaine Bogard, Jean Audibert, Lino Cheang, Chairat Suddhiprakarn, and Scott Bamford. Dr. Jean Audibert served as the Project Manager and Administrator, and provided a technical review of this report. Dewaine Bogard planned the testing program, directed the field experiments, and produced this report. Lino Cheang and Dr. Suddhiprakarn assisted in the field experiments, while Scott Bamford provided tactical support from our Houston office.

In addition to the Earth Technology project team, special notes of appreciation are due Dr. Chandrakan Desai of The University of Arizona, who visited the site and provided the services of two graduate students, Messrs. D. Rigby and H. Waphugala, whose assistance during the field activities is greatly appreciated.

TABLE OF CONTENTS

	<u>Page</u>
ABSTRACT	
1.0 INTRODUCTION	1
2.0 OBJECTIVES OF THE RESEARCH	2
3.0 SITE DESCRIPTION AND SOIL PROPERTIES	4
4.0 TEST EQUIPMENT	
4.1 The Portable Loading and Control System	5
4.2 Methods of Installation	5
4.3 Data Acquisition	6
4.4 The 3-Inch Diameter Pile Segment Model	7
4.5 The 1.72-Inch Diameter Pile Segment Model	8
5.0 TEST PROCEDURES	
5.1 Planned Sequence of Experiments	10
5.2 Log of Experiments and Load Tests	11
6.0 TEST RESULTS	
6.1 The Full-Displacement 3.0-Inch Diameter Probe	14
6.2 The Full-Displacement 1.72-Inch Diameter X-Probe	17
6.3 The 3.0-Inch Diameter, 0.125-Inch Wall Probe Tests	19
6.4 The 3.0-Inch Diameter, 0.065-Inch Wall Probe Tests	21
6.5 The 1.72-Inch, 0.043-Inch Wall Probe Tests	24
6.6 Summary of Experimental Results	25

7.0 SUMMARY AND CONCLUSIONS	29
--	-----------

FIGURES

APPENDICES:

Appendix A: Soil Test Data

Appendix B: Self-Boring Pressuremeter Tests

ABSTRACT

A series of experiments have been performed at a site near Sabine Pass, Texas, using two types of pile segment models. The models were 1.72 and 3.00 inches in diameter, and were instrumented to simultaneously measure the total radial pressure, the pore pressure, the shear transfer, and the relative pile-soil displacement during insertion, consolidation, and static and cyclic axial loading.

The experiments were performed at a depth of 50 ft in five parallel borings, so that the soil conditions would be very similar. The 3.00-inch diameter models were driven into the soil below the bottom of cased boreholes, while the 1.72-inch diameter models were pushed into place. The models were provided with both open-end and fully-plugged cutting shoes, in order to investigate the effects of the degree of cavity expansion on the magnitudes of the lateral soil pressures which were developed, and on the rates of consolidation and the parallel increases in the shear transfer capacity of the soil.

In order to develop curves relating the increase in shear transfer capacity with time after installation, quasi-static loadings to failure in tension were performed at various times after installation in each experiment. Near the end of consolidation (as determined by the magnitudes of the remaining excess pore pressures) two-way cyclic loading was performed, with alternate loadings to failure in tension and compression, so as to degrade the soil resistance to a stable minimum value. Upon completion of the cyclic tests, additional loadings were performed with a wide variation in the rate of displacement, in order to ascertain the effects of slip rate on the shearing resistance of the soil.

The effects of diameter on the rate of consolidation are clearly demonstrated in the results obtained using the fully-plugged 1.72-inch and 3.00-inch diameter models. The effects of the amount of cavity expansion are demonstrated in the results of the experiments with the 3.00-inch and the 1.72-inch diameter models with varied wall thicknesses of the cutting shoes. As noted in a comparison of the results of the experiments, the rate of consolidation shows a significant dependence on the relative

D/wt ratio (Diameter to wall thickness); a dependence which is of equal or greater importance as the diameter itself.

Although the effects of diameter and D/wt ratio on magnitudes of the radial pressures and on the rate of consolidation are clearly demonstrated, no effects on the magnitudes of the ultimate (long-term) static shear transfer capacity were observed. That is, at equal degrees of consolidation, very similar magnitudes of peak static shear transfer were measured, regardless of the boundary conditions during consolidation. Thus, the observed behavior suggests strongly that the development of a total stress-based approach to axial pile design should be relatively straightforward; an effective stress-based approach will require considerably more effort, and reliance on unproved (and unmeasurable) effective stress-time-deformation relationships.

1.0 INTRODUCTION

During recent years, considerable effort has been expended in improving the analytical methods used to predict the behavior of axially-loaded piles. Existing theoretical concepts of pile-soil interaction have been based on intuition and on the results of laboratory tests on clay soils in which the boundary conditions during consolidation and axial shearing are quite dissimilar to those which exist in the clay adjacent to a pile. Existing axial pile design procedures are based on the quasi-statistical treatment of the results of axial pile load tests, in which few were instrumented, and in which little consideration was given to the effects of time after driving on the development of shear transfer capacity in the soil.

In order to obtain a base of high-quality experimental data by which existing and future theoretical concepts could be checked, and upon which reliable and accurate design procedures could be developed, The Earth Technology Corporation has developed two in situ pile segment models. The models are instrumented to measure the soil parameters which were felt to control, or contribute to, the development of shear transfer capacity in clay soils.

The tools have been deployed at the onshore sites of two large-diameter pile load tests, the Shell Beta pile test site in Long Beach, California and the Chevron pile test site in Empire, Louisiana; at the offshore site of the Conoco pile load tests on large-diameter driven and drilled-and-grouted piles; and at two additional onshore sites (including the Sabine Pass site) where large-diameter pile load test data are not available.

Four of the sites contain predominately soft, normally consolidated clays, with the Long Beach site consisting mostly of a stiff silty clay. At each site, very similar patterns of behavior were observed; the similarity of the patterns of behavior, and the acquisition of the parallel results of load tests during the full range of consolidation on a fully-instrumented large-diameter pile at the Conoco offshore site, have resulted in the compilation of a well-documented data base upon which accurate and reliable axial pile design procedures can be developed and verified.

2.0 OBJECTIVES OF THE RESEARCH

During the experiments which have been performed earlier (the results of which remain proprietary), it was found that the relative wall thickness of the cutting shoe of a pile (expressed as the D/wt ratio) had an effect on the rate of consolidation and, thereby, the rate of increase in axial shear transfer capacity. The effects indicated that the D/wt ratio was of equal importance with the pile diameter in determining the time-rate of consolidation. Accordingly, the experiments reported herein were planned to provide additional experimental verification of such effects.

Although it was recognized at the outset that a sufficient number of experiments could not be performed within the available budget to fully explore such effects, and that the results of only one experiment with each D/wt ratio would have little statistical significance in terms of obtaining mean, or average patterns of response, it was felt that such data would be extremely valuable in understanding and in guiding future theoretical (and empirical) developments in the area of axial pile-soil interaction.

The research program was thus developed to examine the following aspects of axial pile-soil interaction:

1. The effects of the amount of cavity expansion (i.e., D/wt ratio) on the rate of consolidation and setup
2. The effects of diameter on the rate of consolidation and setup
3. The role of radial effective pressures and pore pressures with regard to axial shear transfer capacity, that is, (1) Do direct relationships exist between the radial effective pressure and the shear transfer, or is the relationship more complex? and, (2) Does the degree of consolidation, as denoted by the relative degree of dissipation of excess pore pressures, yield a more reliable indicator of the relative increase in static axial capacity than does the magnitude of the radial effective pressure?

The program of experiments at the Sabine site was also expected to provide an addition to the data base which has been developed by The Earth Technology Corporation during the past four years; although much proprietary research has been performed, little data is yet available for publication.

Prior to the development of the tools, very little high-quality experimental data in the area of axial pile-soil interaction was available; existing theoretical concepts and design procedures were therefore based on very limited information, and were, therefore, similarly limited in accuracy and reliability. By providing a more complete picture of the evolution of soil behavior during pile installation, consolidation, and static and cyclic loading, it is expected that a better understanding of the behavior of axially loaded piles can be achieved, and that the reliability and accuracy of axial pile design procedures can be vastly improved.

3.0 SITE DESCRIPTION AND SOIL PROPERTIES

The location of the test site, shown in the map in Figure 1, is approximately 4 miles south of Sabine Pass, Texas. The soil of interest, at the 50-ft depth, is a normally consolidated gray marine clay having a Liquid Limit of 100 and a Plasticity Index of 72, which plots well above the A-line in the region of high plasticity. An idealized soil profile was developed by combining the data obtained in the six boreholes drilled at the site to perform the pile segment tests. A composite Boring Log is shown in Figure 2.

The results of laboratory strength and consolidation tests on 3-inch diameter push tube samples taken at the site are given in Appendix A, and are summarized below.

Three Miniature Vane tests made on samples from depths of 51.5 to 56.0 ft indicated an average peak undrained shear strength of 0.75 ksf, with a residual value of 0.34 ksf.

Three Unconsolidated Undrained Triaxial Compression tests indicated an average undrained shear strength of 0.51 ksf, with the average of two UU tests on remolded samples indicating a remolded shear strength of 0.34 ksf.

The results of three consolidation tests on samples of the clay indicated a value of approximately $1 \text{ inch}^2 / \text{day}$ for the coefficient of consolidation, c_v , in the range of radial consolidation pressures measured during the experiments.

As an out-of-scope effort to this project, The Earth Technology and International Underwater Contractors (IUC) funded a test of the Self Boring Pressuremeter (PAM) developed by the French Institute of Petroleum Research (IFP) at the Sabine site. The test was performed on September 23-24, 1985 and was witnessed by several representatives of the oil industry and government agencies. Due to the presence of a thick shell hash layer, the pressuremeter probe could not advance beyond 11.5 m (38 ft). The results of this investigation are included in Appendix B of this report.

4.0 TEST EQUIPMENT

The testing apparatus consisted of a loading frame upon which a through-hole hydraulic ram was mounted, digital and analog recording systems, and two each of the 1.72-inch and 3.00-inch diameter pile segment models.

4.1 The Portable Loading and Control System

The portable loading system is shown schematically in Fig 3. The load is applied to a short section of N-rod which has a circular flange welded at one end. The displacement of the hydraulic ram is transferred to the probes by the N-rods, through the hollow centers of which the instrument cables are passed to the surface.

The rate of travel of the hydraulic ram is controlled by one-directional flow control valves, arranged so as to restrict the outflow of the ram, with unrestricted input flow. The direction of travel of the ram is controlled by an electrical four-way solenoid valve which is mounted on the upper steel plate near the ram. During the static and cyclic tests reported herein, the solenoid valve was operated manually.

The nominal rate of travel of the ram during the quasi-static load tests was, for the majority of the tests, less than 0.001 inch/sec. During the fast-rate tests, the rate of travel was increased to approximately 0.02 inch/sec.

4.2 Methods of Installation

Prior to installing the probes, a boring was drilled and cased to a depth of 3.5 ft above the center of the shear measurements (for the 3-inch-diameter probes), at which depth the pressure transducers were located at the end of driving. For the shorter 1.72-inch-diameter probes, the borehole was advanced slightly deeper.

The process of installation of a 3-inch-diameter probe with a thin-wall cutting shoe is shown schematically in Fig 4. As shown in the figure, the probe is first lowered into the boring, and then slowly released, until the probe and the N-rod string are supported by the soil. The probe is then driven into place using a 300-lb casing hammer, with a drop of 3-ft on each blow. As the cutting shoe advances into the soil, the cutting shoe fills, becoming plugged after a penetration of 7 ft. Driving is continued for an additional 7 ft, for a total penetration of 14 ft below the bottom of the borehole.

At the end of driving, the sensitive section of the probe rests near the center of the zone of soil which was penetrated by the open-end cutting shoe prior to plugging. Thus, the radial pressures in the sensitive zone are equivalent to those created by a thin-wall pile, while those at the deeper depths are equivalent to those created by a closed-end pile. The upper load cell (used to measure the shear transfer) is driven to a depth of 2.5 ft below the bottom of the boring, which is approximately 10 probe diameters below the vertical stress relief at the bottom of the borehole. Similarly, the bottom load cell is 2 ft (about 8 diameters) above the depth at which the cutting shoe became filled with soil and plugged. The pressure transducers are located an additional 15 inches away from the load cells. Thus, the sensitive length of the probe is well isolated from the complex pressure gradients at the bottom of the boring and at the depth at which the cutting shoe plugged.

4.3 Data Acquisition

The data acquisition system is shown schematically in Fig 5. The system consists of parallel analog and digital data acquisition systems, with each being used to supplement and to verify the other. The digital system was used to record data during consolidation, with both systems being used in parallel to record data during the load tests.

The analog data acquisition system consisted of a signal conditioner and amplifier and two x-y-y recorders. The strain gage signals from the 3-inch diameter probes were amplified, filtered, and then recorded on the analog plotters. The 1.72-inch

probe has signal-conditioning and amplifying circuitry in the probe itself; the output from these probes was plotted directly.

The digital data acquisition system was designed to utilize a Hewlett-Packard 3497A Scanning Digital Voltmeter as an analog-to-digital converter, with the digitized voltages being stored on 8-inch floppy discs by a Digital Equipment Corporation MINC 11/23 microcomputer.

The HP3497A has a precision of \pm one microvolt, with an accuracy of 6-1/2 digits. Thus, the output voltages from strain gage bridges can be read and recorded directly, without requiring strain gage balancing or amplifying circuitry.

The data are recorded on the floppy discs as raw voltages, with the voltages being converted to engineering units prior to being displayed on the CRT screen and relayed to the line printer.

The final data reduction from raw voltages to engineering units is done in the office, with a Hewlett-Packard 9872A Digital Plotter being used to prepare graphic records of the data.

4.4 The 3-Inch Diameter Pile Segment Model

A 3-inch diameter pile segment model, or probe, is shown schematically in Fig 6. The probe is equipped with two load cells separated by a distance of 31.6 inches, corresponding to a shaft surface area of 2.00 sq ft between the load measuring points. The strain gages in the load cells are connected in a single Wheatstone bridge in such a manner so that the output of the bridge is proportional to loads applied between the two cross-sections.

The pressure transducers are located midway between the two load cells. The total pressure transducer is sensitive only to forces normal to the outer face of the unit, thus measuring the total radial pressure acting against the surface of the probe. The face of the transducer is shaped to conform to the pile wall and is of a diameter chosen to have one sq inch of surface area. The pore pressure transducer

is a commercially-available Statham P856-500A. The transducer diaphragm forms the rear wall of a cylindrical cavity, with the front face of the cavity being a porous Carborundum stone which shields the diaphragm from intergranular soil pressures, but allows free passage of water to transmit pore fluid pressures.

A slip-joint arrangement is located at the connection between the body of the probe and the cutting shoe. The body of a DC-LVDT is mounted in the body of the probe; the core of the LVDT is attached to the cutting shoe. The cutting shoe serves as a reference anchor for the measurement of relative pile-soil displacement, enabling the direct measurement of shear transfer versus displacement relationships.

The axial load cells were calibrated by applying a series of loads on each load cell independently using a specially-fabricated calibration jig. The calibration factor for the combination of the two load cells was then calculated, accounting for the slight differences in sensitivity of the two units.

The total and the pore pressure transducers were calibrated by placing the probes in a 30-inch diameter, 10-ft long pressure chamber, which was then filled with water and subjected to a series of known values of hydrostatic pressure. Prior to calibrating the pressure transducers, the probes, complete with the cables, were subjected to an overnight period of 100 psi hydrostatic pressure, to ensure that the probes were water-tight.

4.5 The 1.72-Inch Diameter Pile Segment Model

A 1.72-inch diameter pile segment model (denoted as the X-probe) is shown schematically in Fig 7. The probe, which is 56.5 inches in length, consists of a number of independent housings which contain a total pressure transducer, a pore pressure transducer, a shear-sensing element (friction sleeve), and a displacement transducer.

In a manner similar to the 3-inch probe, the total pressure transducer is a load cell which measures the total force acting on an active face which is shaped to conform to the outside surface of the probe shaft.

The pore pressure transducer is mounted in a housing which contains an internal cavity connected to the outer surface of the probe through three holes. At the surface of the probe, porous stones are placed, so that only the pore fluid pressure is transmitted to the inner cavity.

The shear sensing element consists of a cylindrical sleeve (friction sleeve) which is supported by a load cell. The outer sleeve, which is not connected to the probe except through the load cell, gives a measure of the average shear transfer on the 31-sq inch surface area of the sleeve.

At the tip of the probe, a slip-joint arrangement is placed, with the body of a DC-LVDT being housed in the probe and the core of the LVDT being attached to a short anchor section.

The transducers of the X-probe are simultaneously calibrated in a cylindrical pressure chamber. An annular sleeve, with o-ring seals, is attached to the friction sleeve. When the probe is inserted into the cylindrical chamber, the annular sleeve forms a hydraulic piston. The shaft of the probe is restrained from movement, and hydrostatic pressure is applied sequentially to each end of the pressure chamber. The applied pressure is then converted into equivalent values of shear transfer.

At the same time, the total and pore pressure transducers are read and calibrated.

5.0 TEST PROCEDURES

Prior to mobilizing to the test site, a sequence of experiments and load tests were developed which would maximize the productivity of the drilling crew and which would also yield the desired technical information. Based on earlier experiments performed at the site in September 1982, with the 3-inch probes, and on the work performed at Empire, La., with both types of probe, the time required for various degrees of consolidation in each experiment was precalculated. Static tension tests, with no cyclic loading, were planned for each experiment with different diameters and D/wt ratios in order to observe the increase in static shear transfer capacity during consolidation.

Two-way cyclic tests were performed near the end of consolidation, in order to record the cyclic minimum shear transfer.

5.1 Planned Sequence of Experiments

For each experiment, the following sequence of installation and load testing were followed.

1. Install the probes, either by pushing (the x-probes) or by driving (the 3-inch probes).
2. Perform a load test to failure in tension as soon as possible after installation.
3. Observe the process of consolidation, and estimate the degree of consolidation.
4. Perform slow load tests to failure in tension, at degrees of consolidation of approximately 20, 40, 60, 80, and 90+ percent.

5. During the final tension test, perform two additional cycles of unloading, then reloading to failure in tension.
6. Perform a two-way cyclic test, with failure in both tension and compression, in order to fully degrade the soil.
7. Perform one cycle of loading at the fastest possible load rate, then repeat one slow-rate cycle of loading.
8. Perform one large-displacement loading to failure in tension, with the load rate varied during plastic slip.

The sequence of load tests were performed in order to observe the evolution in static shear transfer capacity during (relatively) undisturbed consolidation. Ideally, each load test at each degree of consolidation would require an independent installation and period of truly undisturbed consolidation prior to loading. Practically, the required number of borings (and total consolidation times) were not possible. It will later be shown that the tension loadings to failure resulted in only slight perturbations of the consolidation, and had no significant effect on the magnitudes of shear transfer recorded in the later tests.

Due to failures and malfunctions of various pieces of equipment, it was not possible to follow Step 4 exactly. It should be noted, however, that the exact degree of consolidation at the time of each test is not important, so long as a number of tests are performed, and the degree of consolidation known.

5.2 Log of Experiments and Load Tests

A chronological log of the load tests which were performed within each experiment is tabulated below.

<u>DATE</u>	<u>TIME</u>	<u>EXPERIMENT / TEST</u>
18 July 1986	10:11	Install 3-inch, full-displacement probe
	10:43	Perform static tension test, U = 18 percent
	12:51	Perform static tension test, U = 37 percent
20 July 1986	10:41	Perform static tension test, U = 92 percent
23 July 1986	08:56	Perform static tension test, U = 100 percent Follow with two-way cyclic tests
	10:59	End of tests, probe removed from boring
20 July 1986	08:04	Install 1.72-inch, full-displacement probe
	08:29	Perform static tension test, U = 22 percent
	09:36	Perform static tension test, U = 40 percent
	12:24	Perform static tension test, U = 60 percent
21 July 1986	07:29	Perform static tension test, U = 87 percent
22 July 1986	14:39	Perform static tension test, U = 97 percent Follow with two-way cyclic tests
23 July 1986	11:18	Probe removed without testing, U = 99 percent
20 July 1986	14:52	Install 3-inch, 0.065 wall, probe
	15:54	Perform static tension test, U = 39 percent
	18:45	Perform static tension test, U = 72 percent
20 July 1986	21:53	Perform static tension test, U = 85 percent
21 July 1986	13:58	Perform static tension test, U = 99+ percent Follow with two-way cyclic tests
	15:44	Tests completed, probe removed from boring

21 July 1986	18:32	Install 3-inch, 0.125 wall, probe
	18:46	Perform static tension test, U = 16 percent
	19:28	Perform static tension test, U = 36 percent
	21:30	Perform static tension test, U = 57 percent
22 July 1986	07:19	Perform static tension test, U = 86 percent
23 July 1986	07:32	Last stable pressure data, U = 93 percent
	14:07	Perform static tension test, followed by two-way cyclic tests; probe removed from boring
22 July 1986	09:09	Install 1.72-inch, 0.043 wall, probe; note only 0.12 ksf excess pore pressure, 0.05 ksf excess total pressure
	10:12	Perform static tension test, U = 58 percent
	13:14	Perform static tension test, U = 92 percent
	17:27	Perform static tension test
23 July 1986	07:27	Perform static tension test, followed by two-way cyclic test
	11:58	Probe removed from boring

As noted in the table above, all the experiments were successful; however, the 1.72-inch probe with the 0.043-inch wall cutting shoe did not develop excess pore pressures nor excess total pressures during installation. The reasons for this behavior are not known. It should be noted, however, that, in addition to the absence of consolidation, no setup occurred; the magnitude of the shear transfer remained almost constant, and equal to the value measured immediately after driving in the other experiments (approximately 1/2 the remolded shear strength).

6.0 TEST RESULTS

The results of the experiments will be presented in this chapter of the report, in the same order as tabulated in Section 5.2.

6.1 The Full-Displacement 3.0-Inch Diameter Probe

As noted earlier, the full-displacement 3.0-inch diameter probe was installed by driving on 18 July 1986, and was removed on 23 July 1986. During the five-day period the probe was installed, four separate static tension tests were performed, with a cyclic test being performed after the final tension test.

The variation in the total and pore pressures during consolidation are shown in the upper graph in Fig 8, with the radial effective pressure, calculated as the difference in the two measured pressures, being shown in the lower graph. The breaks in the curves correspond to each of the static load tests, with the final load test being performed at the end of the time shown. It may be noted in the curves that the static loadings to failure in tension did not create a significant amount of disturbance in the consolidation process, with the variations in pressure with time rapidly returning to the pretest patterns after the end of loading.

The maximum total pressure recorded at the end of driving was 8.2 ksf, with a corresponding maximum pore pressure of 7.9 ksf. During consolidation, the total radial pressure decreased to a near-constant value of 5.2 ksf, with the pore pressure stabilizing at 3.3 ksf. Thus, the radial effective pressure increased from 0.3 to 1.9 ksf during the same period.

The results of the static tension tests performed at various times after driving are shown in Fig 9. As seen in the figure, the static shear transfer capacity increased from 0.20 ksf 31 minutes after driving to 0.55 ksf 119 hours after driving.

Upon the completion of three cycles of loading, unloading, and reloading to failure in tension, the probe was subjected to five cycles of loading to failure in both tension and compression. The results of the five cycle of two-way loading are shown in Fig 10. As seen in the figure, the shear transfer decreased during the first three cycles, then stabilized at a value of 0.46 ksf; a reduction of 16 percent in the peak shear transfer.

The recorded variations with time in the soil and pore pressures during the cyclic tests shown in Figs 9 and 10 are given in Fig 11, with the shear transfer included in the lower graph. It will be noted that the shear and the normal pressures are plotted to the same scale, for convenience in comparing the relative magnitudes of the changes in the pressures during cyclic loading. As seen in the two upper graphs, the cyclic shearing resulted in a general increase in the pore pressure, with a resultant decrease in the radial effective pressure. Upon completion of the load tests shown in Fig 11, the total pressure had decreased to 4.9 ksf, with an increase to 3.7 ksf in the pore pressure, resulting in a decrease in the radial effective pressure from 1.9 to 1.2 ksf.

The shear transfer versus displacement behavior recorded during the last cycle is compared in Fig 12 with that recorded during the first tension test, which was shown in Fig 9. As seen in the figure, the yield displacement remained reasonably constant, with the peak shear transfer reducing from 0.55 to 0.46 ksf.

Upon completion of the five cycles of two-way loading, which were performed at a displacement rate of 0.0015 inch/sec, the rate of displacement was increased to 0.016 inch/sec, and one cycle of loading performed. The rate of displacement was then decreased, and one final cycle of two-way loading performed.

The recorded shear transfer behavior during the tensile loading portion of the two cycles are given in Fig 13. As seen in the figure, the increase of about 10 to 1 in the rate of loading resulted in an increase in the peak shear transfer from 0.47 to 0.51 ksf; somewhat less than 9 percent increase per log cycle of increase in the slip rate.

At the end of the rate-effect test, the probe was subjected to a large-displacement loading in tension, which was continued for several inches to break loose the cutting shoe. During the first half-inch of travel, the load rate was increased during plastic slip, from 0.003 to 0.016 inch/sec, with the results shown in Fig 14. As seen in the figure, the peak shear transfer on the initial loading was 0.43 ksf, which decreased to 0.41 ksf with continued displacement at the slow rate. When the rate was increased, the magnitude of the shear transfer increased to a maximum of 0.47 ksf. This corresponds to a rate of loading effect of the order of 13% per log cycle. Near the end of the load test shown, the rate was decreased, with a resulting decrease in the shear transfer back to the smaller value.

The variations in the soil pressures which were recorded during the load test shown in Fig 14 are given in Fig 15. Also shown in Fig 15 is a continuation of the pullout of the probe, during which time the slip joint had reached a mechanical stop; displacement data are therefore unavailable. The load test shown in Plate 14 appears in the first 2 minutes of Fig 15. Near the 4-minute mark, the load rate was again increased, resulting in a near-constant shear transfer value of 0.44 ksf being recorded.

As seen in the upper two graphs, the radial effective pressure increased significantly when the rate of loading was increased. With a near-constant value of 0.44 ksf for the shear transfer, the radial effective pressure increased from 1.7 to 2.7 ksf. The increase in the radial effective pressure was not solely due to decreases in the pore pressure, which were only 0.3 ksf; the increase in the total pressure, from 5.3 to 6.0 ksf, contributed the greatest effect.

During the loading sequence shown in Fig 15, the decrease in the pore pressure (from beginning to end) was from 3.7 to 3.3 ksf; the parallel increase in the total radial pressure was from 5.0 to 6.0 ksf, resulting in an increase in the calculated value of radial effective pressure from 1.3 to 2.7 ksf. This increase is greater than that observed during the 5 days of consolidation, and indicates clearly that the magnitude of the shear transfer is independent of the magnitude of the radial effective pressure (i.e., that clay soils are not frictional materials).

6.2 The Full-Displacement 1.72-Inch Diameter X-Probe

The 1.72-inch diameter probe was installed on 20 July 1986, and the experiment was continued until 23 July 1986, for a total consolidation time of over 4500 minutes.

Static load tests were performed at times when the degree of consolidation was 22, 40, 60, 87, and 98 percent, with a two-way cyclic test performed after the final static test. After the completion of the two-way cyclic test, the radial pressures were monitored for an additional 1200 minutes, during which time the degree of consolidation increased to 99 percent.

The variation in the measured soil and pore water pressures during the three days in which the probe was installed are shown in Fig 16. The maximum total pressure recorded immediately after the probe was installed was 7.7 ksf; the accompanying pore pressure was 7.5 ksf.

The breaks in the curves shown in Fig 16 correspond with the times at which the load tests were performed. As seen in the figure, the static load tests resulted in only minor disruptions in the process of consolidation.

Near the end of consolidation, the total pressure had reduced to 5.4 ksf and the pore pressure had decreased to 3.4 ksf, yielding an increase in the radial effective pressure from 0.2 to 2.0 ksf.

The results of the static tension tests performed 25 minutes, 4 hours 20 minutes, 23 hours 25 minutes, and 54 hours 35 minutes after installation are shown in Fig 17. As shown in the figure, the static shear transfer capacity increased during this period, from 0.19 to 0.55 ksf. In addition to the tests shown in Fig 17, one additional test was performed 1 hour 32 minutes after driving; the peak shear transfer measured during this test was 0.25 ksf.

During the final static tension test, the analog recorder was, unfortunately, not activated; the initial cycle of loading was therefore not recorded. The peak shear transfer recorded by the digital system was 0.53 ksf, however, without a parallel analog record, the actual peak value can not be verified. Due to the peak-residual

form of the curves, the digital system did not always capture the peak value of shear transfer; the digital data was thus augmented by hand-digitizing the analog records. For this particular loading, the absence of parallel analog records precluded such augmentation.

Since the analog recorder was not activated, 0.2 inches of displacement were accumulated before the error was discovered. In order to perform the two-way cyclic test, the probe was therefore pushed downward until the LVDT was centered, and the test sequence was resumed. During the compressive loading (not shown), the recorded peak shear transfer was 0.50 ksf.

Upon completion of the static tension test performed 3270 minutes after installation, the probe was loaded to near failure in compression, then loaded to failure in tension. During the two subsequent loadings to failure in tension, the shear transfer at failure decreased to 0.38 and 0.37 ksf, respectively, below the residual value of 0.41 ksf shown in Fig 17.

Five cycles of loading to failure in tension and compression were then performed, with the results shown in Fig 18. After one loading to failure in tension, the load rate was increased; as a result, the magnitude of the shear transfer also increased.

The variation of the shear transfer, the pore pressure, and the radial effective pressure during the sequence of static and cyclic loading are shown in Fig 19. As seen in the figure, the radial effective pressure increased significantly during the initial tension loading, from 2.1 to 3.5 ksf; an increase almost as large as that recorded during monotonic consolidation.

The simultaneous variation in the shear transfer and the soil pressures during two cycles of the two-way cyclic test are shown in Fig 20, with the time scale expanded. As shown in the figure, the increase in the radial effective pressure, which was due primarily to decreases in the pore pressure, occurred during plastic slip, as the magnitude of the shear transfer decreased from the peak to the residual value. During the first cycle shown in Fig 20, the radial effective pressure increased from 1.3 ksf (at the peak shear of 0.53 ksf) to 2.4 ksf (at the maximum displacement, with

the residual shear transfer being 0.43 ksf). Again, the absence of truly frictional clay behavior is clearly evident.

The effects of cyclic loading on the soil resistance is shown in Fig 21, in which the shear transfer recorded on the final, slow loading to failure in tension is compared to that on the first recorded tension test (shown in Fig 17). As shown in the figure, the peak shear transfer decreased from 0.55 to 0.51 ksf; a decrease of only 7 percent. As noted earlier, the magnitude of the initial static peak shear transfer was not recorded, and was, no doubt, greater than the value of 0.55 ksf measured on the second failure in tension.

6.3 The 3.0-Inch Diameter, 0.125-Inch Wall Probe Tests

The experiment with the 3.0-inch diameter pile segment model with a cutting shoe having a wall thickness of 0.125 inch was begun on 21 July, and was completed on 23 July, after 44 hours of consolidation. During this experiment, leakage of moisture into the probe created instability in the pressure data after 37 hours of consolidation. At the time the pressure data became unstable, the degree of consolidation was approximately 93 percent; thus, the loss of the pressure data did not invalidate the experiment.

Slow loadings to failure in tension were performed 14 minutes, 56 minutes, 3 hours, 13 hours, and 44 hours after installation, at which times the degree of consolidation was 16, 36, 57, 86, and 95 (estimated) percent.

The variations in the measured and the calculated soil and pore water pressures during consolidation are shown in Fig 22.

During this experiment, the total pressure recorded immediately after driving was 6.8 ksf. Unlike the behavior observed in the two experiments discussed earlier, the total pressure increased with time after driving, reaching a maximum value of 7.1 ksf after 80 minutes. The total pressure then decreased, remaining near 6.0 ksf after 900 minutes had elapsed.

The maximum pore pressure, which was recorded immediately after driving, was also 6.8 ksf, indicating near-zero radial effective pressures immediately after driving. At the time of the moisture intrusion, the pore pressure had decreased to 3.5 ksf, only 0.2 ksf above the ambient value of 3.3 ksf observed in the earlier experiments.

It is quite interesting to note that the radial effective pressure near the end of consolidation had increased to 2.5 ksf; a value larger than the near-equal values of 1.9 and 2.0 ksf measured in the experiments with full-displacement cutting shoes.

The breaks in the smooth curves correspond to the times at which the static load tests were performed. As noted earlier, the load tests had little effect on the soil pressures.

The results of the static tension tests performed at various times after driving are shown in Fig 23. As shown in the figure, the magnitude of the peak shear transfer increased from a value of 0.17 ksf 14 minutes after driving to 0.66 ksf after 44 hours.

During the test performed 44 hours after driving, the probe was twice unloaded, then reloaded to failure in tension. During the second and the third loadings, the peak shear transfer was 0.62 and 0.61 ksf, respectively.

The probe was then subjected to five cycles of loading to failure in tension and compression, as shown in Fig 24. During the cyclic tests, the shear transfer decreased to 0.52 ksf, a reduction of 21 percent.

In Fig 25, the behavior recorded during the fifth cycle of loading is compared to that recorded during the first loading to failure. As shown in the figure, the cyclic degradation in resistance was accompanied by a softening of the clay, with the yield displacement remaining nearly constant.

6.4 The 3.0-Inch Diameter, 0.065-Inch Wall Probe Tests

The 3.0-inch diameter probe with the 0.065-inch wall cutting shoe was installed on 20 July and was removed on 21 July, after 23 hours of consolidation. Static load tests were performed 62 minutes, 3 hours 48 minutes, 7 hours, and 23 hours after driving, at which times the degrees of consolidation were 39, 72, 85, and 99+ percent, respectively.

The variation in the measured and calculated soil and pore water pressures during consolidation are shown in Fig 26. As shown in the figure, the maximum total pressure immediately after driving was 6.1 ksf, slightly smaller than the maximum pore pressure, which was 6.5 ksf. The apparent negative value of radial effective pressure should not be considered to be real, but indications of nearly-equal total and pore water pressures. The pressure transducers are separated vertically by a distance of approximately 2 inches, so that the differences in the pressures may indicate vertical pressure variations. It should also be noted that the pressure transducers were designed for offshore applications, and have a linear range of more than 100 ksf; a difference of 0.4 ksf represents only 0.4 percent of full scale.

During consolidation, the total pressure initially decreased, to a minimum value of 5.1 ksf. At the end of the experiment, the total pressure had increased slightly, to 5.3 ksf. The pore pressures decreased throughout the consolidation period, from the maximum value of 6.5 ksf immediately after driving, to 3.3 ksf after 43 hours. Again, as shown in the figure, the static load tests created only temporary perturbations in the process of consolidation, but had no permanent effects.

The magnitude of the radial effective pressure near the end of consolidation was 2.0 ksf; equal to the values of 1.9 and 2.0 ksf which were measured in the experiments with the full-displacement cutting shoes, and less than the maximum value of 2.5 ksf measured in the experiment with the 0.125-inch wall cutting shoe. Again, this behavior is unexpected; a smaller value of radial effective pressure would be expected for both the experiments with the thin-wall cutting shoes, as compared with the full-displacement end conditions.

The results of the static load tests performed at various times after driving are shown in Fig 27. As shown in the figure, the peak shear transfer increased from 0.22 ksf one hour after driving to 0.58 ksf after 43 hours. During the load tests performed 43 hours after driving, the probe was twice unloaded, then reloaded to failure, as shown in Fig 27. On the second and third loadings to failure in tension, the values of peak shear transfer were 0.55 and 0.54 ksf, respectively, only slightly smaller than the initial peak value of 0.58 ksf.

After the conclusion of the tension tests shown in Fig 27, the probe was subjected to 6 cycles of loading to failure in both tension and compression, as shown in Fig 28. As shown in the figure, the peak shear transfer of 0.54 ksf on the first cycle decreased to 0.47 ksf on the fifth cycle, with the post-peak residual value decreasing from 0.51 to 0.41 ksf.

The variations in the measured and calculated soil and pore water pressures are shown in Plate 29. In the figure, the rapid decrease in the pore pressure, and the corresponding rapid increase in the radial effective pressure, occur during plastic slip, with near-constant shear transfer. It should also be noted that the three cycles of loading to failure in tension prior to the two-way cyclic test had reduced the at-rest radial effective pressure from a pre-test value of 2.0 ksf to 1.6 ksf. After the conclusion of the two-way cyclic tests, the radial effective pressure had decreased still further, to 1.2 ksf, only 60 percent of the pre-test value.

Upon completion of the two-way cyclic tests, one fast-rate cycle of loading to failure in tension and compression was applied, followed by one cycle at the same rate as the static tension test. The results of the slow-rate cycle of loading are compared to the initial static test in Fig 30. As seen in the figure, the peak shear transfer had decreased from 0.58 to 0.46 ksf, a decrease of almost 21 percent. As noted earlier, the yield displacement remained nearly constant during cyclic degradation.

The tension-loading portions of the cycles of loading with different rates are shown in Fig 31. As shown in the figure, the increase in displacement rate from 0.00011 to 0.011 inch/sec resulted in an increase in the shear transfer from 0.46 to 0.52 ksf,

corresponding to approximately a 7 percent increase in shear transfer per log cycle of increase in rate.

The probe was then subjected to one large-displacement loading in tension, with the rate of displacement being increased from 0.00003 inch/sec to 0.016 inch/sec during plastic slip. The results of the test are shown in Figure 32. As shown in the figure, the shear transfer increased from 0.42 to 0.54 ksf, an increase of 10 percent per log cycle of increase in rate. As seen in the figure, the load rate was decreased after approximately 0.5 inches of displacement, whereupon the magnitude of the shear transfer decreased, to 0.44 ksf. Upon increasing the rate of displacement a second time, the shear transfer again increased. At this point, the slip joint had reached a mechanical stop; the load test, however, was continued.

The load test, with the additional loading for which displacement data are not available, are shown in Fig 33, which contains the variation with time in the shear transfer, the pore pressure, and the radial effective pressure during the tests shown in Fig 32. As seen in Fig 33, only slight changes in the soil and water pressures accompanied the slow-rate plastic slip, with the radial effective pressure increasing from 1.3 to 1.5 ksf. When the rate of loading was increased, the radial effective pressure increased from 1.5 to 3.2 ksf; the pore pressure decreased from 3.6 to 2.4 ksf, below the ambient pore pressure.

After the completion of the tests shown in Fig 32 (the small spike near the end of the curves), the load rate was again increased, and the probe pulled upward approximately 6 inches. During the large displacement at the fast rate, as shown in Fig 33, the shear transfer increased to 0.63 ksf, with the radial effective pressure simultaneously increasing to over 3.5 ksf.

Again, the effects of volume changes in the clay adjacent to the pile during plastic shearing resulted in changes in the radial pressures which were almost equal to those which occurred during consolidation.

6.5 The 1.72-Inch, 0.043-Inch Wall Probe Tests

A 1.72-inch diameter probe was fitted with a cutting shoe having a wall thickness of 0.043 inch. Since interior of the probe body is sealed, four weep holes were drilled in the cutting shoe near its point of attachment to the probe.

The probe was installed on the morning of 22 July, and was removed at noon on 23 July.

At the end of installation of the probe, by pushing with the drawworks of the rig, only small values of excess pore pressure were measured. At the end of installation, the total radial pressure was 3.0 ksf, with a pore pressure of 3.4 ksf. During the following 27-hour period, the pore pressure decreased to 3.3 ksf, with the total pressure remaining essentially constant.

The reasons for the low values of total pressure (below hydrostatic) are not clear. The transducer calibration was carefully checked, and found to be correct. The in-air voltage readings made before and after the experiment were checked, and found to differ by only 0.04 ksf, which is the limit of accuracy in the measured voltages.

The probe was load tested 1, 4, 8, and 22-1/2 hours after installation, with the magnitude of the shear transfer recorded in the tests being 0.15, 0.16, 0.16, and 0.15 ksf, respectively. During a two-way cyclic test performed after 23 hours of consolidation, the shear transfer remained at 0.17 ksf (slightly higher, due to rate effects) for four cycles of loading to failure in tension and compression.

Upon removal of the probe, the cutting shoe was inspected, and the soil plug was found to be intact.

The physical reasons for the lack of consolidation, and for the absence of increases in shear transfer, are not known. The magnitude of the shear transfer, 1/2 the remolded strength, agrees well with the values measured immediately after driving in the other experiments. The absence of increases in the shear transfer with time may have been due to the absence of decreases in void ratio accompanying the dissipation

of excess pore pressures; the low values of total pressure suggest that additional factors (post-holing during installation) may also have contributed.

In any event, due to the nature of the results, the data are not presented in graphic form.

6.6 Summary of Experimental Results

The soil and pore pressure data recorded during consolidation are contained in Table 1.

TABLE 1. SUMMARY OF CONSOLIDATION DATA

Diameter	D/wt ratio	Total		Pore		Effective		t ₅₀	t ₉₀
		Max	Min	Max	Min	Min	Max		
3.00	2	8.2	5.2	7.9	3.3	0.3	1.9	300**	2400
3.00	24	6.8	6.1	6.8	3.5	0.0	2.5	120	1200
3.00	46	6.1	5.1	6.5	3.3	-0.4	2.0	100	570
1.72	2	7.7	5.2	7.5	3.3	0.2	2.0*	150	1600
1.72	40	3.0	3.0	3.4	3.3	-0.4	-0.3	N/A	N/A

** Estimated. The data acquisition system was down for repair.

* Prior to final load test, not at the end of consolidation.

The effects of the amount of cavity expansion (as determined by the wall thickness of the cutting shoe) can be seen in the magnitudes of the excess pore pressures which were developed. For the full-displacement probes, the excess pore pressures

were 4.6 and 4.2 ksf, respectively, which are 8.2 and 7.5 times the undrained shear strength. For the 3.00-inch diameter probe with the 0.125-inch cutting shoe, the maximum excess pore pressure of 3.5 ksf is only 6.3 times the undrained shear strength. The 3.00-inch probe with the 0.065-inch wall cutting shoe developed 3.3 ksf (5.9 S_u) of excess pore pressure.

The magnitudes of the maximum total pressures also reflect the effects of the increasing amount of cavity expansion, with the values increasing from 6.1 to 6.8 to 8.0 (average) ksf as the D/wt ratio decreases from 46 to 24 to 2, respectively.

The effect of the D/wt ratio (Diameter divided by the wall thickness) can be seen in the time required for consolidation. For the three 3.0-inch diameter probes with various wall thicknesses, it can be seen that the rate of consolidation is up to three times faster for the probe with the 0.065-inch wall cutting shoe than for the full-displacement shoe ($D/wt = 2$), and is approximately twice as fast for the probe with the 0.125-inch wall cutting shoe.

The pore pressure data during consolidation are shown dimensionless form in Fig 34. In Fig 34, the degree of consolidation, U , represents the proportionate reduction in the magnitude of the remaining excess pore pressure, expressed as a percentage. The dimensionless time factor T , was determined by the equation

$$T = (t \times C_v) / D^2, \text{ where}$$

$$t = \text{time after driving, in minutes}$$

$$C_v = \text{coefficient of consolidation, in inch}^2 / \text{min (taken as 0.00069, from Appendix A)}$$

$$D = \text{diameter of the probe}$$

As shown in the figure, although the data have been nondimensionalized, the relationships are not normalized, else only one curve would result. In order to normalize the data, the effects of the D/wt ratio must be included.

Although it is possible to normalize the data shown in Fig 34 to account for the D/wt ratio, it should be recognized that only one experiment was performed with each diameter and D/wt ratio. In our past experience with such experiments, a number of such experiments should be performed with each diameter and D/wt ratio, in order to obtain a representative average curve, rather than attempting to fit any single curve.

It can be seen that the rate of consolidation is extremely sensitive to variations in the wall thickness of the cutting shoe. Similarly, slight variations in the amount of soil expelled outward from beneath the wall of the cutting shoe, as compared to the amount of soil which forms the internal plug, will also significantly affect the consolidation time. During installation of the probes, the amount of soil which entered the cutting shoe (or was expelled outward) was not controlled. Without control of the process, exact replication of the experiments with various D/wt ratios is not possible; nor is it likely that the curves obtained for the thin-wall cutting shoes fortuitously represent the average value for each particular D/wt ratio. For these reasons, further normalization of the data was not attempted.

The results of the load test data are summarized in Table 2, with the data also presented in graphical form in Fig 34. As shown in the figure, the magnitude of the peak static shear transfer increases during consolidation, from a value equal to $1/2$ the remolded shear strength ($\alpha = 0.3$) to a value equal to the undrained shear strength, with $\alpha = 1.0$. The scatter in the data is generally within ± 6 percent, which is within the range of variation in the measured values of shear strength, and probably results from the horizontal variability in the soil deposit.

TABLE 2. RESULTS OF STATIC LOAD TESTS

Experiment	Degree of Consolidation Percent	Shear Transfer ksf	Alpha (f/Su)	Effective Pressure	
				Cons.	Fail.
3.0 x Full Displ.	18	0.17	0.30	0.6	0.6
	37	0.29	0.52	0.8	0.9
	93	0.50	0.89	1.9	1.8
	100	0.55	0.98	1.9	1.8
		0.43	0.77		1.3
1.72 x Full Displ.	23	0.16	0.29	0.6	0.6
	41	0.25	0.45	0.9	1.0
	61	0.35	0.63	1.5	1.7
	88	0.42	0.76	2.0	1.9
	98	0.55	0.98	2.0	2.1
		0.51	0.91		1.3
3.00 x 0.125	16	0.17	0.30	0.6	0.6
	36	0.24	0.43	1.5	1.4
	57	0.37	0.66	2.0	1.9
	87	0.56	0.85	2.3	2.3
	95	0.66	1.18		
		0.52	0.93		
3.00 x 0.065	39	0.27	0.48	0.1	0.2
	72	0.36	0.64	0.9	0.7
	85	0.48	0.86	1.4	1.3
	98	0.58	1.04	1.9	N/A
		0.43	0.77		1.4

An examination of the ratios of the shear transfer to the radial effective pressures shows that the ratio varied from 0.16 to 0.40, indicating that direct relationships between the two variables do not exist; i.e., that clays are not frictional materials.

7.0 SUMMARY AND CONCLUSIONS

The results of the experiments have demonstrated that, in normally consolidated clay soils, the magnitude of the shear transfer increases with time at a diminishing rate, eventually approaching a value equal to the undrained shear strength of the soil. Immediately after driving, the shear transfer is very low, being equal to, in these experiments, half the remolded shear strength of the clay.

The consolidation data have shown that, in addition to the diameter, the rate of consolidation is also dependent upon the wall thickness of the cutting shoe. Although the rate of consolidation for open-ended pipe piles is faster than for fully plugged piles, the time required for full setup to occur for prototype-size piles, with diameters in the range of 48 to 72 inches (16 to 24 times the size of the models) is measured in years, rather than days. Thus, any accurate and reliable axial pile design method must include consideration of both diameter and wall thickness on the rate of increase in axial pile capacity.

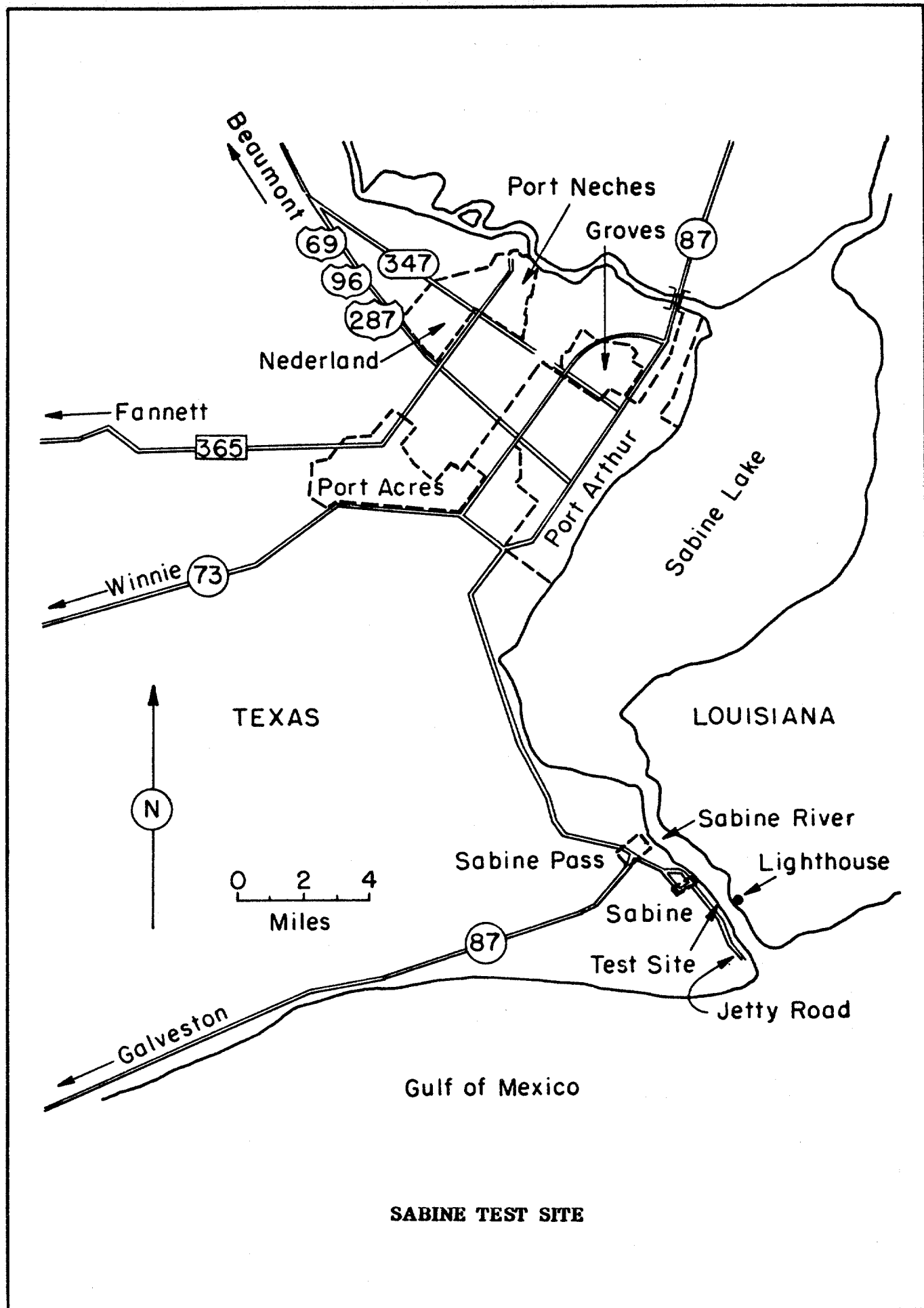
The pressure variations during the load tests have shown that no direct relationships exist between the magnitudes of the radial effective pressure and the shear transfer; that is, that clays do not exhibit truly frictional behavior. The close relationship between the degree of consolidation and the shear transfer suggests that the development of a rational, accurate, and reliable total stress approach to axial pile capacity is quite feasible, although an effective stress-based approach which considers the three-dimensional state of stress should be equally valid.

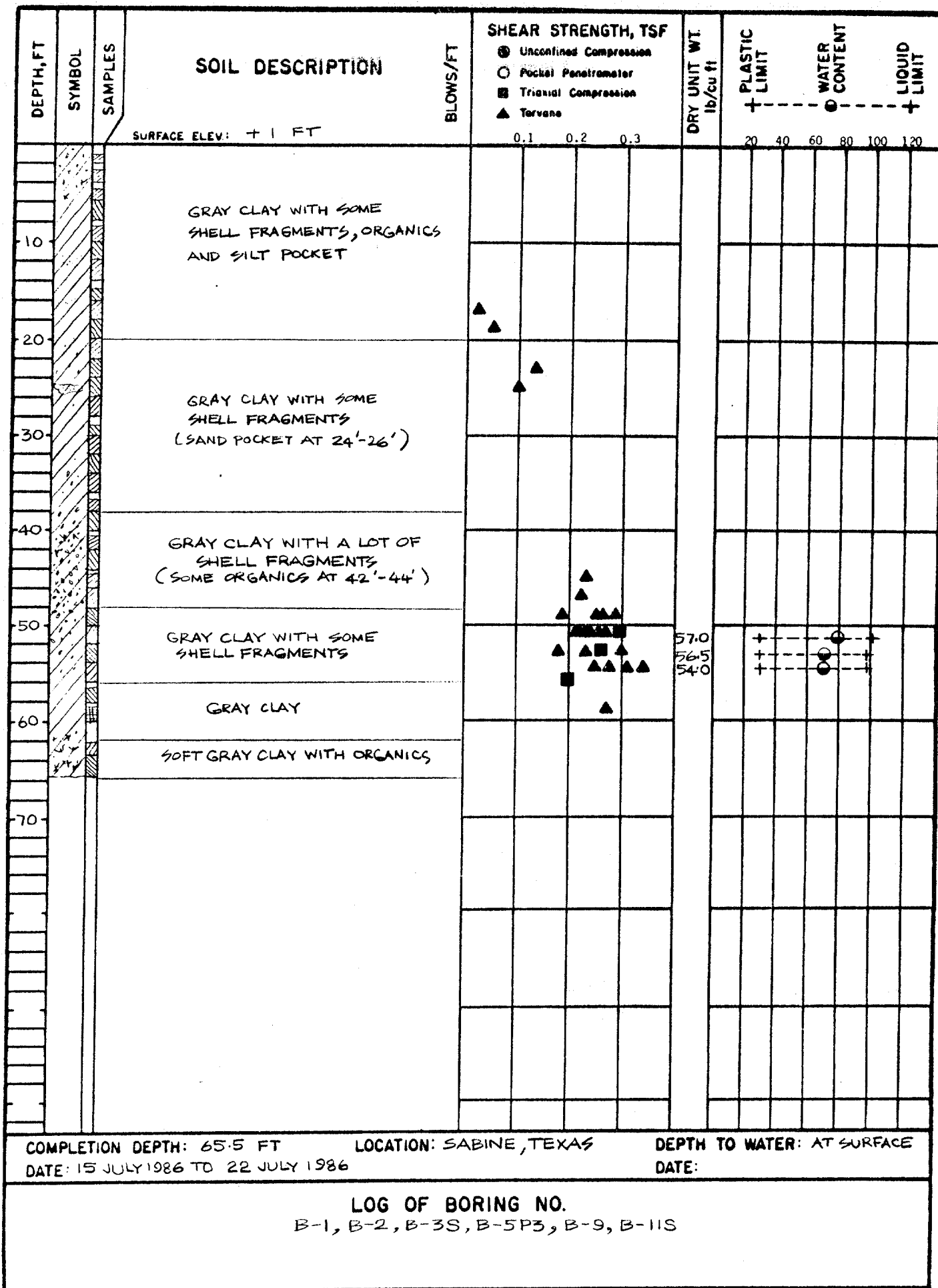
In order to develop any reliable and accurate design method, whether based on total or effective stresses, however, the effects of both pile diameter and wall thickness on the rate of consolidation and setup must be properly considered.

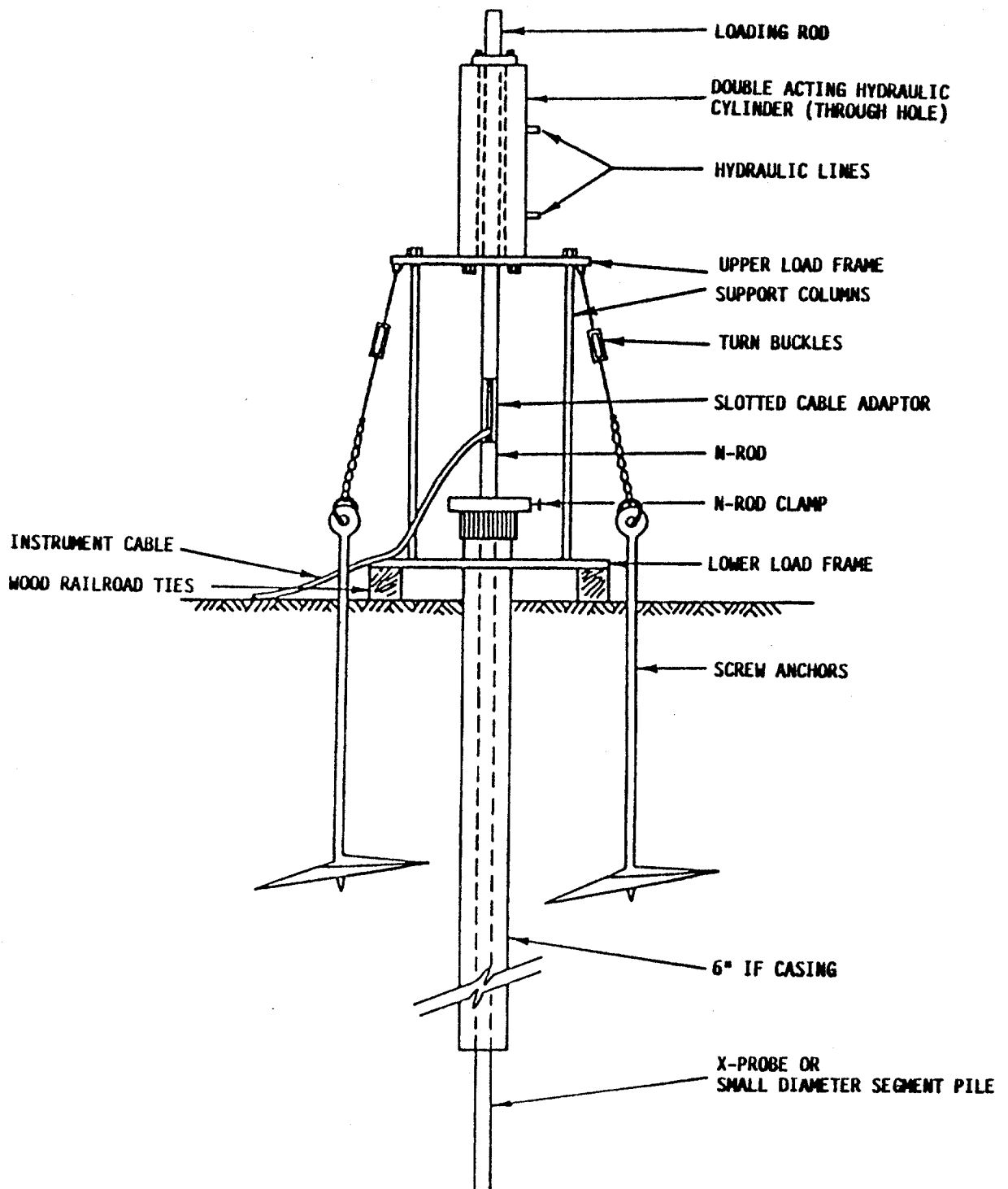
Existing methods for the calculation of axial pile capacity in clays soils have been based on the results of pile load tests in which the effects of time on the shear transfer capacity have not been properly considered. The amount of scatter in the empirical relationships which have been developed by several researchers has severely limited the degree of confidence placed in the methods. An examination of the pile

load test data which has been used to develop the existing design procedures shows that the range in pile diameters was from 4 to 72 inches; the experimental data indicates that, if the time after driving is not considered, the possible range in axial pile capacities is greater than 3 to 1. Thus, to a large degree, proper consideration of the effects of time on the measured axial capacities would probably reduce the scatter, and would allow the development of much more reliable design guidelines than presently exist.

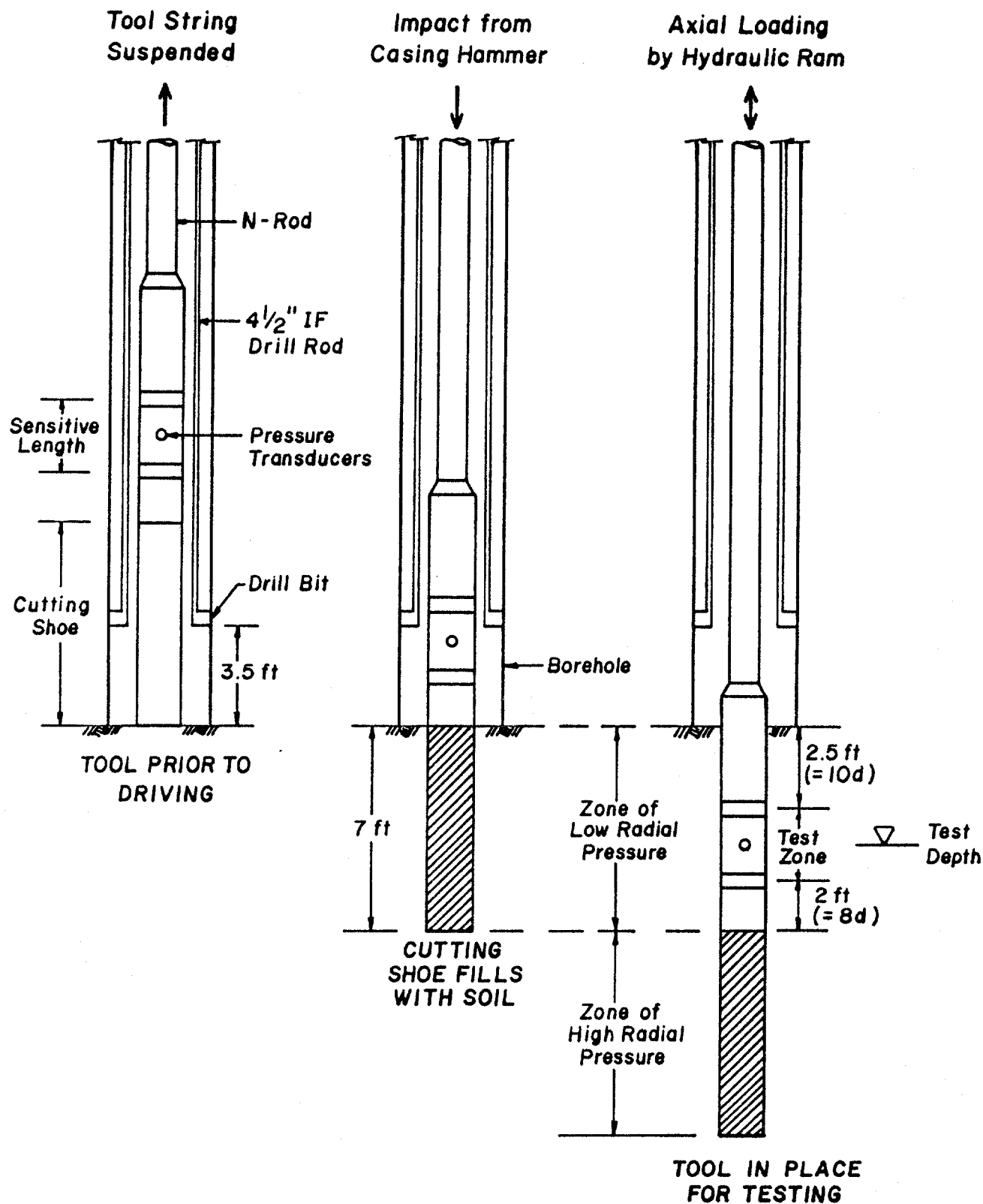
FIGURES



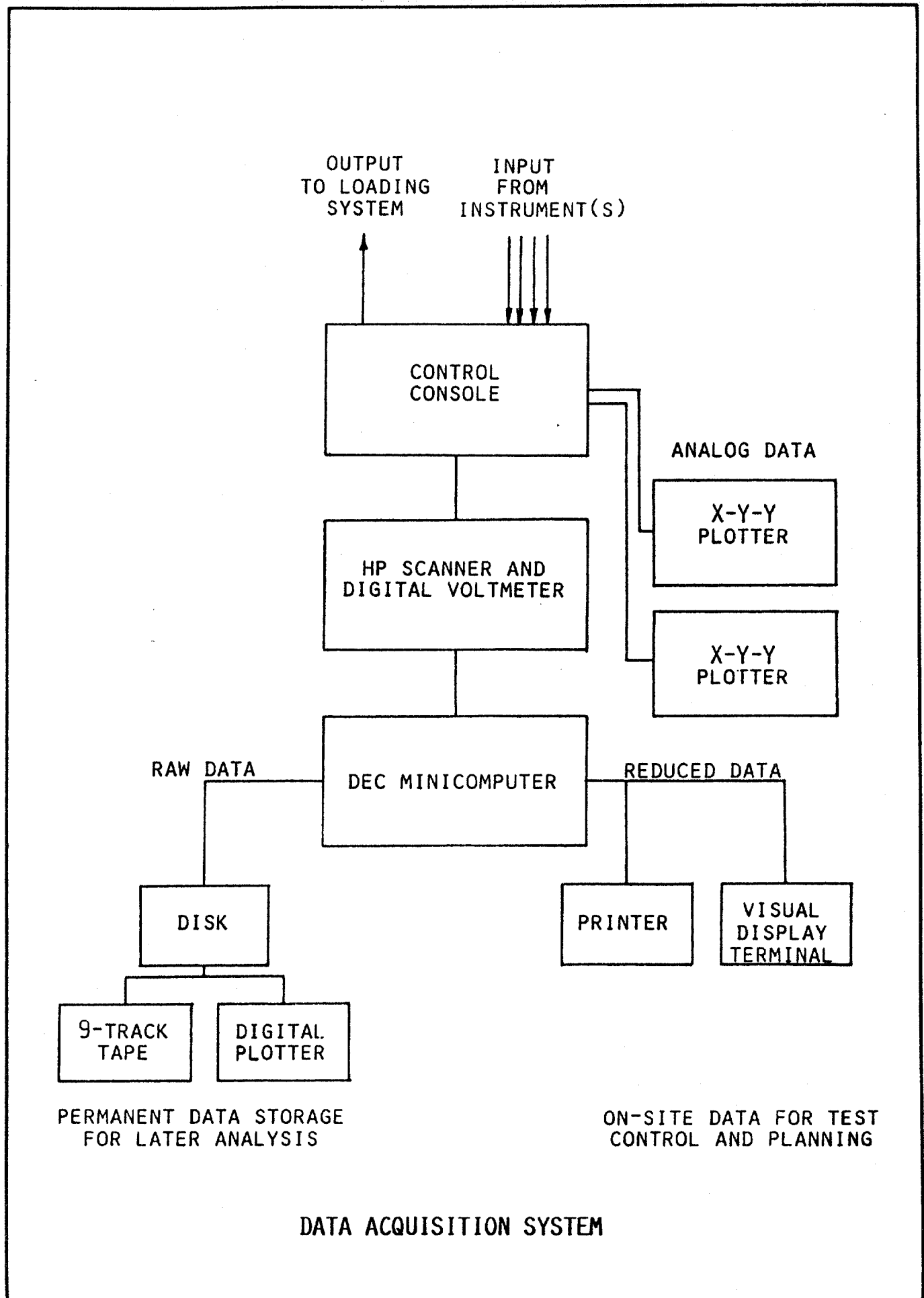


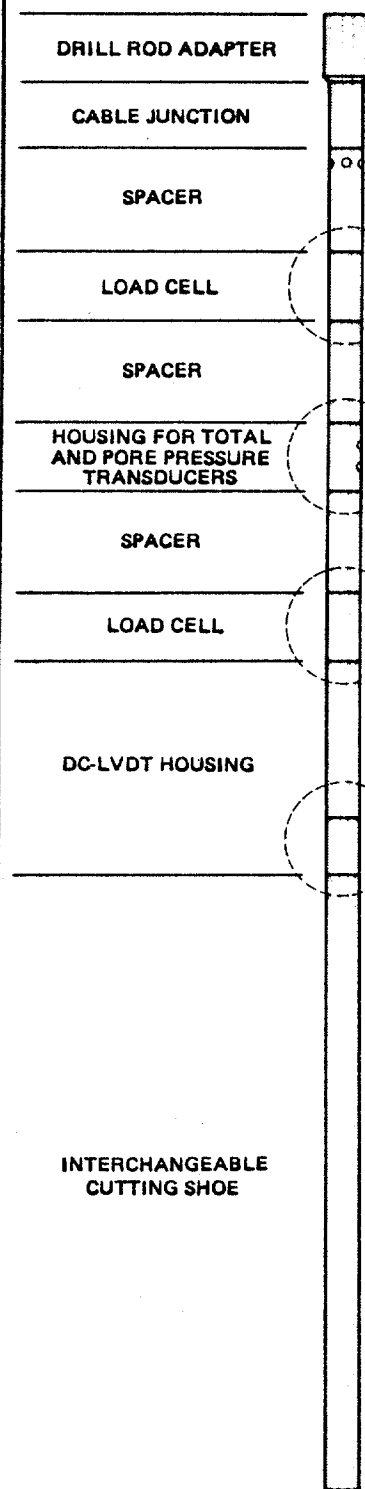


SCHEMATIC DIAGRAM OF PORTABLE LOADING SYSTEM



PHASE OF INSTALLATION OF THE 3-INCH DIAMETER PILE SEGMENT MODEL



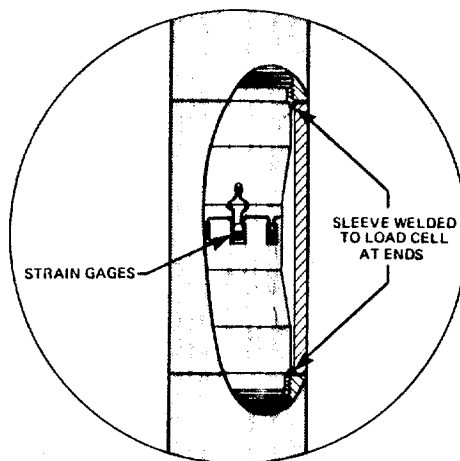


SEE
DETAIL A

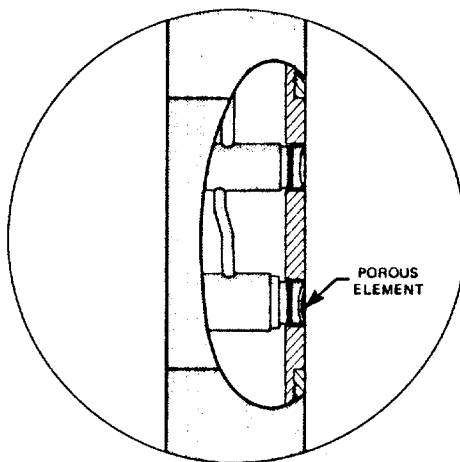
SEE
DETAIL B

SEE
DETAIL A

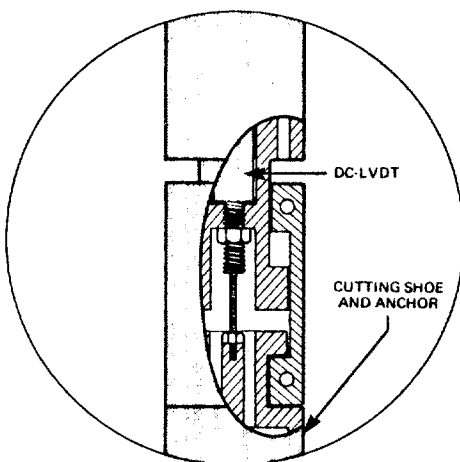
SEE
DETAIL C



DETAIL A
LOAD CELL FOR
FRICTION MEASUREMENT

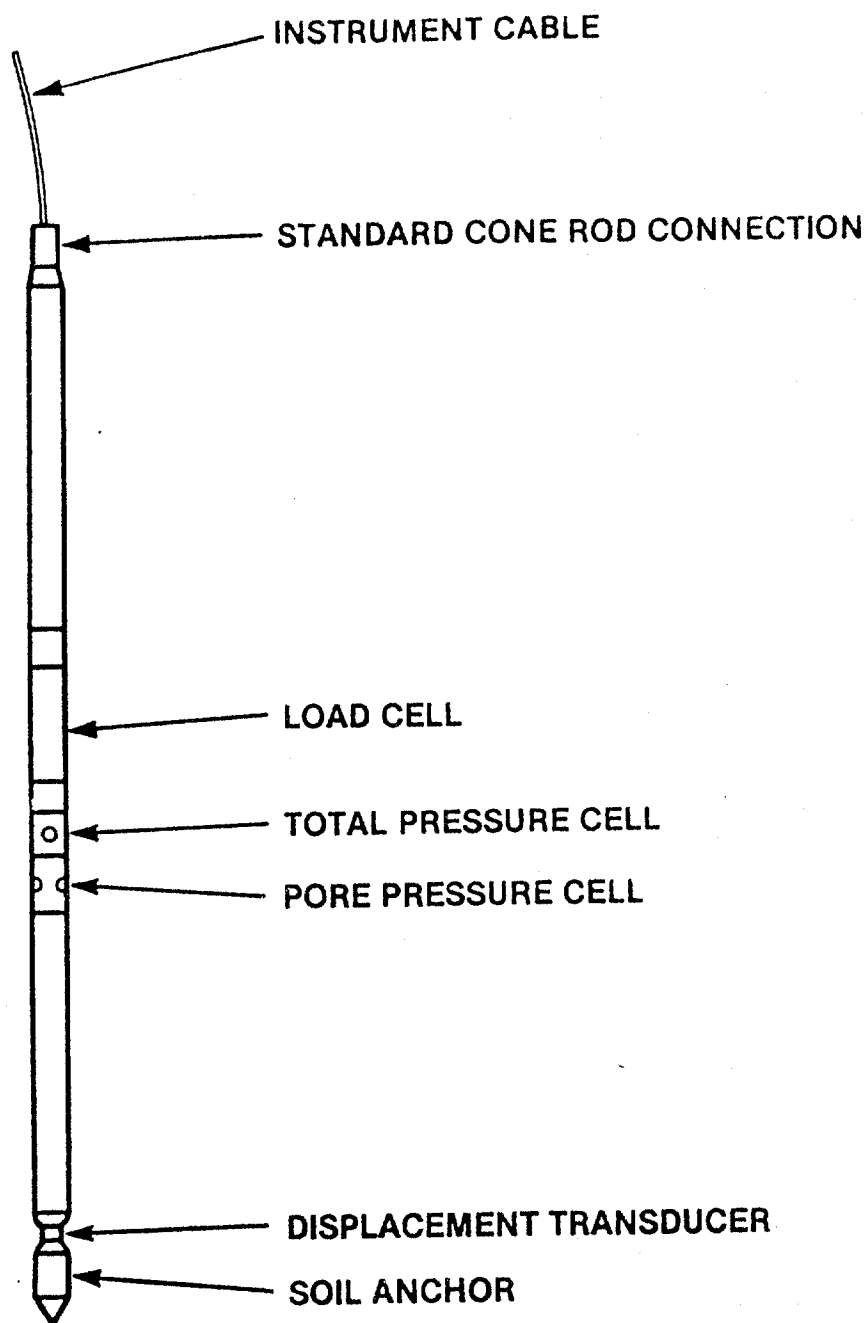


DETAIL B
TOTAL PRESSURE
LOAD CELL AND
PORE PRESSURE
TRANSDUCER HOUSING

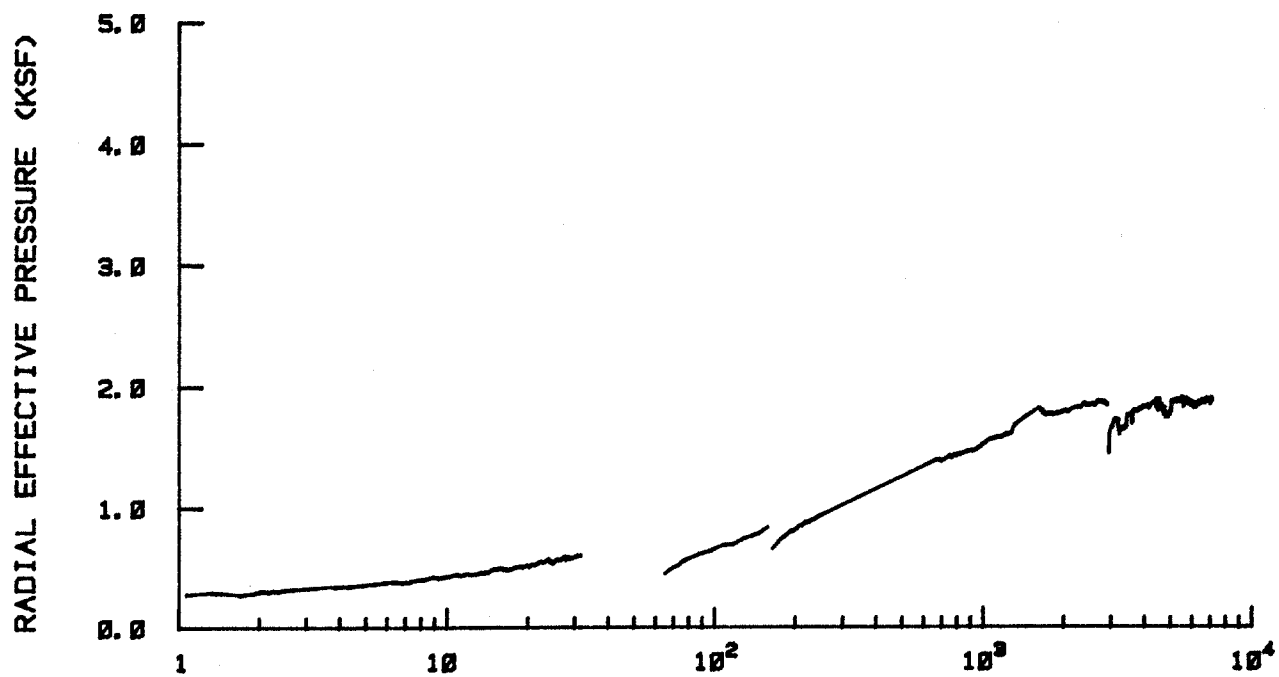
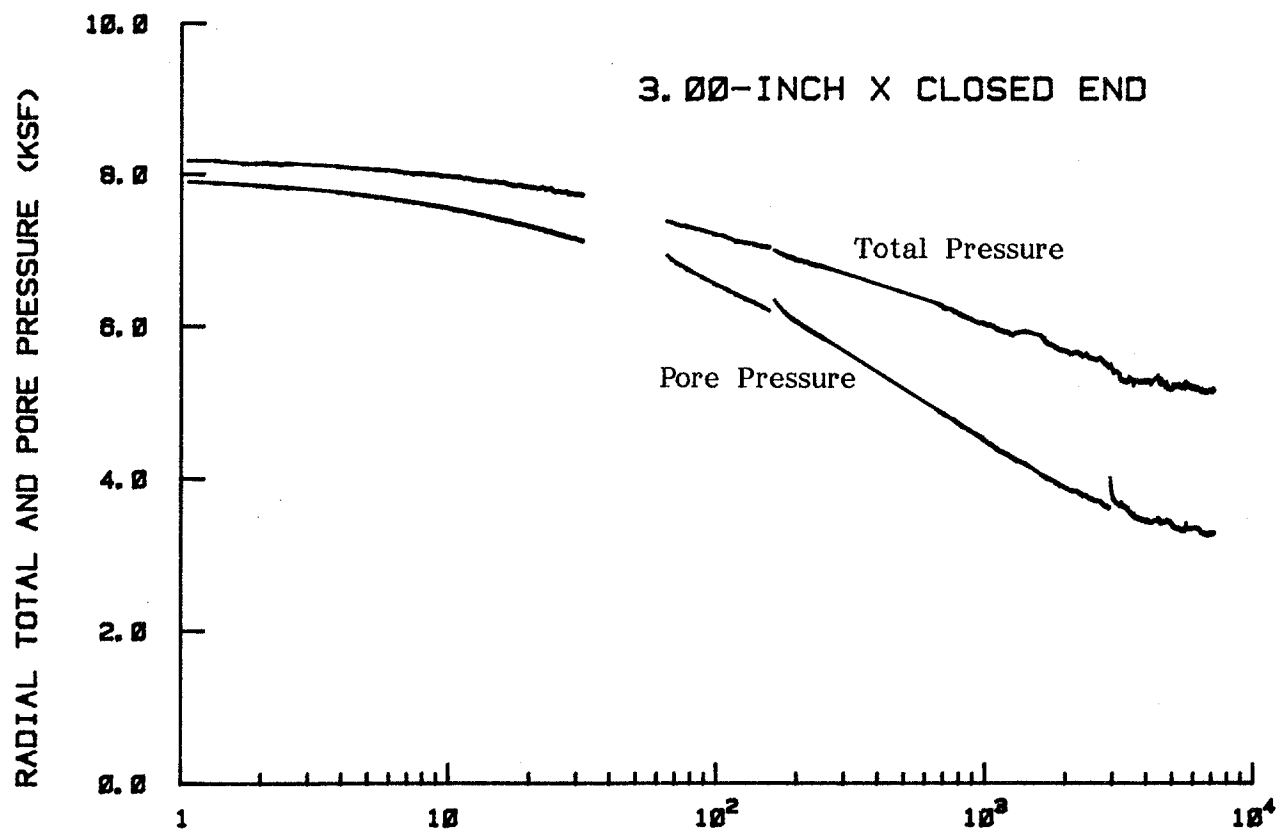


DETAIL C
DC-LVDT FOR
MEASUREMENT OF
RELATIVE DISPLACEMENT

3-INCH DIAMETER PILE SEGMENT MODEL



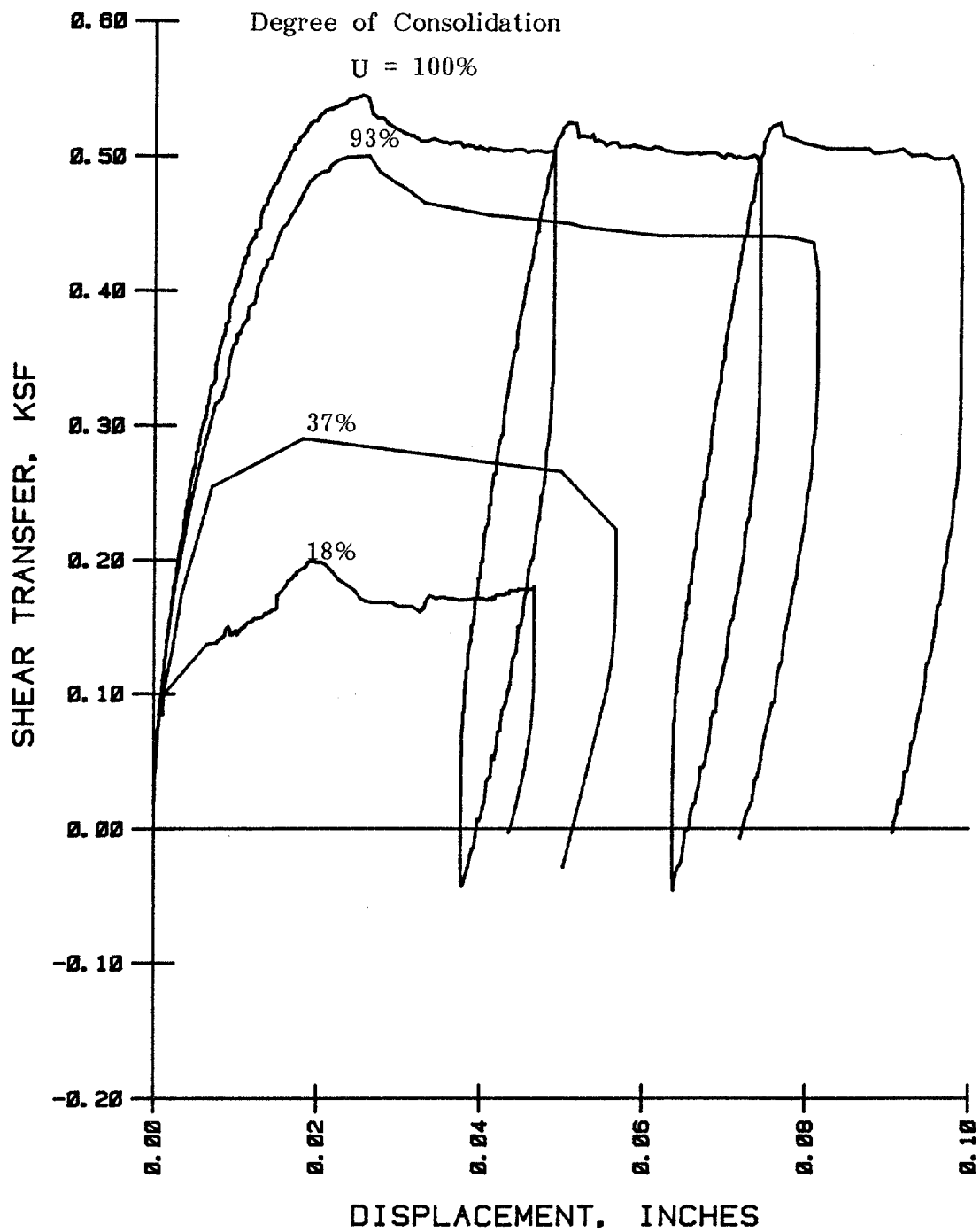
**1.72-INCH DIAMETER PILE SEGMENT MODEL
(DENOTED AS X-PROBE)**



MINUTES AFTER DRIVING

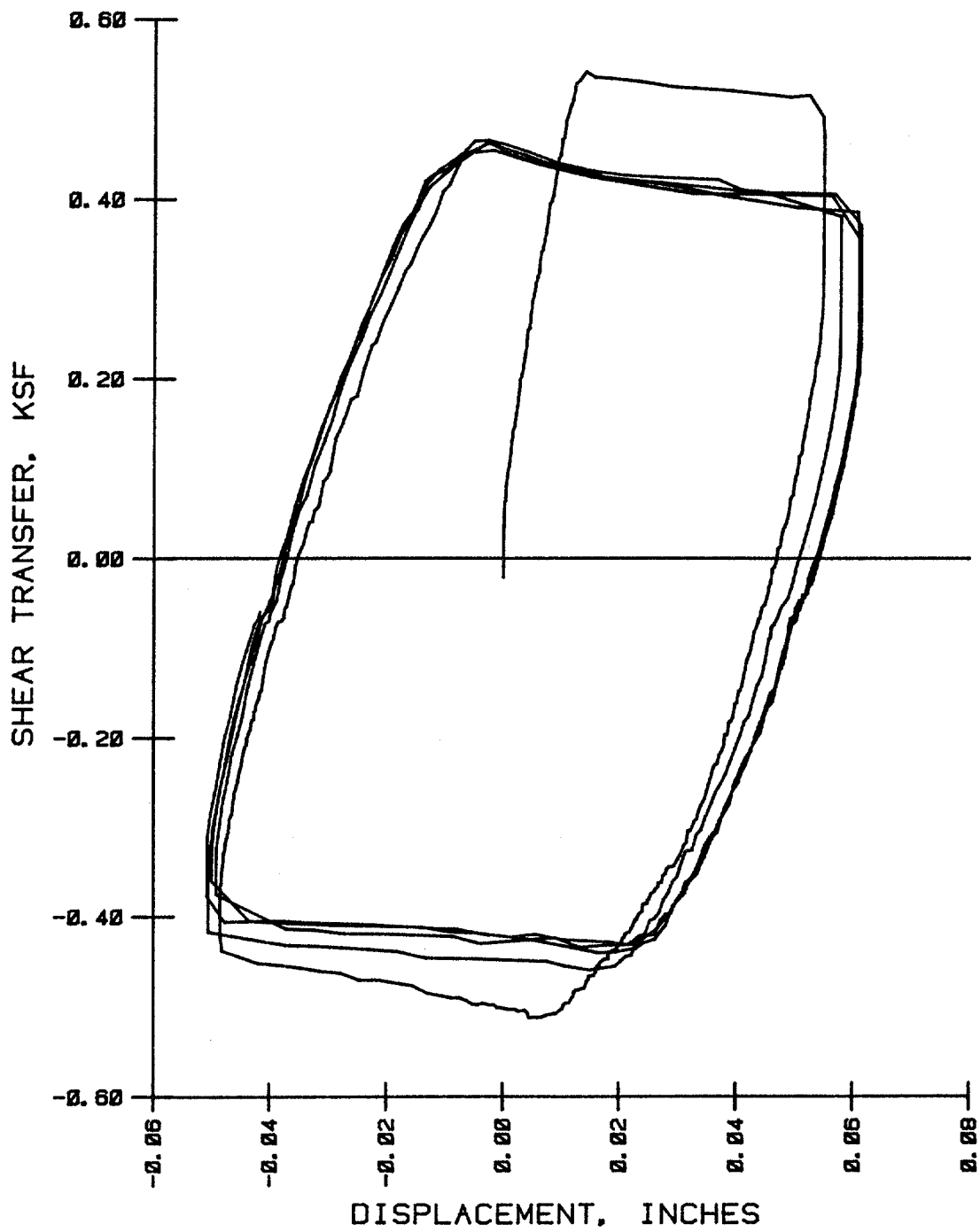
VARIATION OF PRESSURES DURING CONSOLIDATION

3.00-INCH X CLOSED END



RESULT OF STATIC TENSION TESTS

3.00-INCH X CLOSED END



TWO-WAY CYCLIC LOAD TESTS

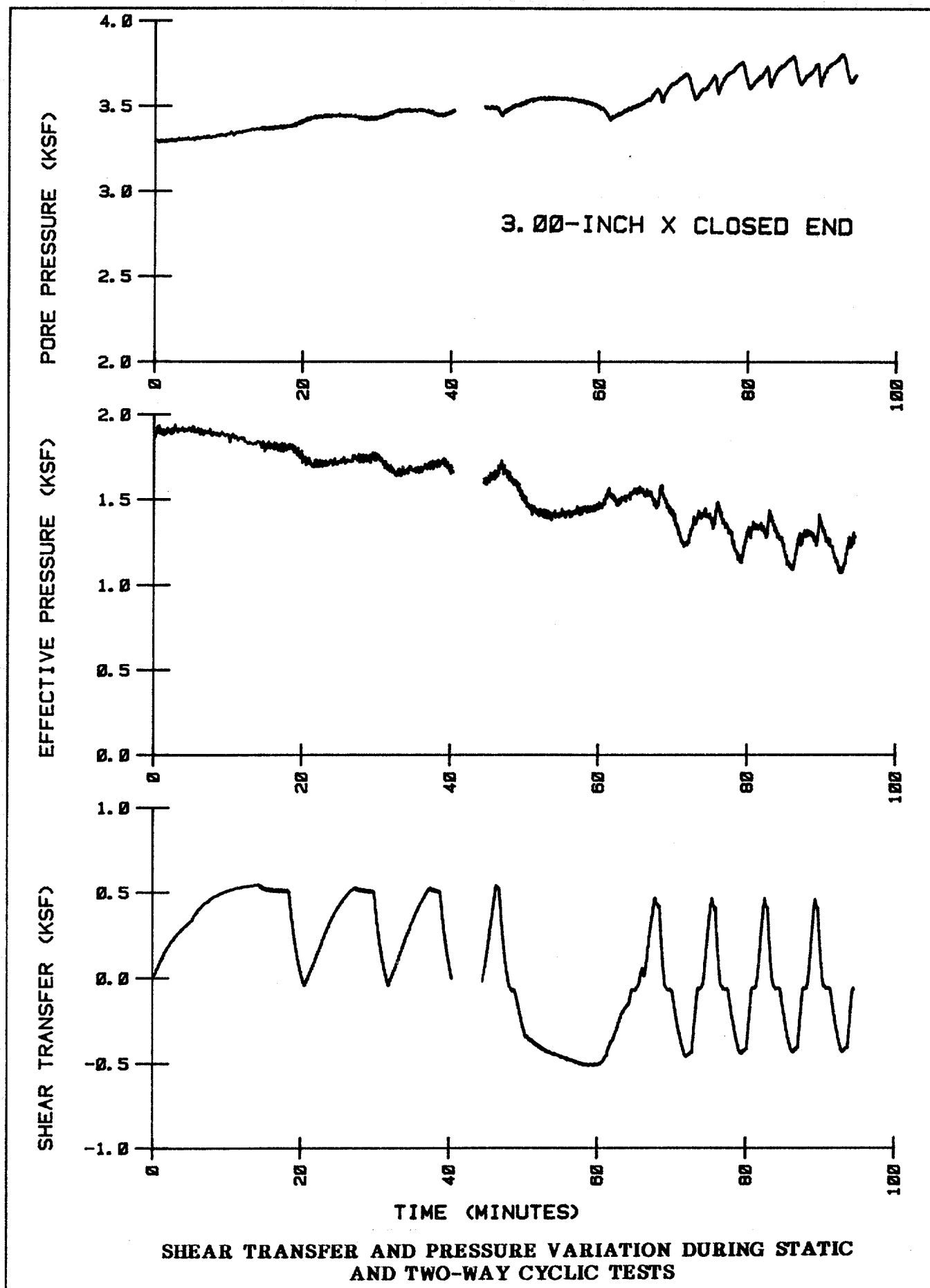
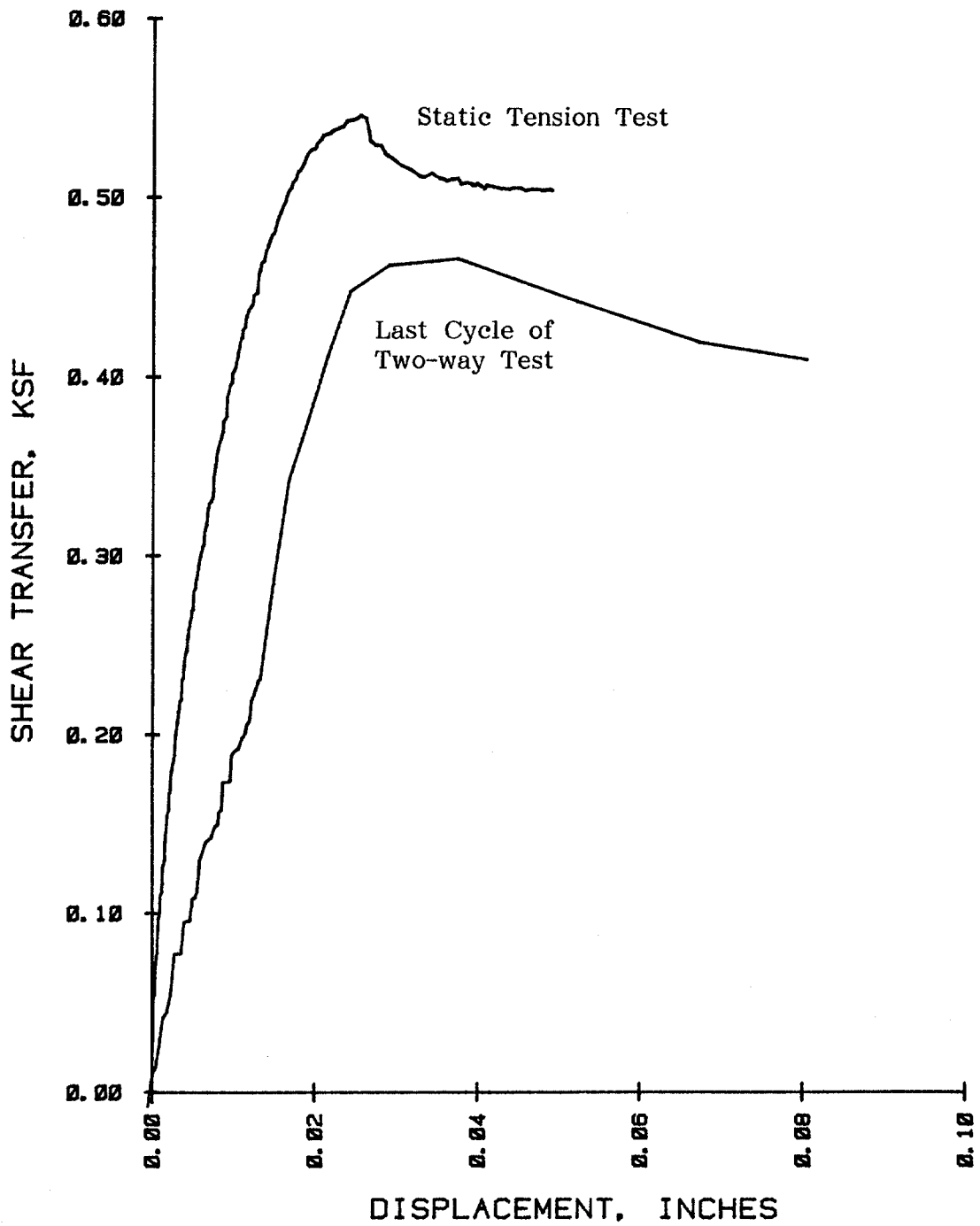


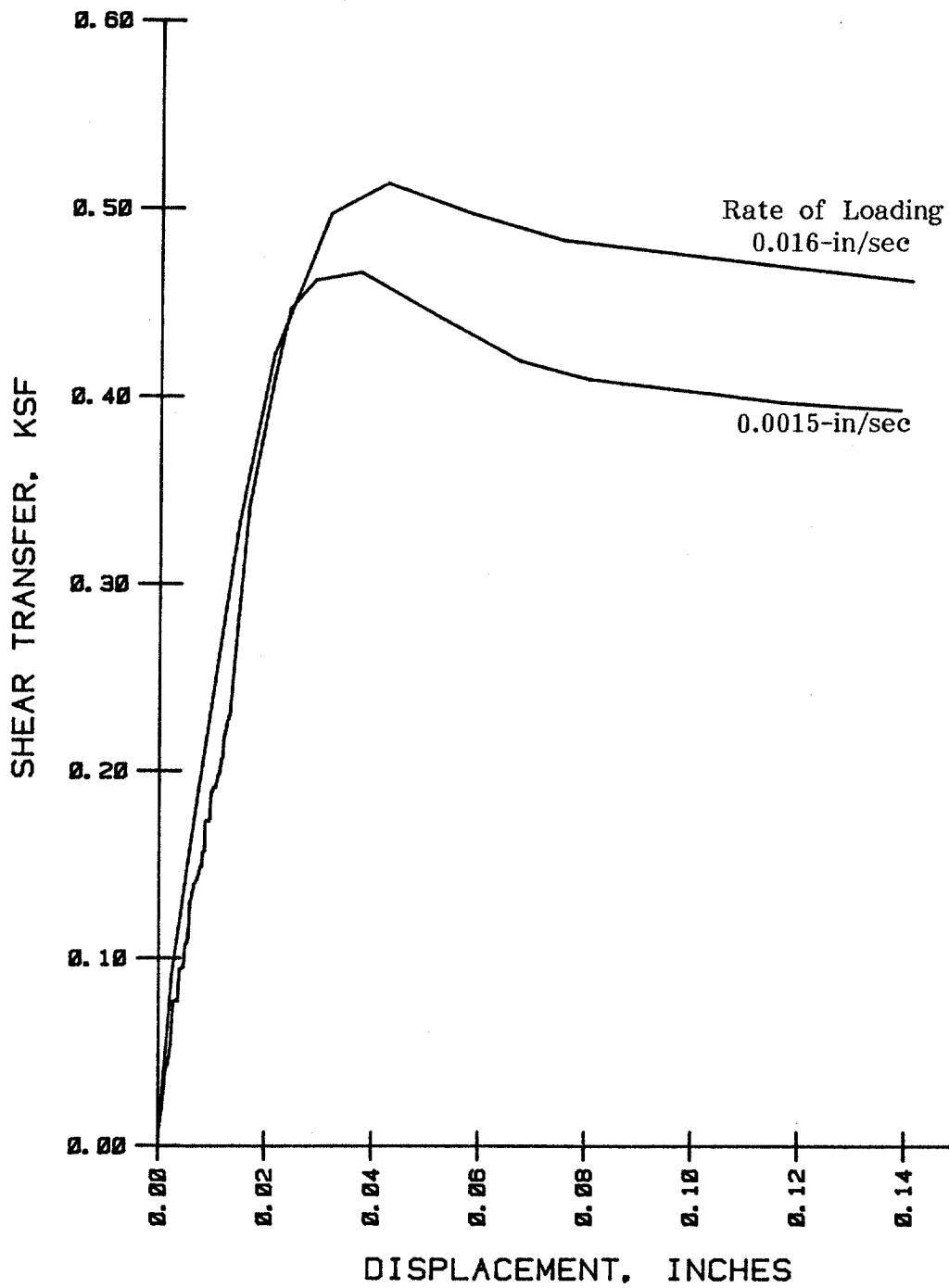
FIG. 11

3.00-INCH X CLOSED END



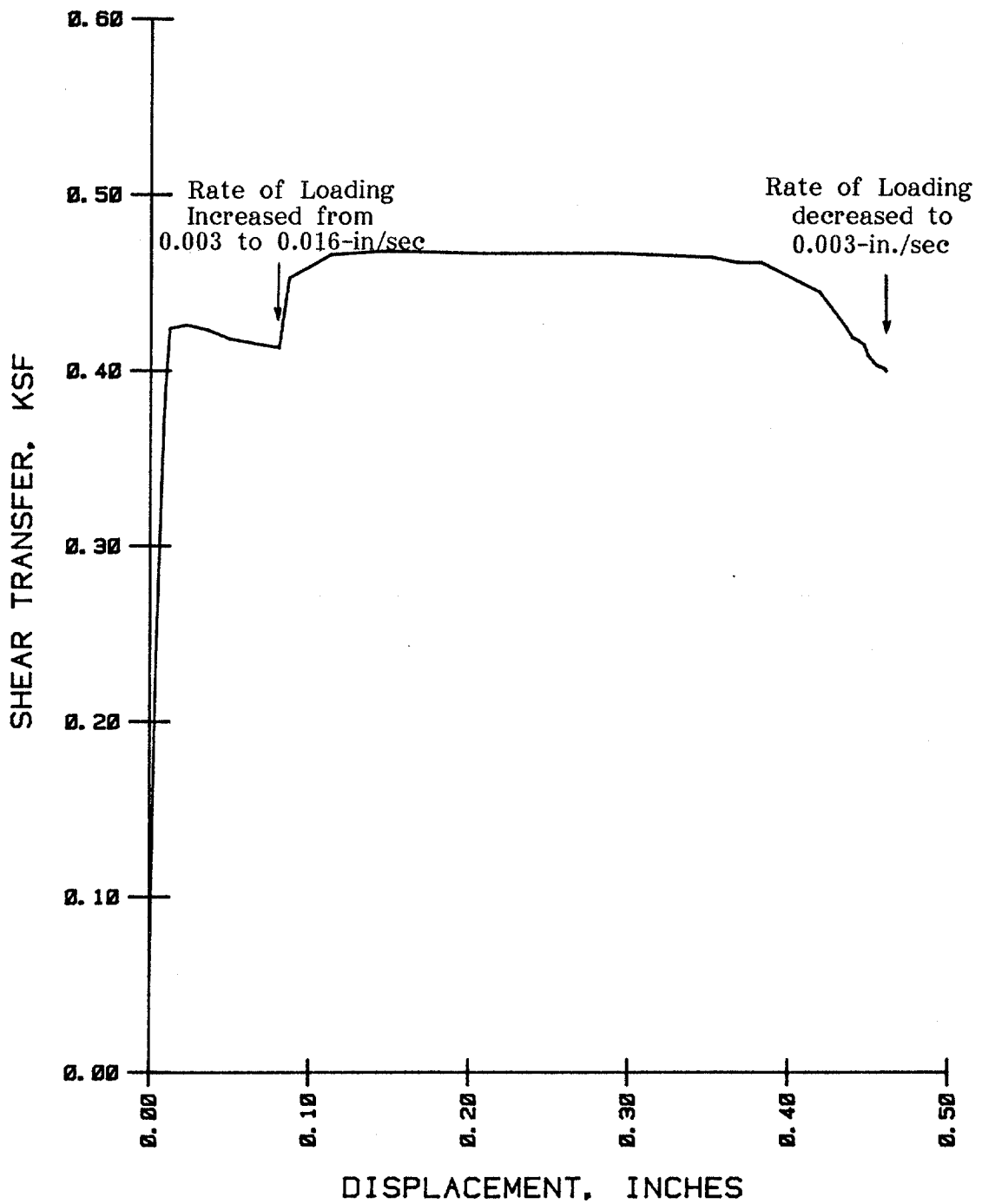
EFFECTS OF TWO-WAY CYCLIC LOADING ON STATIC CAPACITY

3.00-INCH X CLOSED END

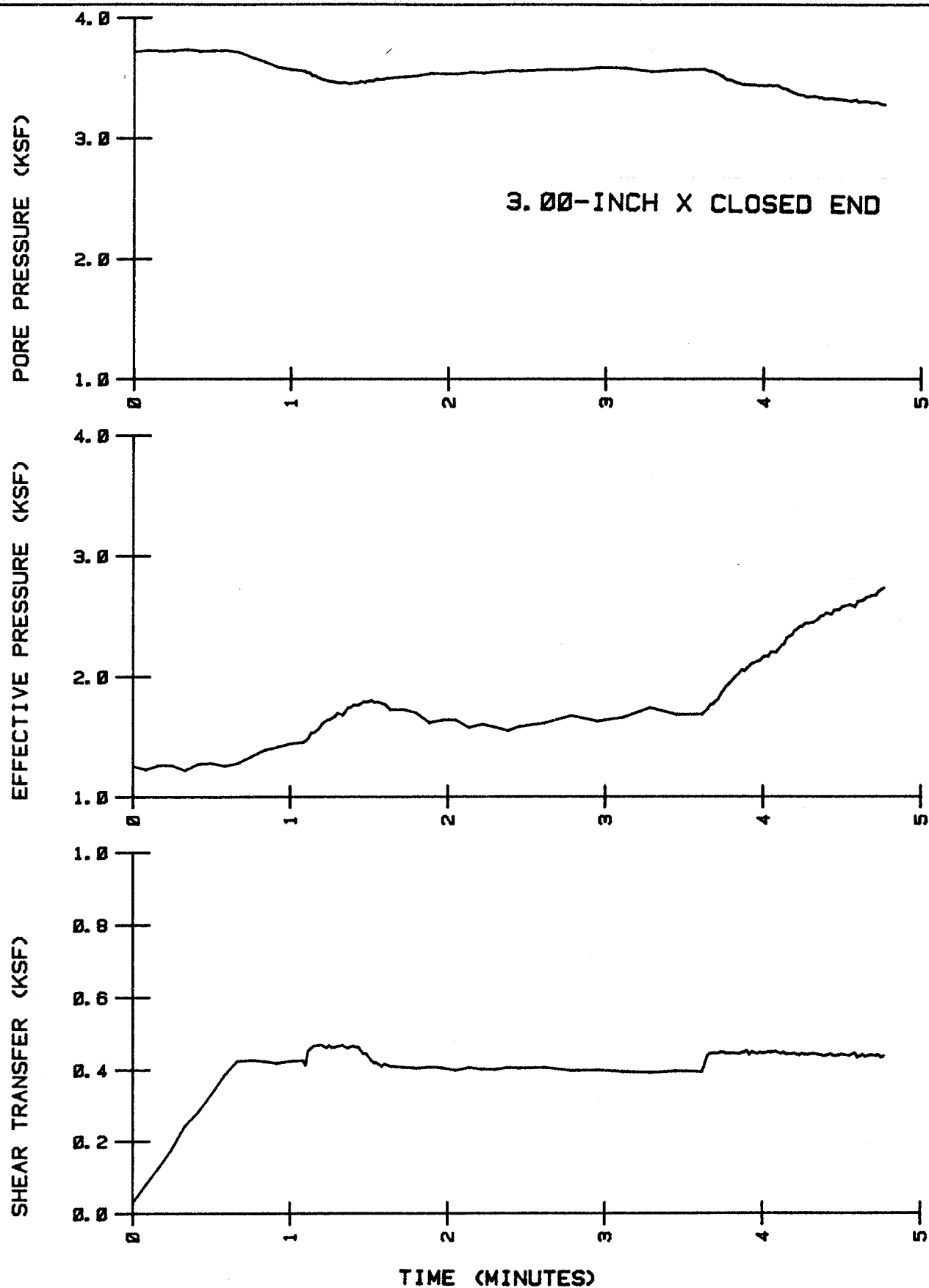


EFFECTS OF RATE OF LOADING ON SHEAR TRANSFER

3.00-INCH X CLOSED END



EFFECTS OF RATE OF LOADING ON RESIDUAL CAPACITY



VARIATION IN SHEAR TRANSFER AND PRESSURE DURING
RATE EFFECT STUDY (SEE FIG. 14)

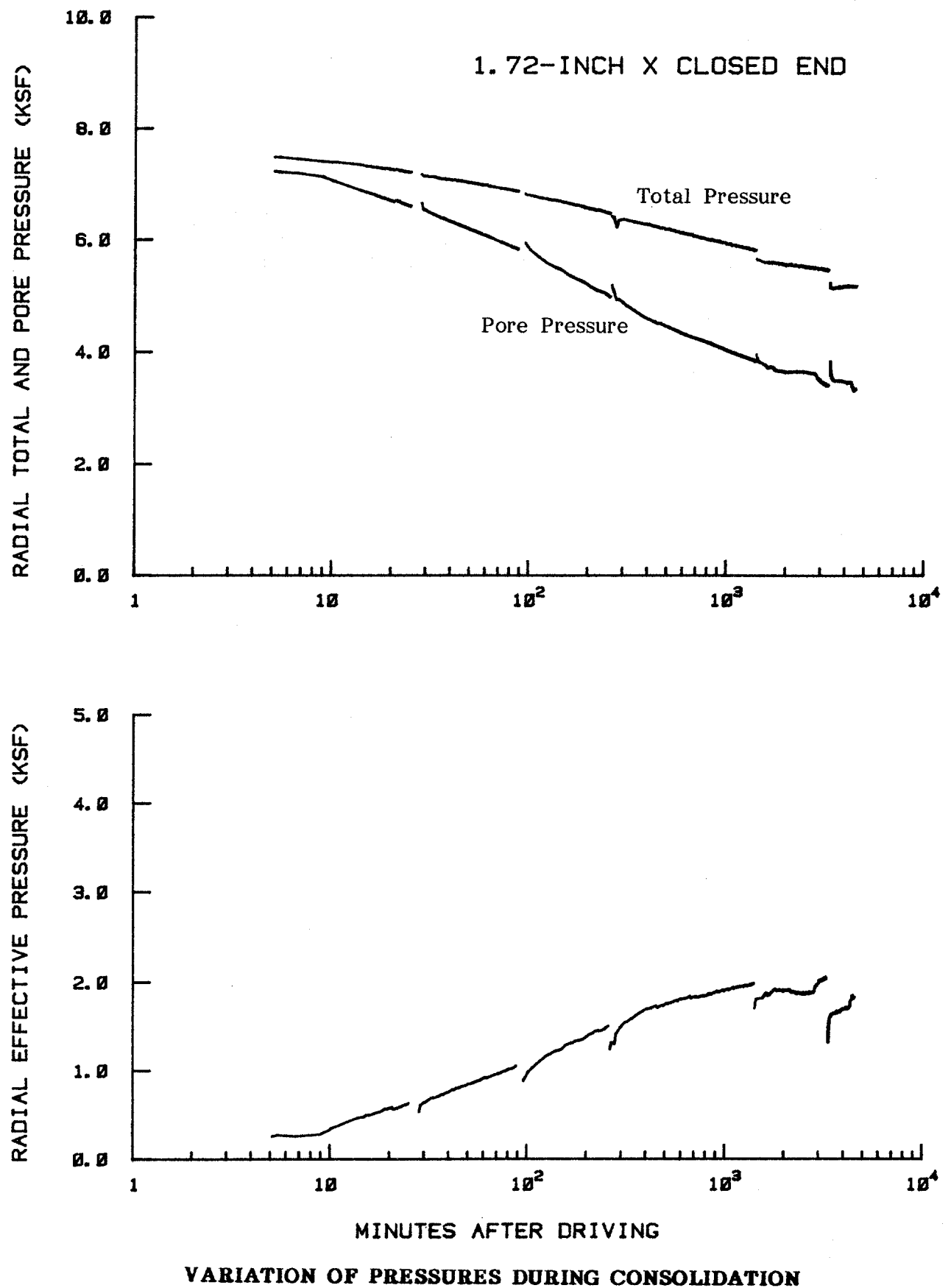
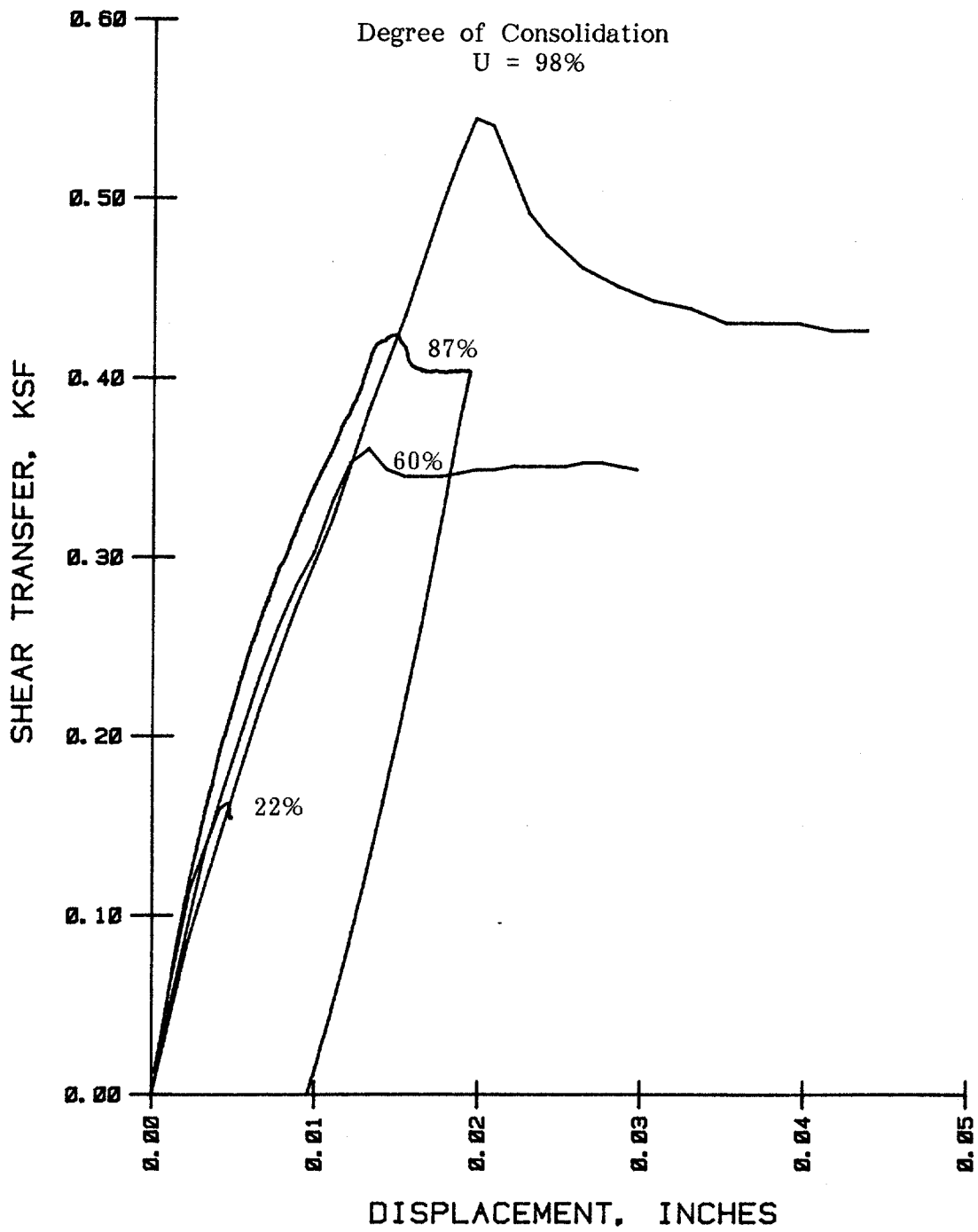


FIG. 16

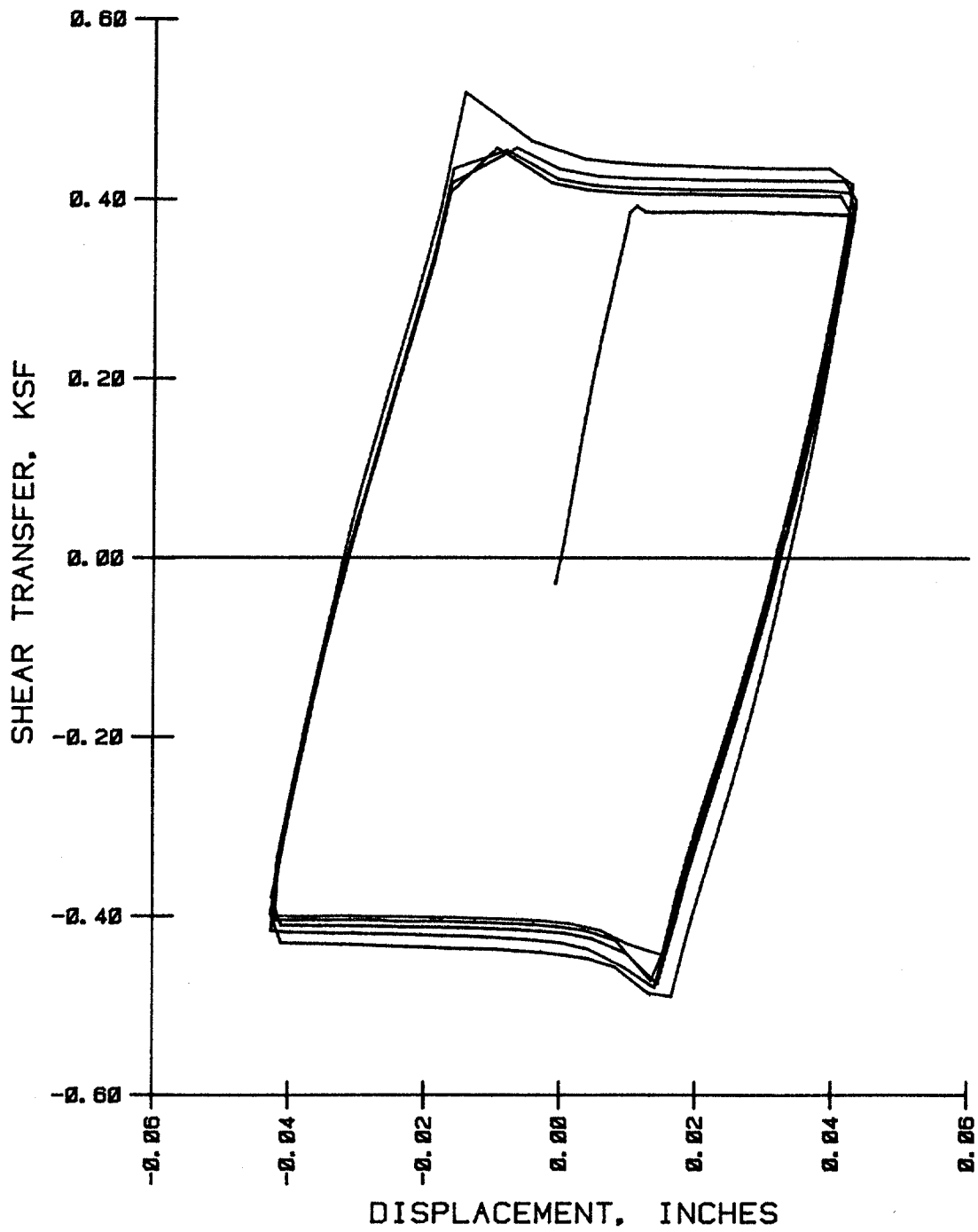
1.72-INCH X CLOSED END



RESULT OF STATIC TENSION TESTS

FIG. 17

1.72-INCH X CLOSED END



TWO-WAY CYCLIC LOAD TESTS

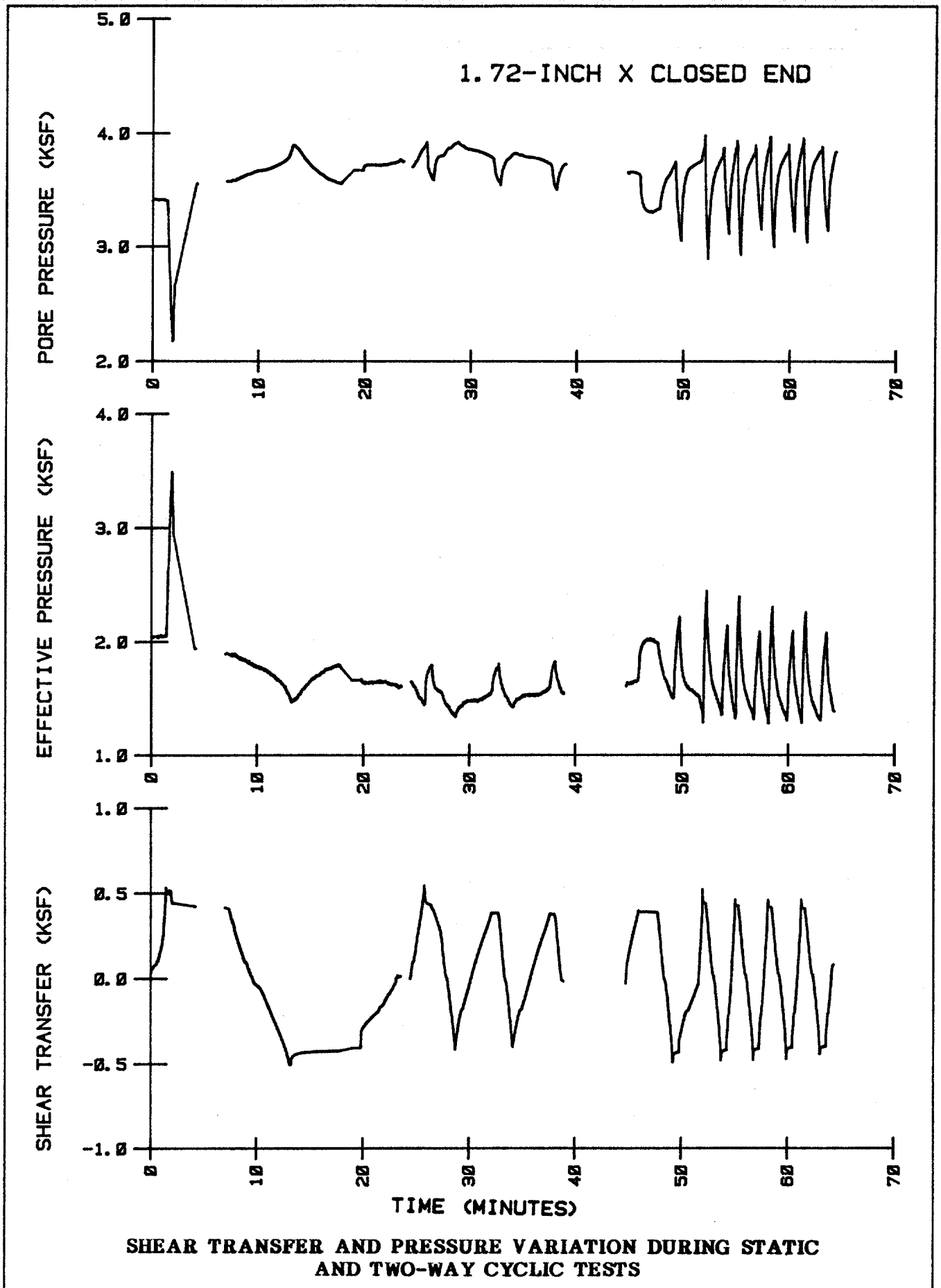
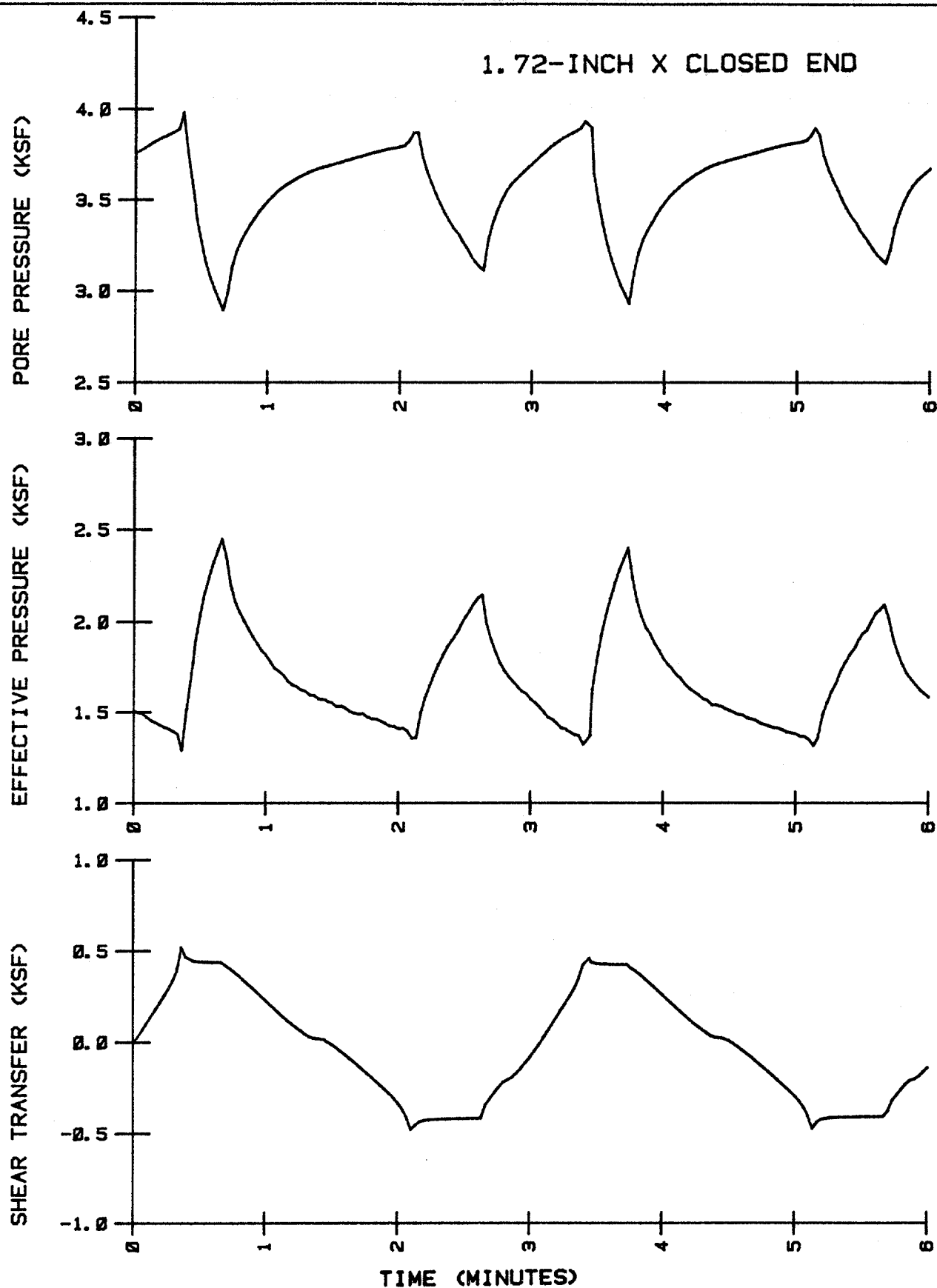
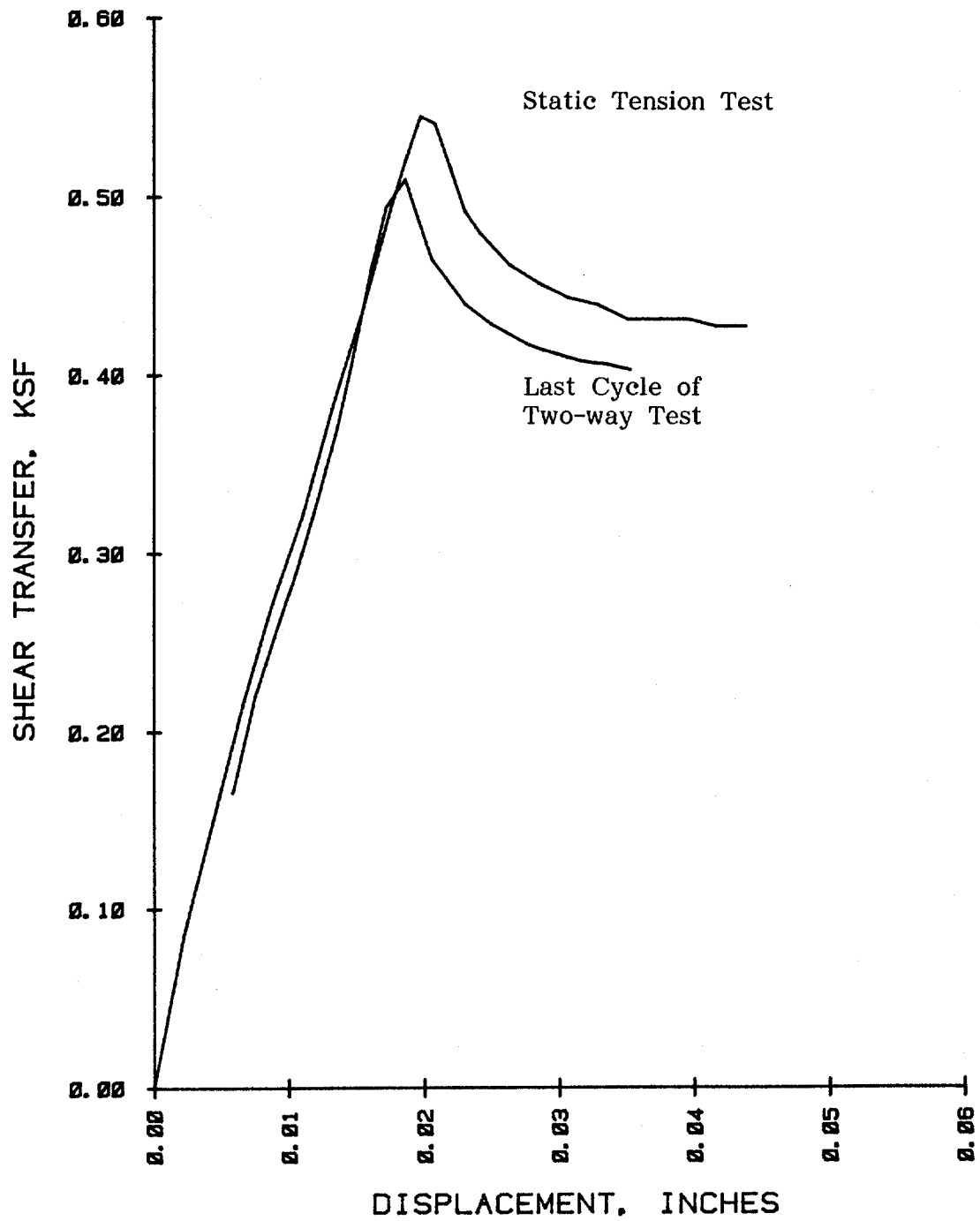


FIG. 19



EXPANDED VIEW OF FIRST TWO CYCLES OF TWO-WAY LOADING FROM FIG. 19

1.72-INCH X CLOSED END



EFFECTS OF TWO-WAY CYCLIC LOADING ON STATIC CAPACITY

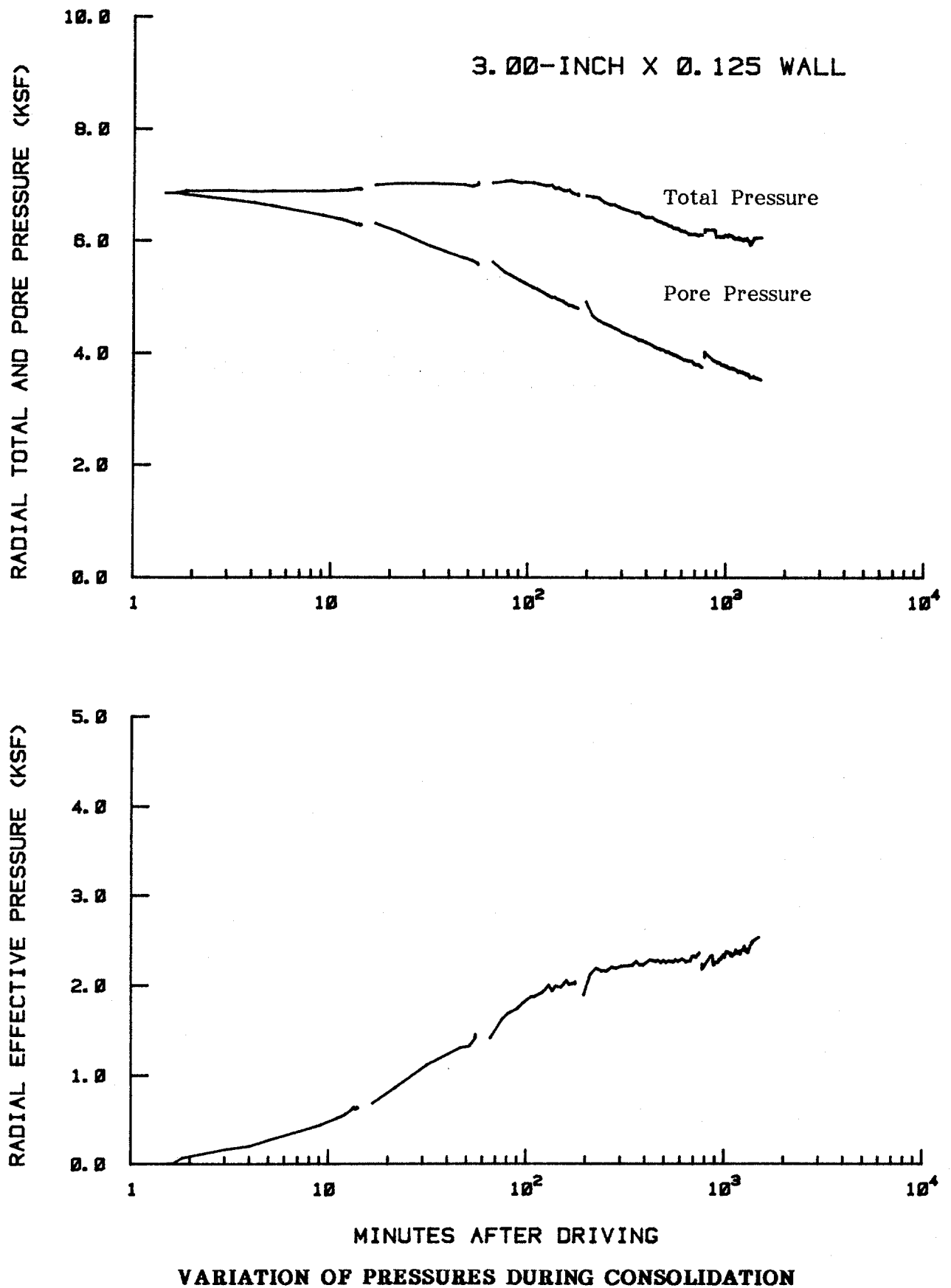
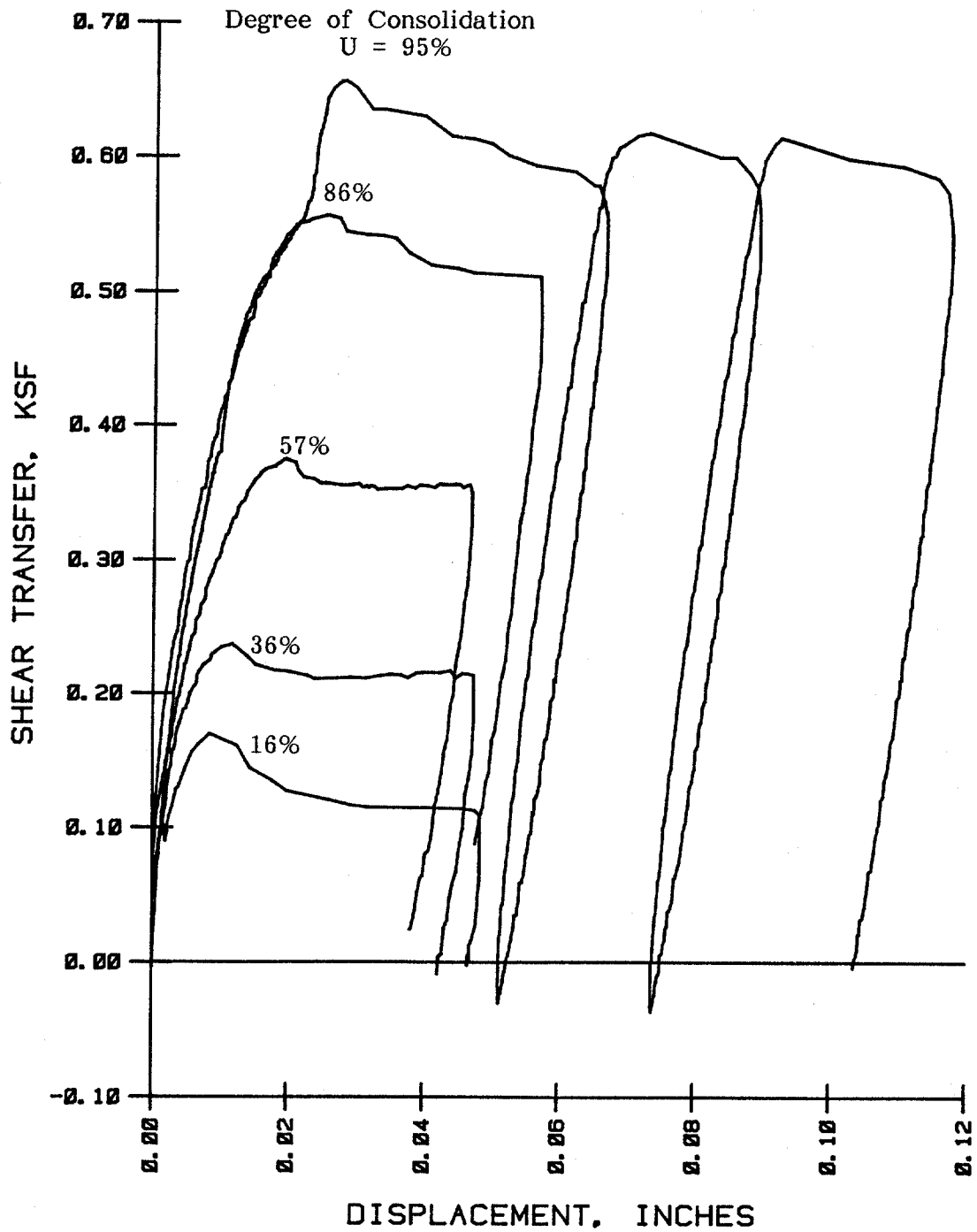


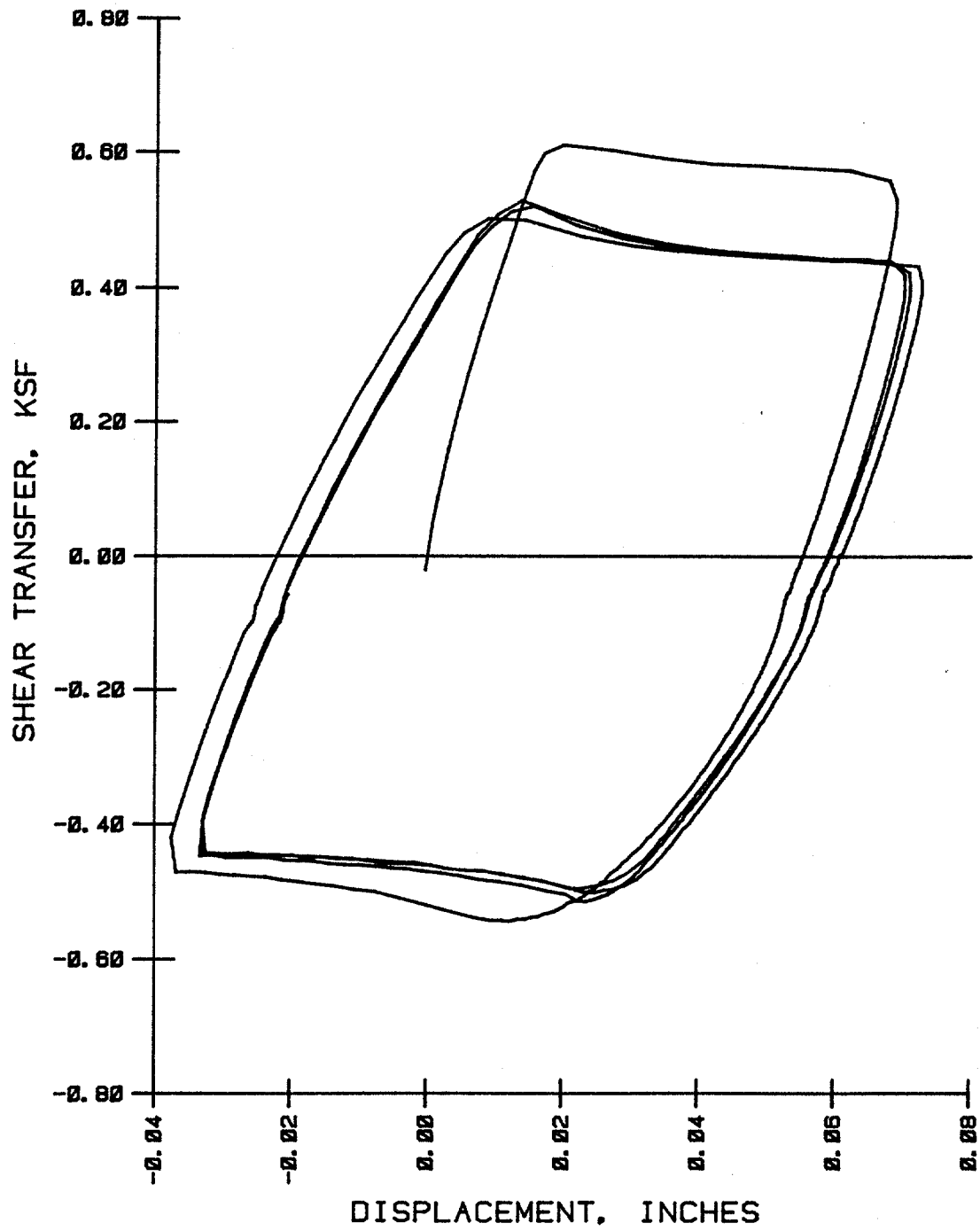
FIG. 22

3.00-INCH X 0.125 WALL



RESULT OF STATIC TENSION TESTS

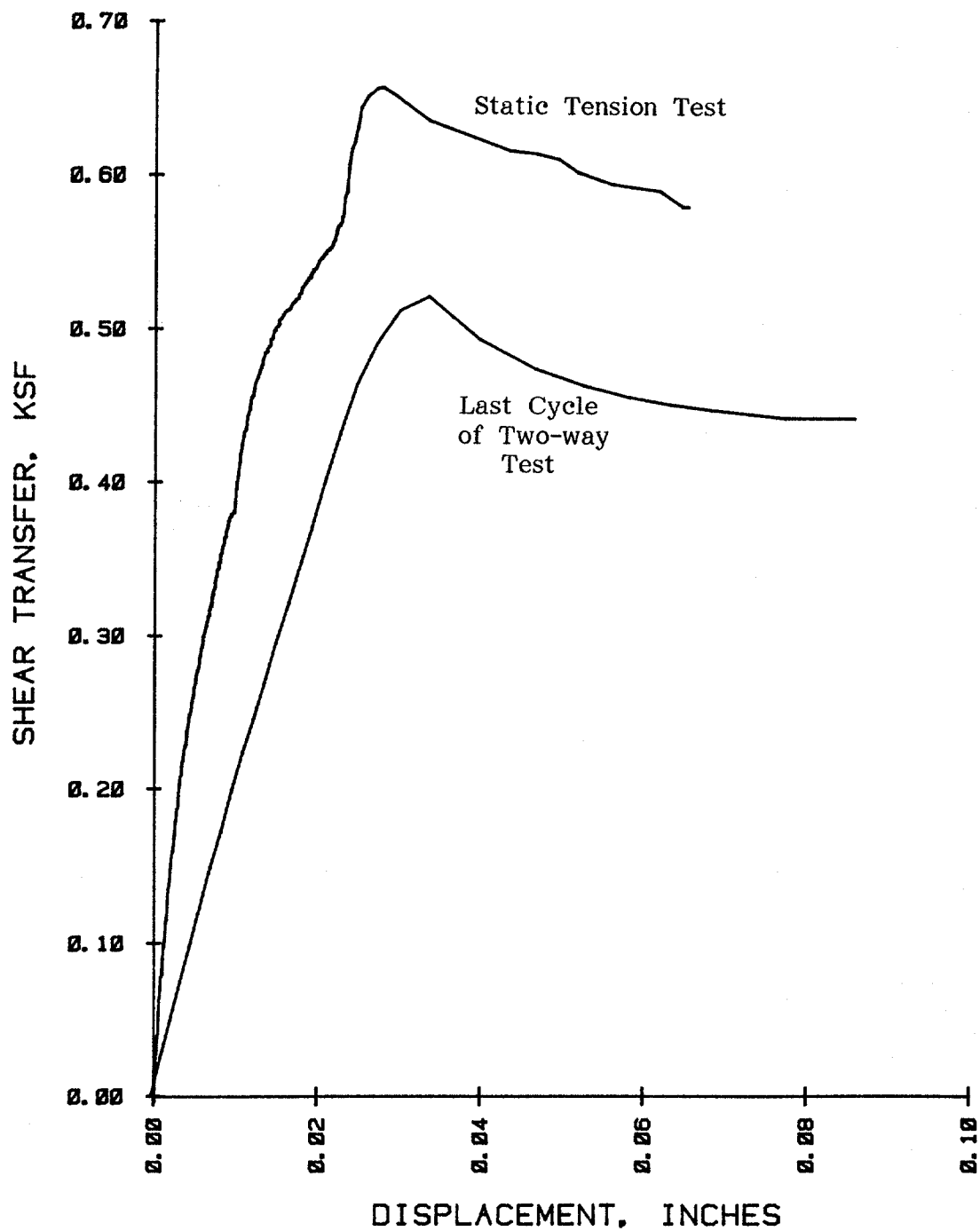
3.00-INCH X 0.125 WALL



TWO-WAY CYCLIC LOAD TESTS

FIG. 24

3.00-INCH X 0.125 WALL



EFFECTS OF TWO-WAY CYCLIC LOADING ON STATIC CAPACITY

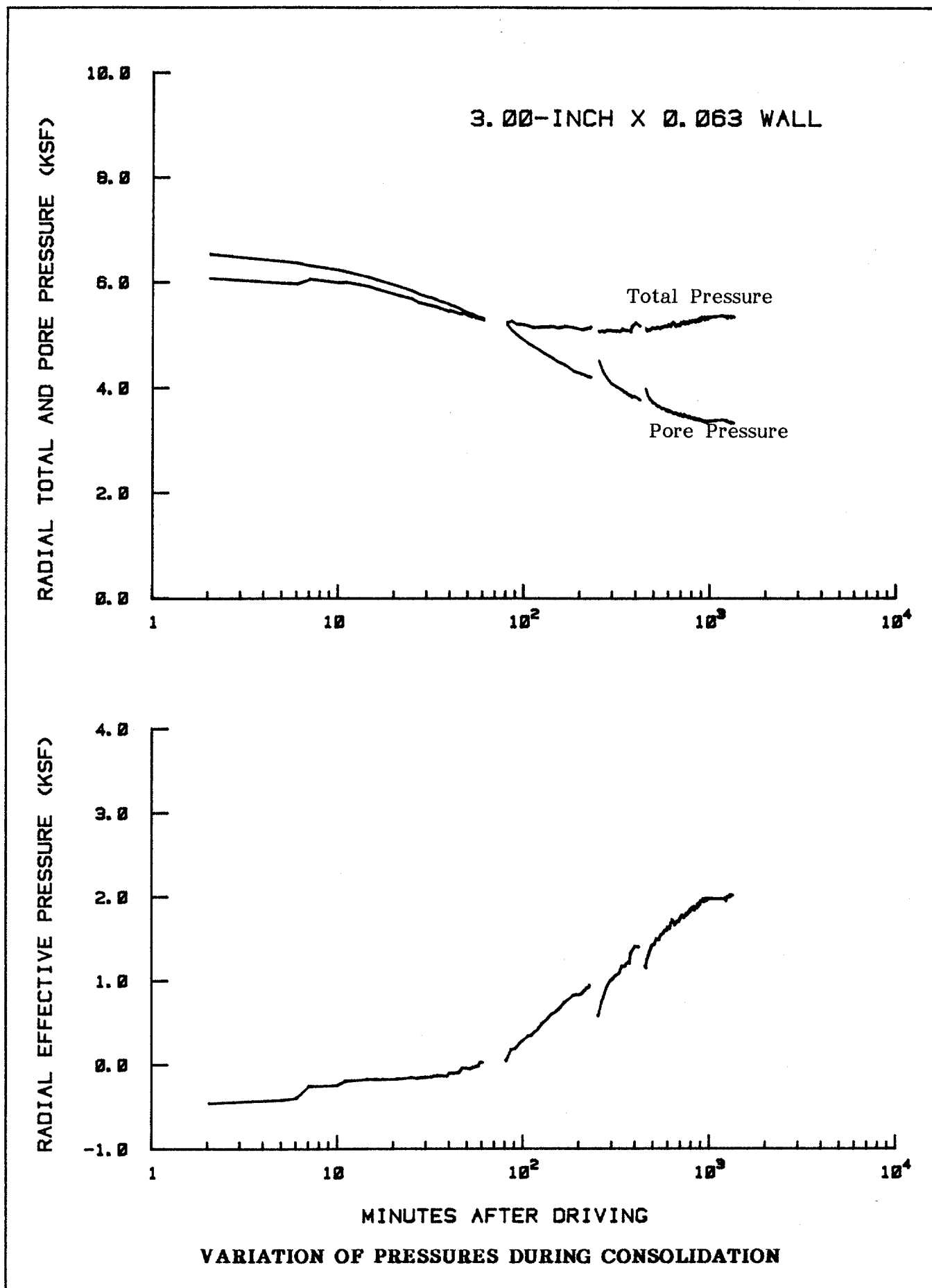
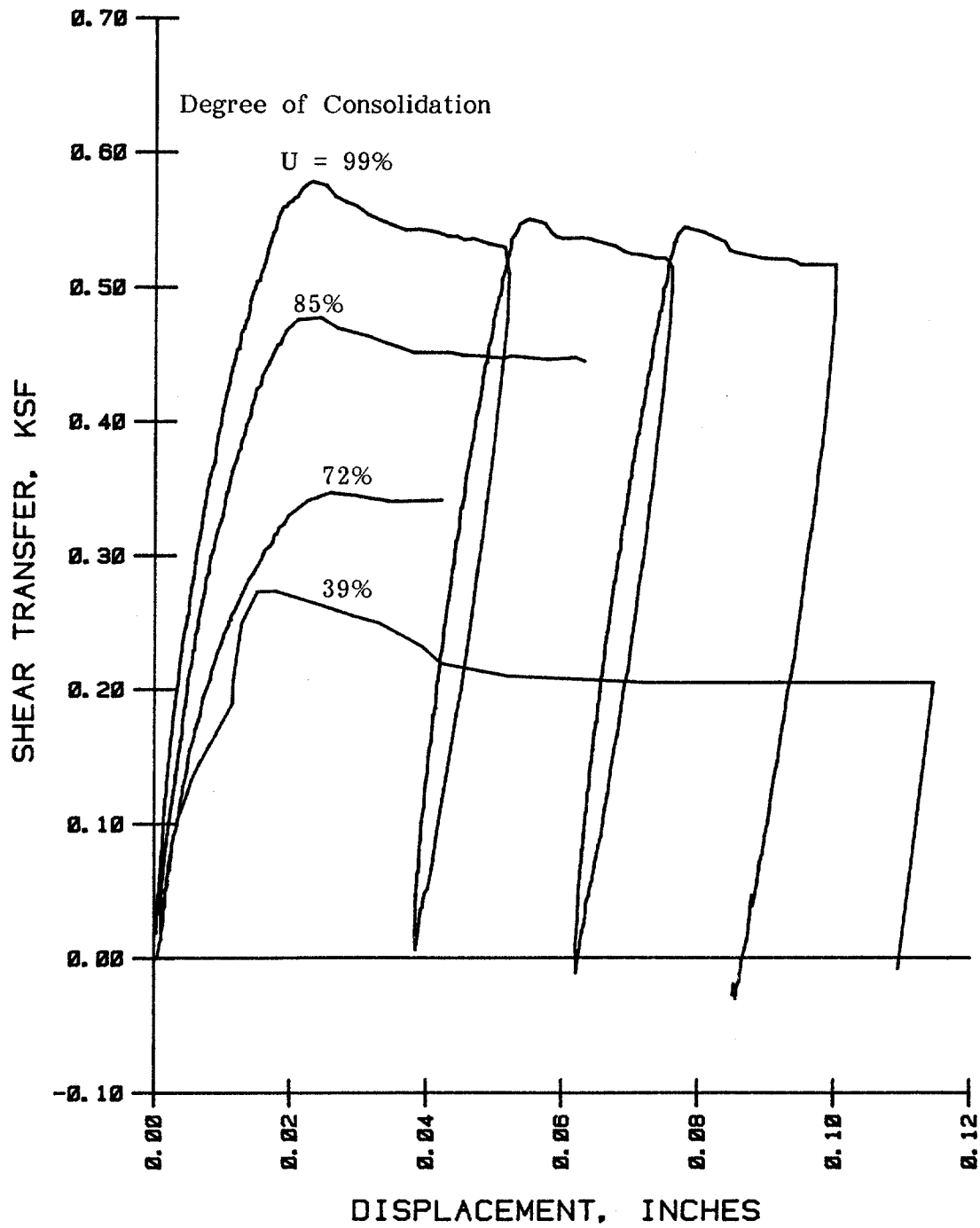


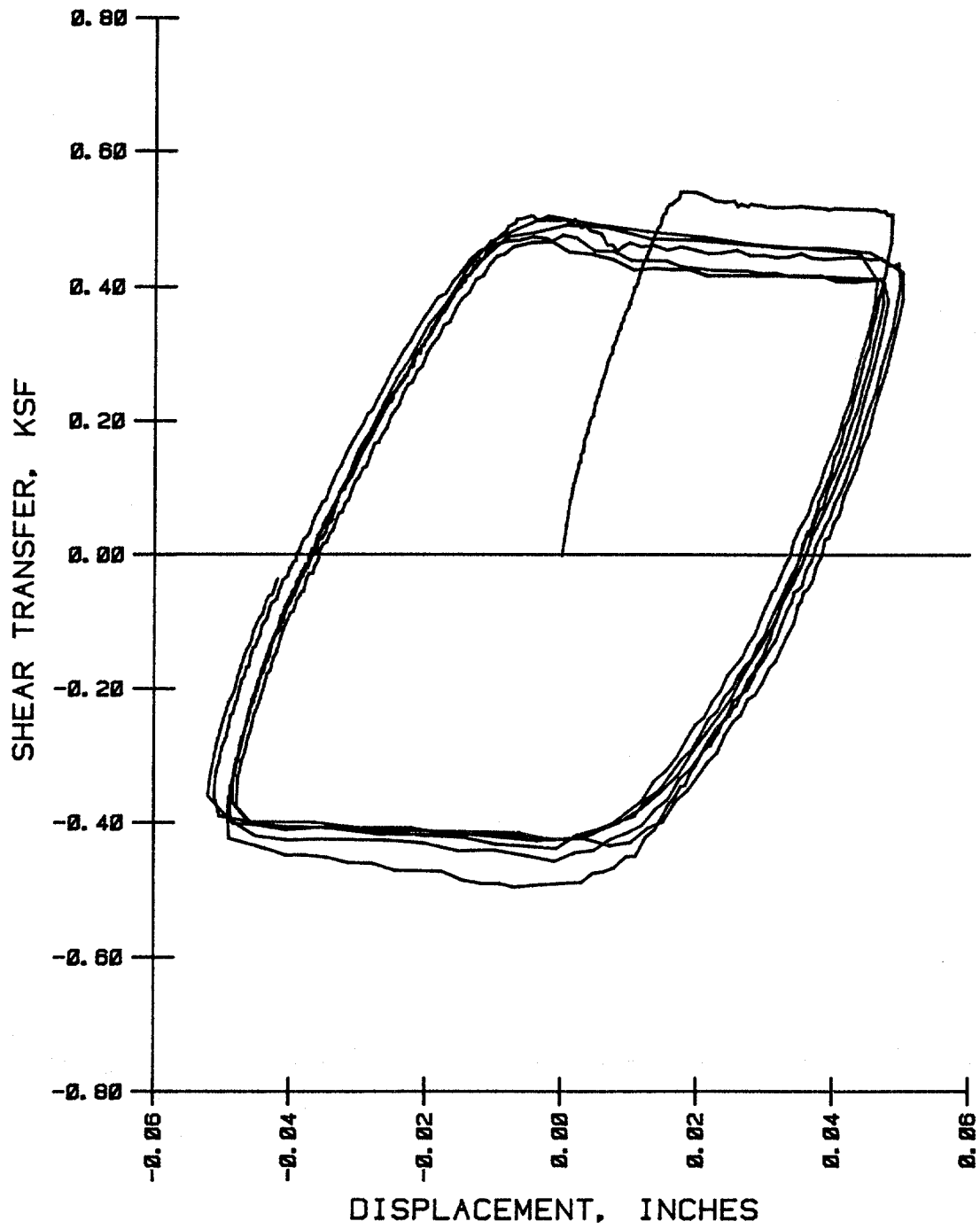
FIG. 26

3.00-INCH X 0.063 WALL

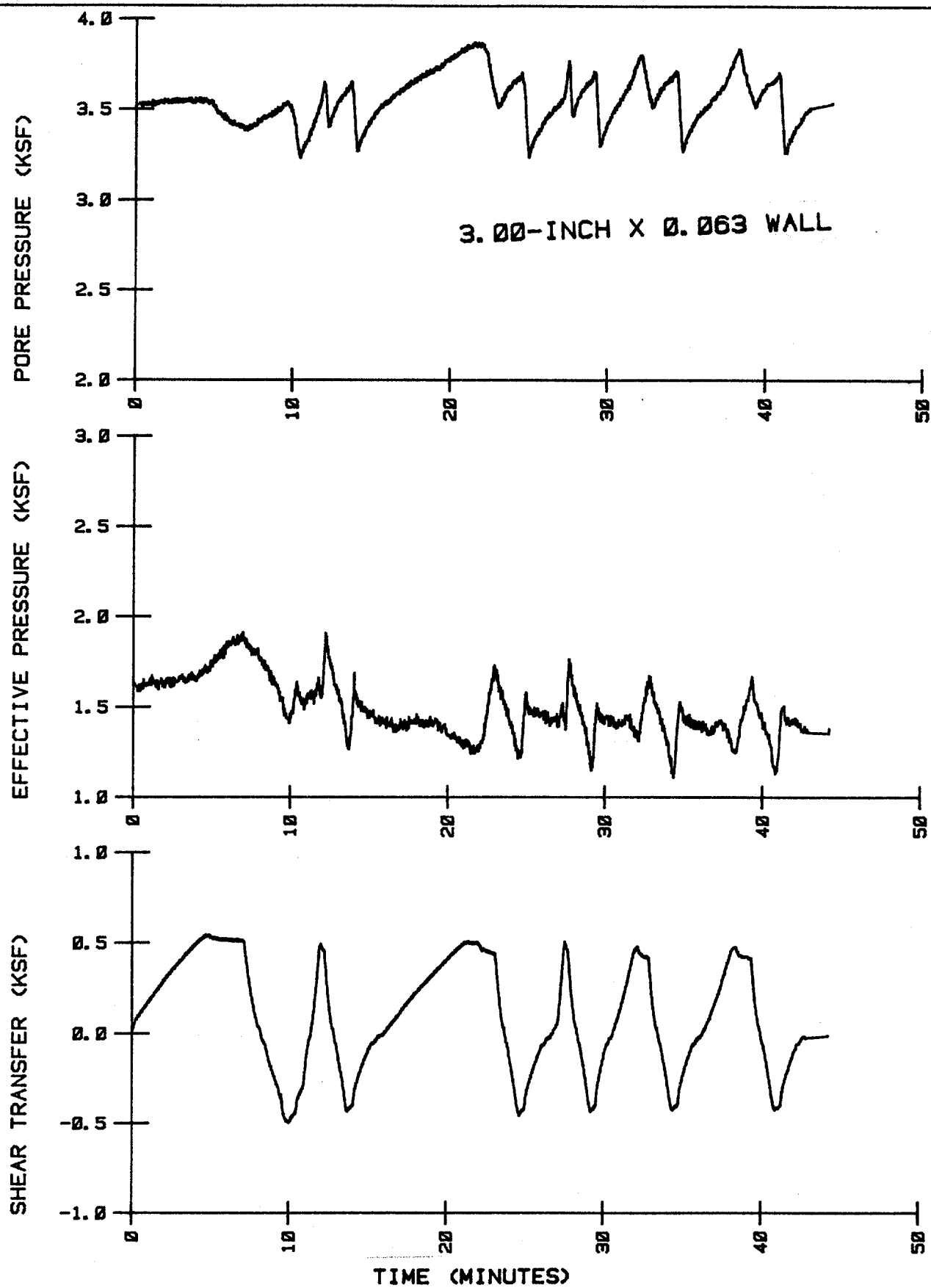


RESULT OF STATIC TENSION TESTS

3.00-INCH X 0.063 WALL

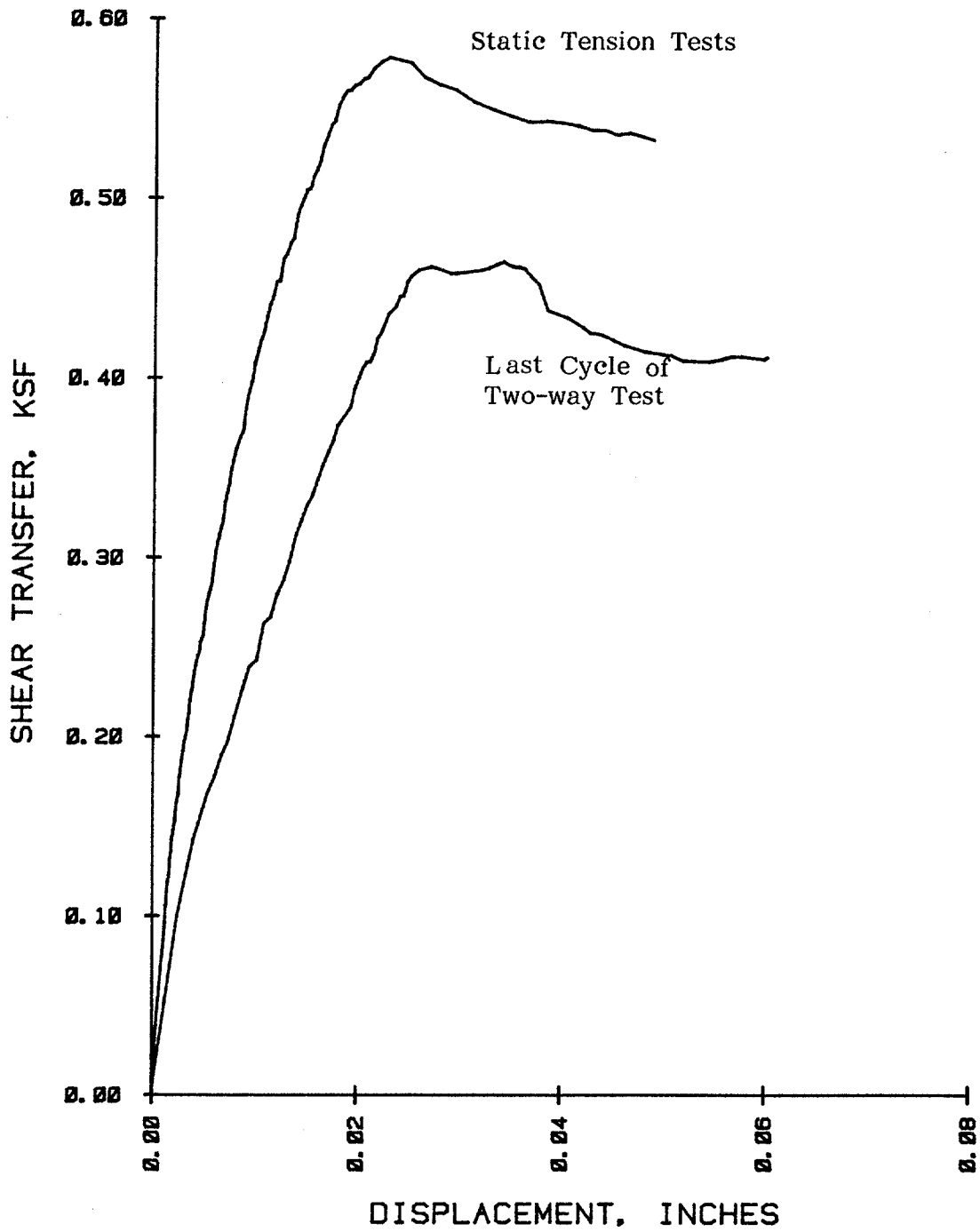


TWO-WAY CYCLIC LOAD TESTS



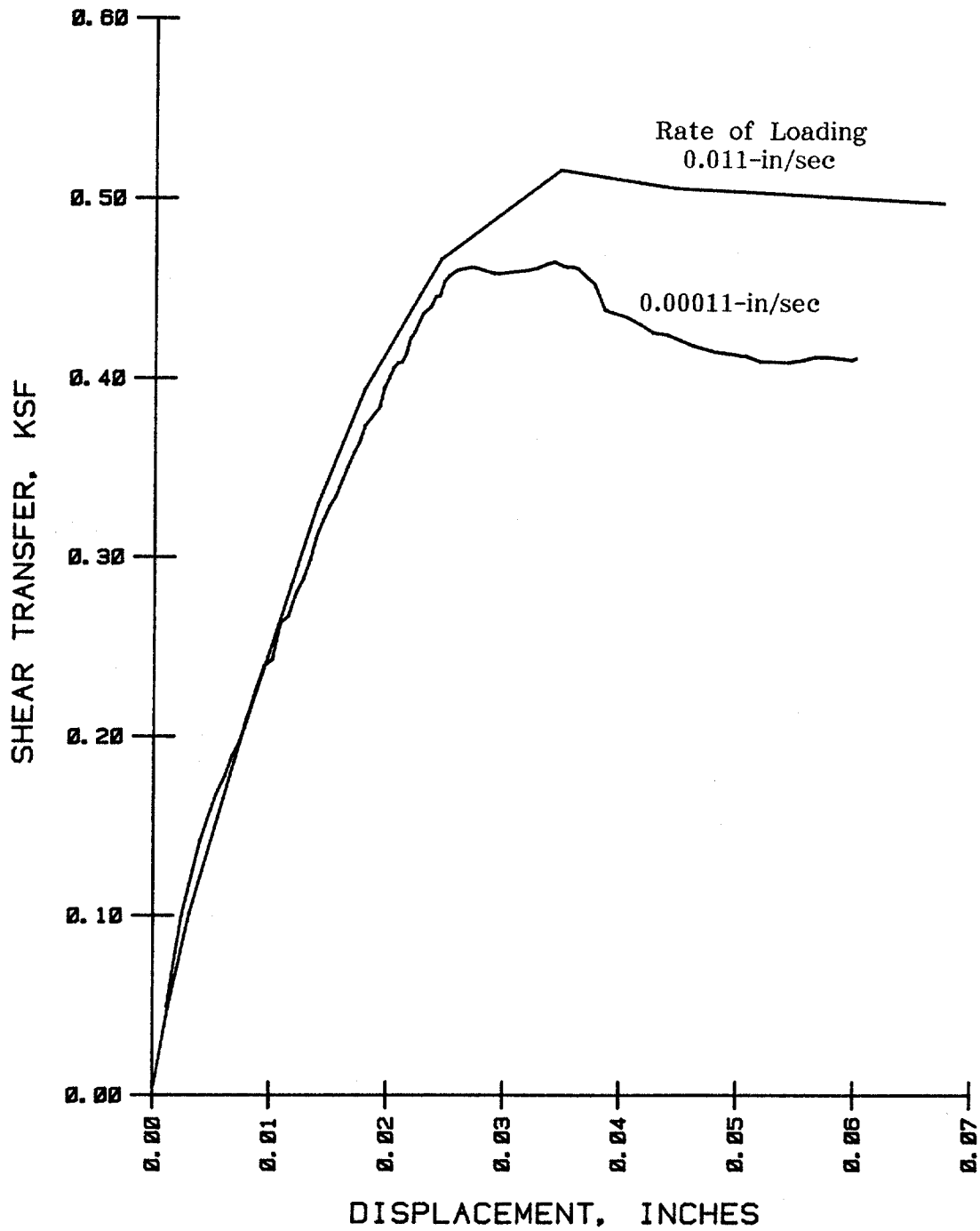
SHEAR TRANSFER AND PRESSURE VARIATION DURING STATIC AND TWO-WAY CYCLIC TESTS

3.00-INCH X 0.063 WALL



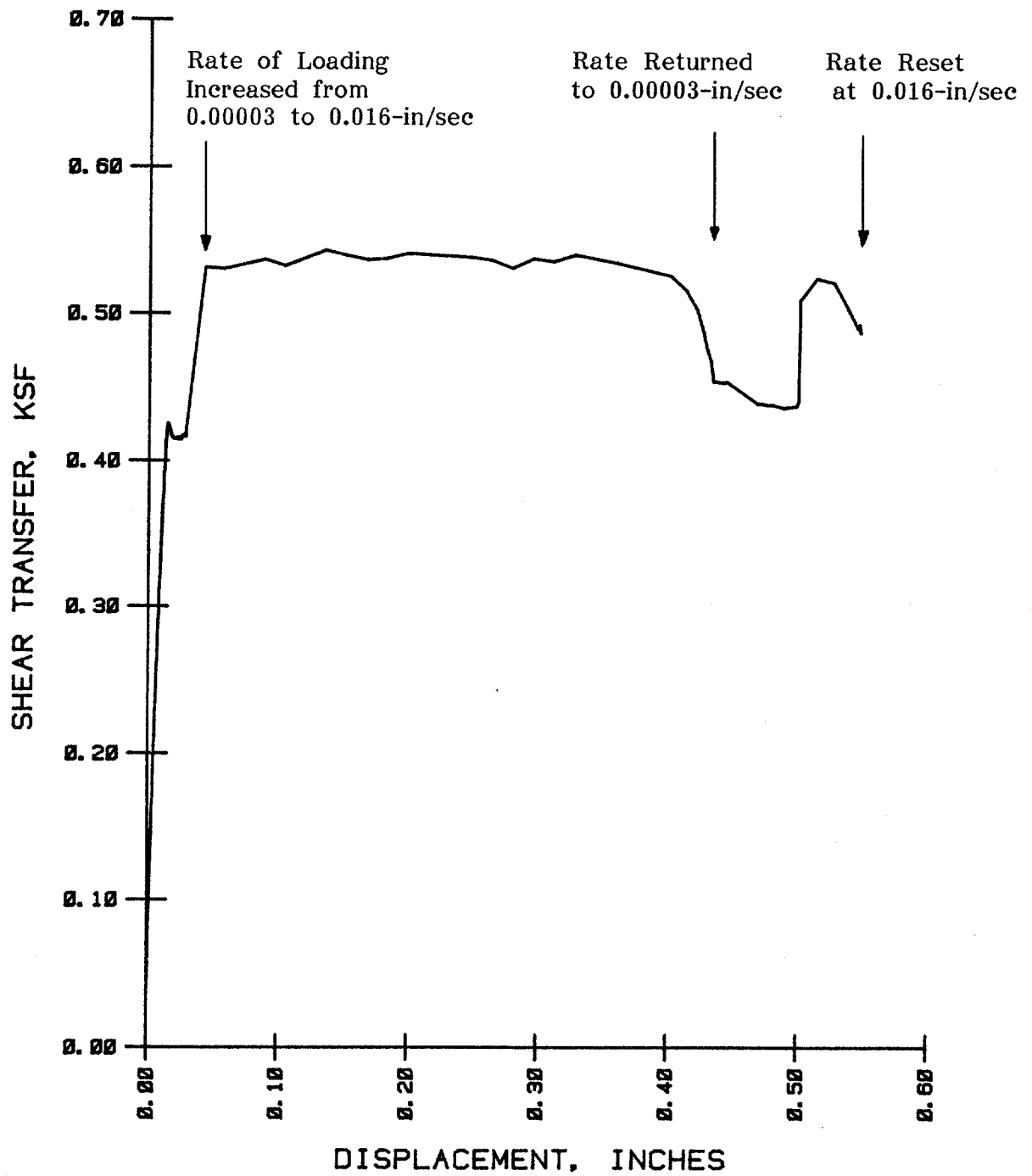
EFFECTS OF TWO-WAY CYCLIC LOADING ON STATIC CAPACITY

3.00-INCH X 0.063 WALL



EFFECTS OF RATE OF LOADING ON SHEAR TRANSFER

3.00-INCH X 0.063 WALL



EFFECTS OF RATE OF LOADING ON SHEAR TRANSFER

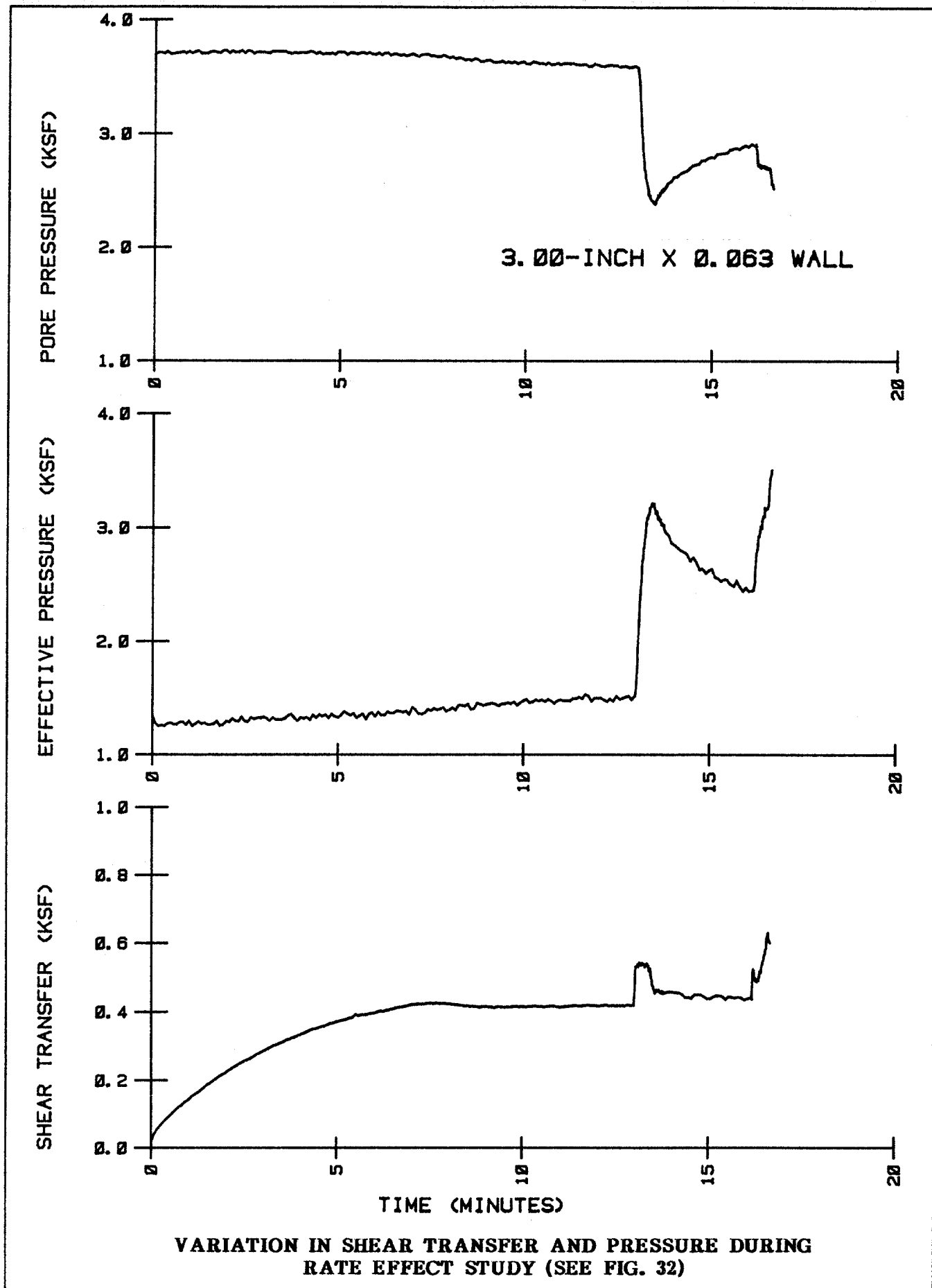
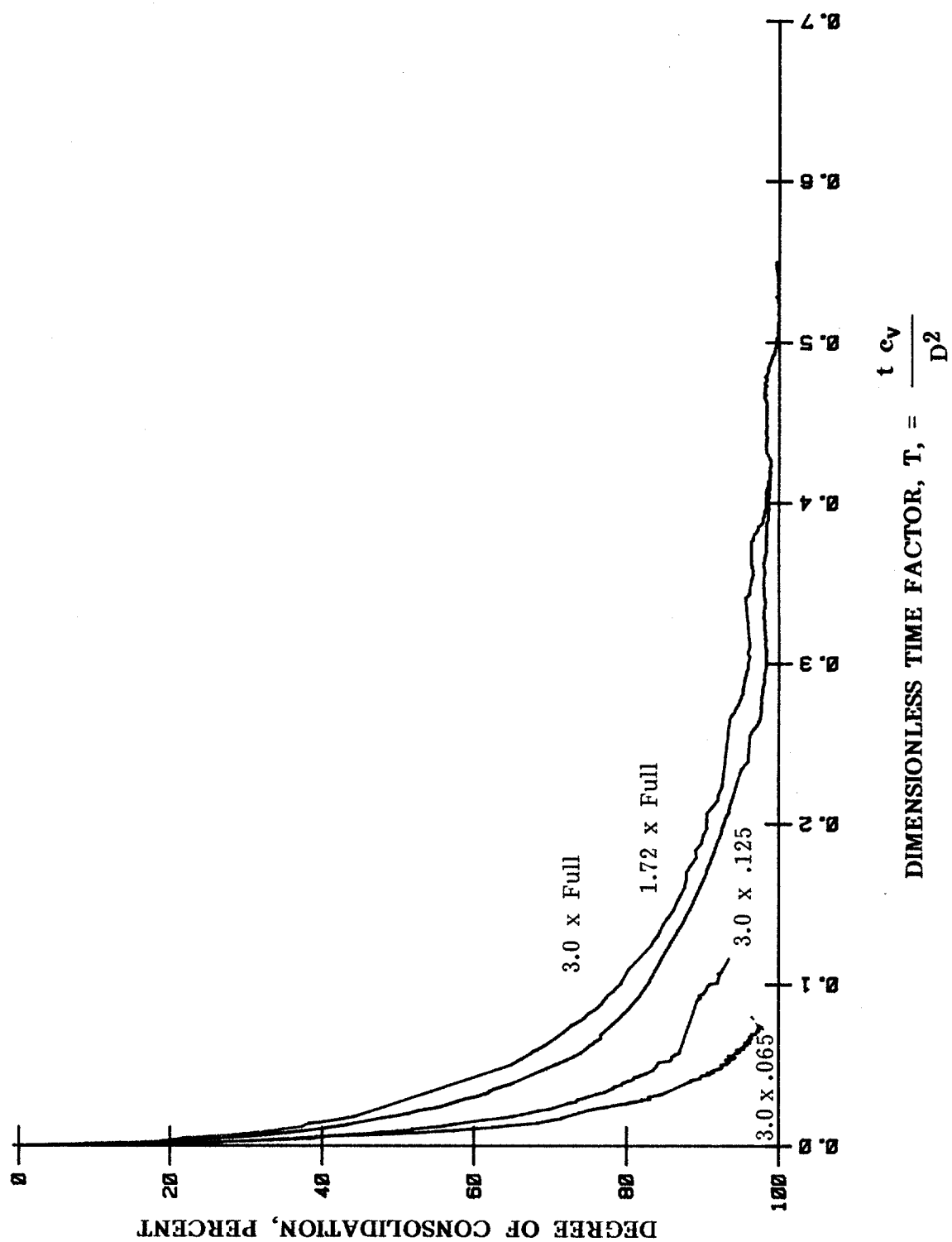
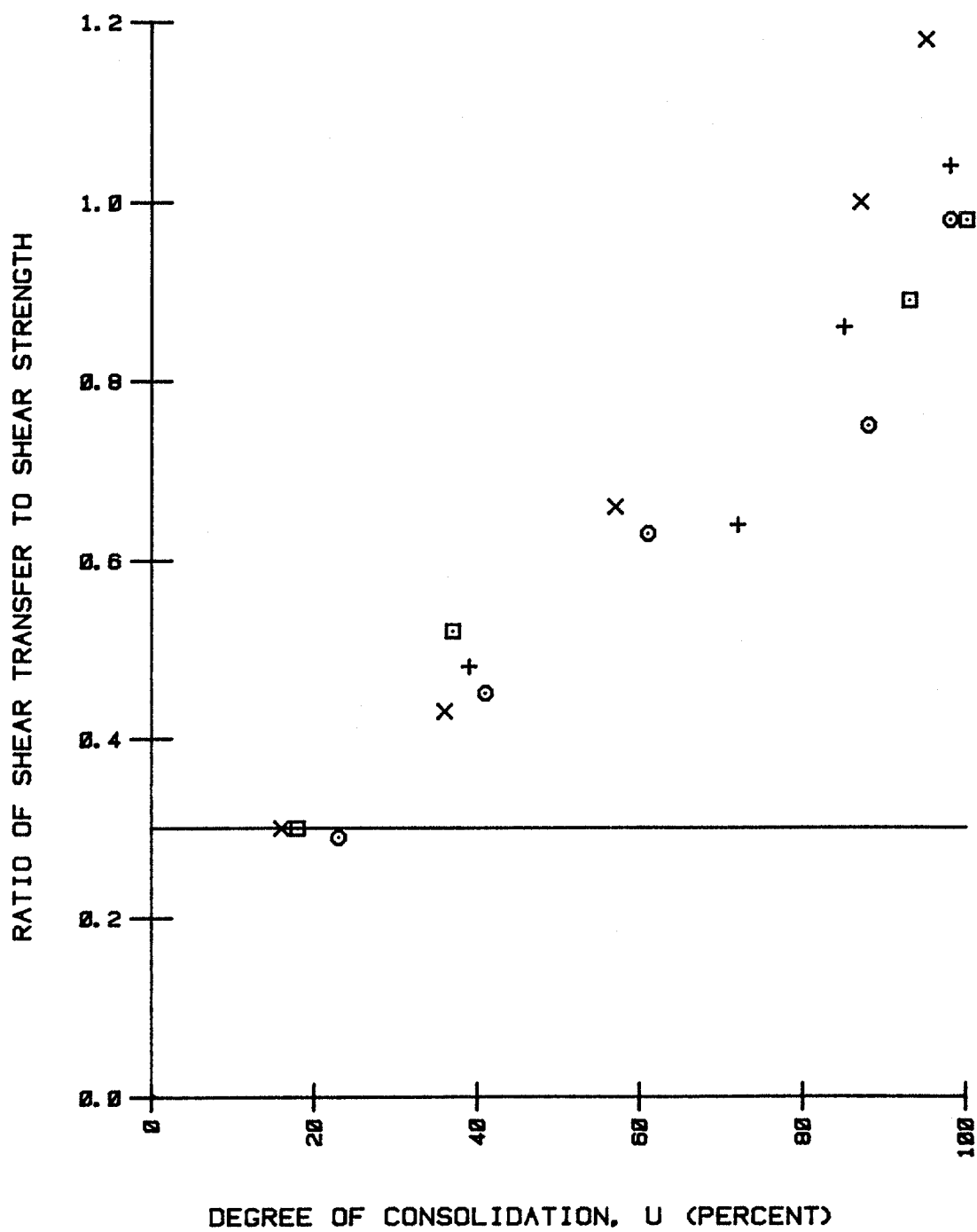


FIG. 33



NONDIMENSIONALIZED CONSOLIDATION CURVES



INCREASE IN STATIC SHEAR TRANSFER DURING CONSOLIDATION

FIG. 35

APPENDIX A
SOIL TEST DATA

		CLASSIFICATION TESTS					STRENGTH ESTIMATE		MINIATURE VANE			COMPRESSION TESTS									
SAMPLE NUMBER	DEPTH ft											TYPE TEST	LATERAL PRESSURE		SHEAR STRENGTH,ksf		ESD STRAIN,%	SUM FAILURE	FAILURE	TYPE FAILURE	
		LI	LL	PL	WM	pcf	%	PEN	TV	UD	REM		RES	WM	ksf	UD					REM
1	49.5																				
2	50.0																				
3	51.0																				
4	51.5	0.70	101	28	79							W	80	8.00	0.60	0.32	0.4	34	2	AC	
4	51.5				76				0.78		0.31										
5	52.0																				
6	53.5	0.67	98	28	71							W	66	8.00	0.53	0.36	0.6	35	4	AC	
6	53.5				71			0.70	0.68		0.28										
7	55.0	0.60	100	28	71							W	68	8.00	0.40		0.4	35	4	AC	
7	55.0				70			0.80	0.78		0.44										
8	55.5																				
9	56.0																				

Legend and Notes

LI = Liquidity Index
 LL = Liquid Limit
 PL = Plastic Limit
 % = Water Content %
 SUM = Submerged Unit Weight
 -200 = % Passing No. 200 Sieve

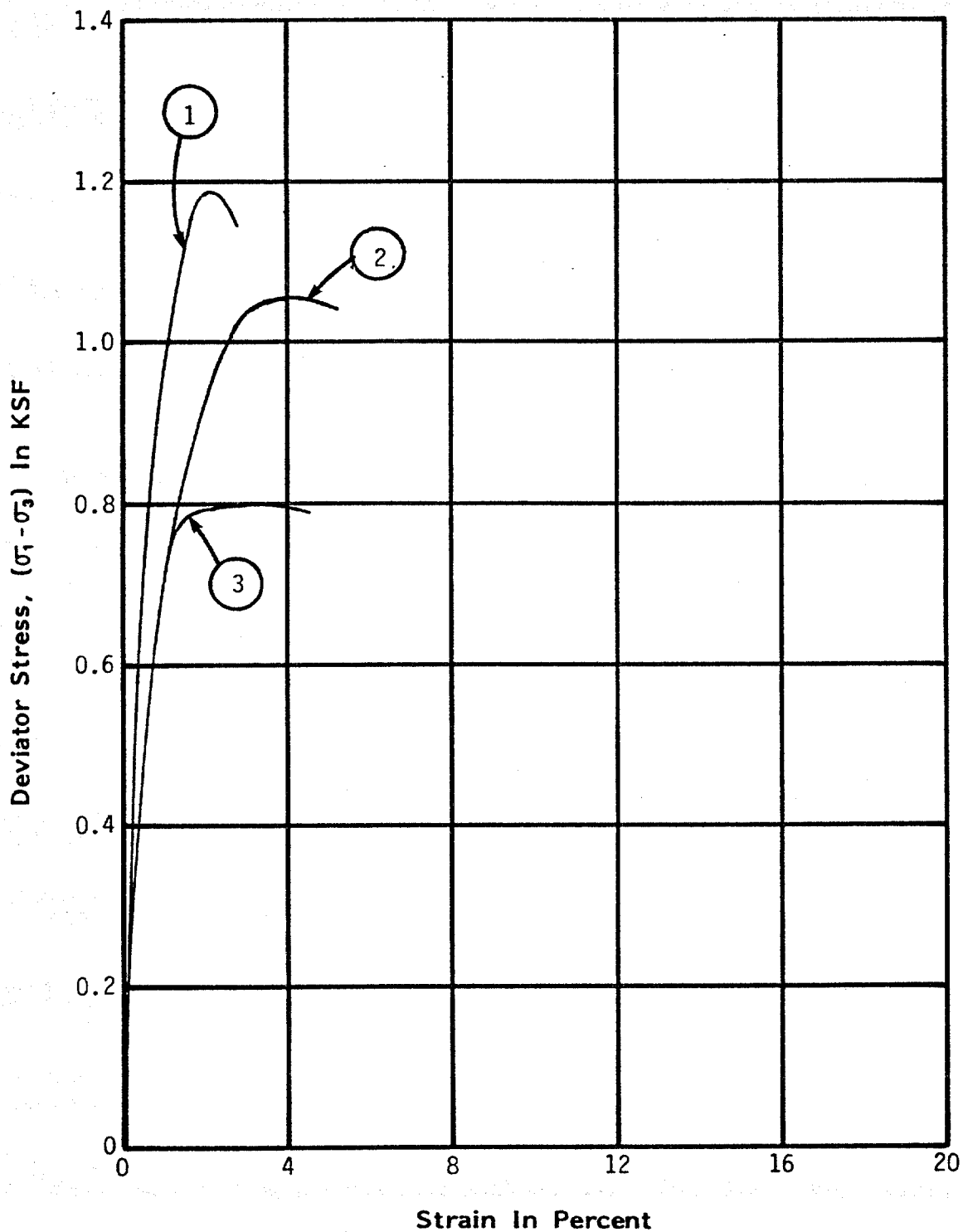
PEN = Pocket Penetrometer
 TV = Torvane
 UD = Undisturbed Test
 REM = Remolded Test
 RES = Residual Test
 ESD = Strain at One Half the Maximum Stress

TEST TYPE:
 U = Unconfined Compression
 W = Unconsolidated-Undrained Triaxial
 CU = Consolidated-Undrained Triaxial

TYPE FAILURE:
 A = Bulge
 B = Single Shear Plane
 C = Multiple Shear Plane
 D = Vertical Fracture

SUMMARY OF TEST RESULTS

BORING B-10
 NSF/UNIVERSITY OF ARIZONA PROJECT
 SABINE, TEXAS



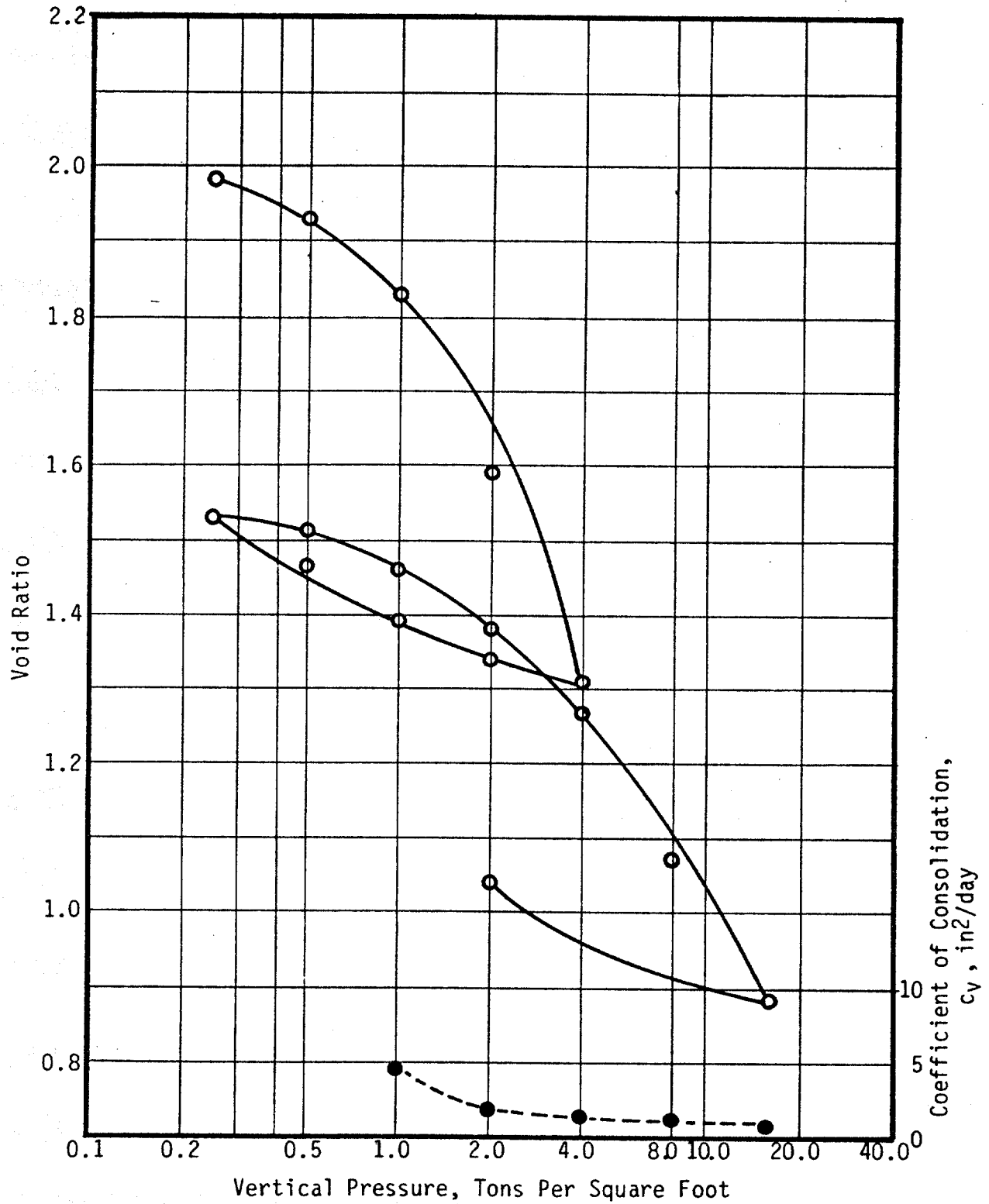
STRESS-STRAIN CURVES

UNCONSOLIDATED-UNDRAINED TRIAXIAL COMPRESSION TEST

<u>Curve No.</u>	<u>Boring No.</u>	<u>Penetration, ft</u>	<u>Confining Pressure, ksf</u>
1	B-10	51.5	8.00
2	B-10	53.5	8.00
3	B-10	55.0	8.00

SAMPLE: S-6 DEPTH: 53.5'
SOIL TYPE: Dark Gray Clay

MOISTURE CONTENT: 64%
LIQUID LIMIT: 93
PLASTIC LIMIT: 28

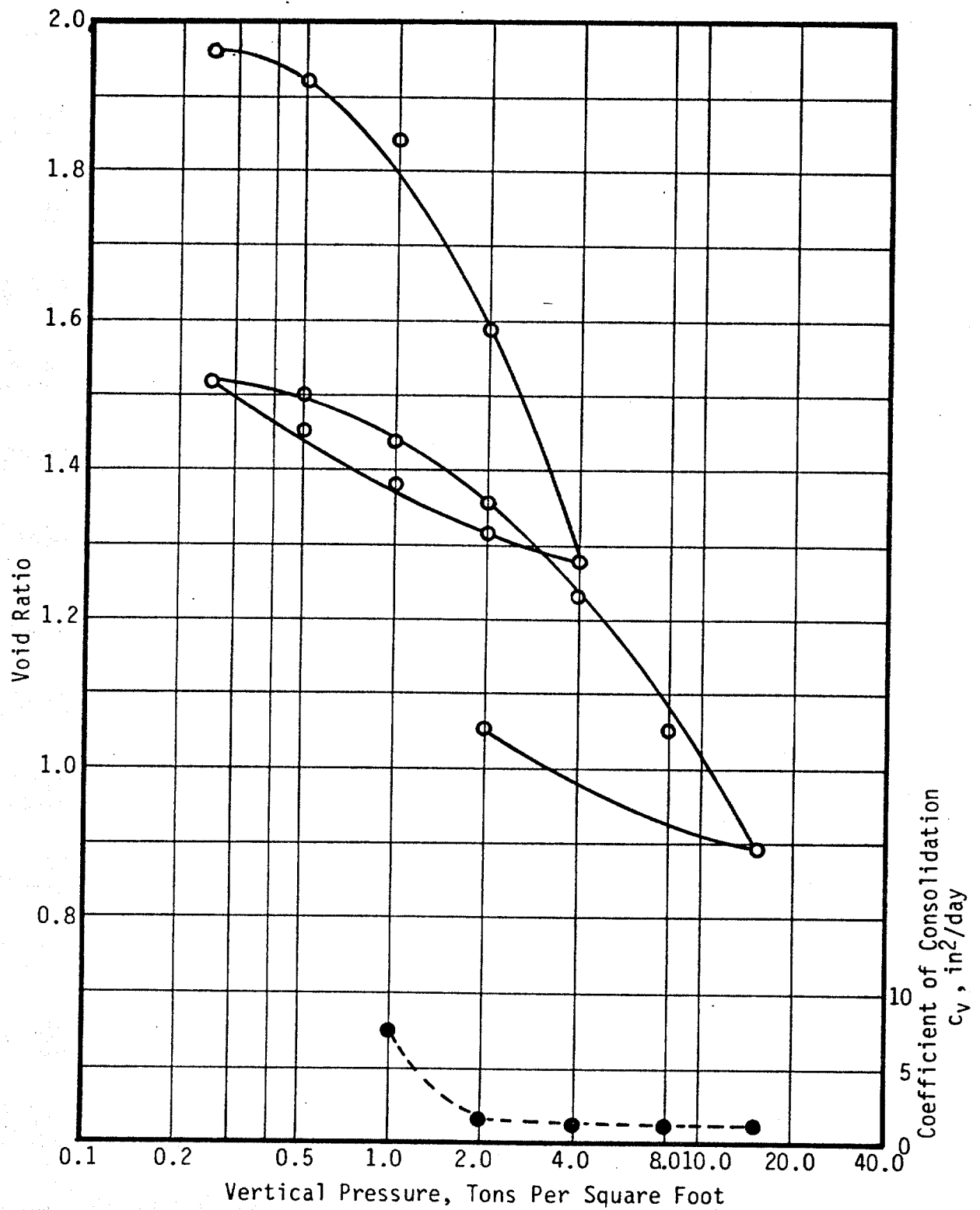


CONSOLIDATION TEST RESULTS

NSF/UNIVERSITY OF ARIZONA PROJECT
SABINE, TEXAS

SAMPLE: S-4 DEPTH: 51.5'
SOIL TYPE: Gray Clay

MOISTURE CONTENT: 65%
LIQUID LIMIT: 101
PLASTIC LIMIT: 28

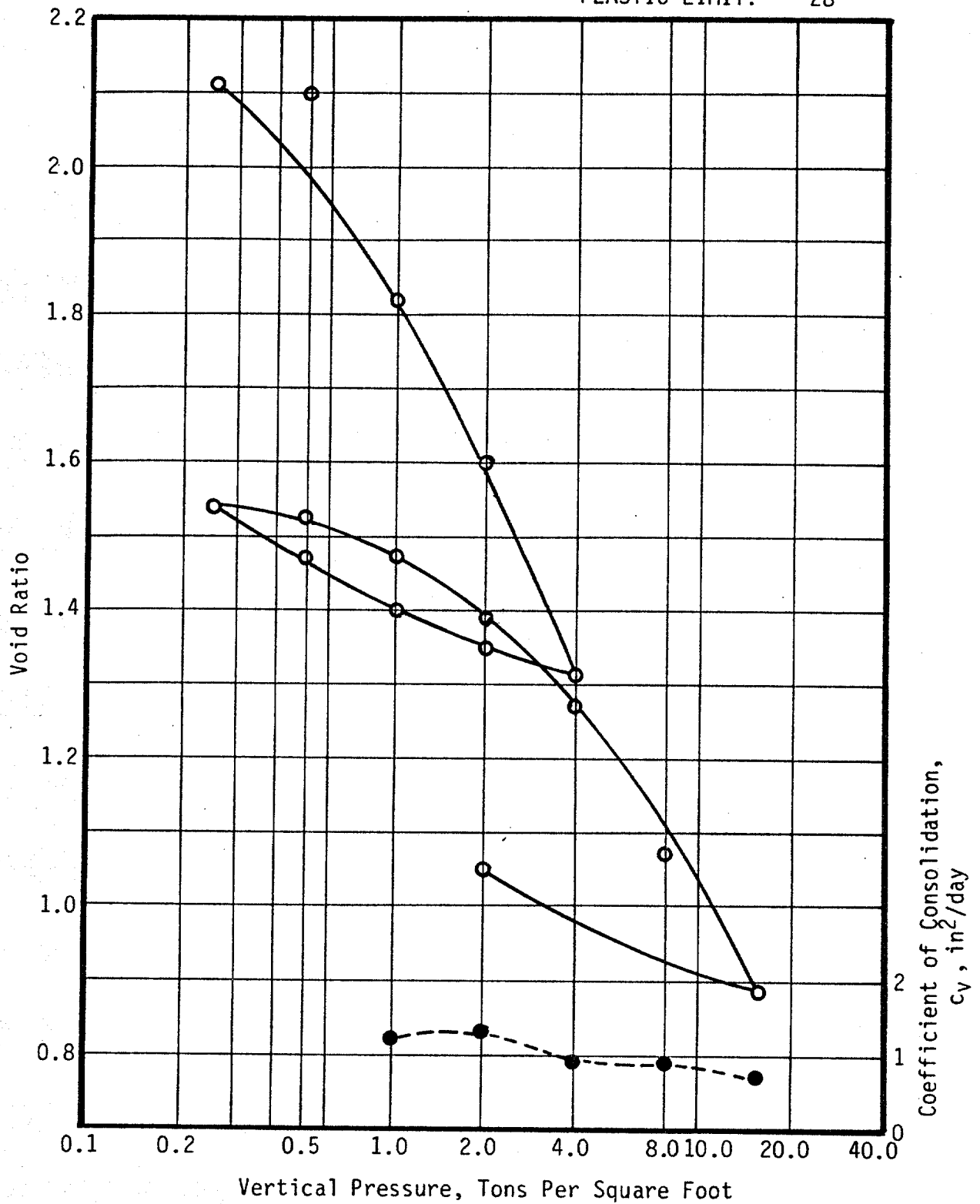


CONSOLIDATION TEST RESULTS

NSF/UNIVERSITY OF ARIZONA PROJECT
SABINE, TEXAS

SAMPLE: S-7 DEPTH: 55'
SOIL TYPE: Dark Gray Clay

MOISTURE CONTENT: 70%
LIQUID LIMIT: 100
PLASTIC LIMIT: 28



CONSOLIDATION TEST RESULTS

NSF/UNIVERSITY OF ARIZONA PROJECT
SABINE, TEXAS

APPENDIX B

SELF-BORING PRESSUREMETER TESTS

February 1986



**Institut
Français
du
Pétrole**

THE PAM DEMONSTRATION AT SABINE SITE

September 23-24, 1985

Ref. 33 872

INSTITUT FRANCAIS DU PETROLE

Direction de recherche
"Exploitation en Mer"

THE PAM DEMONSTRATION AT SABINE SITE

SEPTEMBER 23-24, 1985

RÉFÉRENCE : 33 872

FEBRUARY 1986

DIRECTION DE RECHERCHE
EXPLOITATION EN MER

Projet : B 4439008
Référence : 33 872
Exemplaires : 20

Abstract

The PAM (Offshore Self-Boring Pressuremeter) developed by the Institut Français du Pétrole was demonstrated on September 23-24, 1985, for the Earth Technology Corporation at the onshore Sabine test site near the mouth of the Sabine River, 15 miles south of Port Arthur, Texas. After the pressuremeter tests on the WD 58 area, this demonstration had the goal of showing representatives from U.S. oil companies what the PAM was capable of doing. Representatives from ten oil companies attended this demonstration.

The PAM demonstration on the Sabine site illustrated the effectiveness of self-boring in normally consolidated clayey formations. The probe was stopped at the depth of 11.5 meters because of the presence of shells and gravels incompatible with the self-boring process which is especially well suited for reconnaissance in fine clayey and sandy soils.

THE PAM DEMONSTRATION AT SABINE SITE

SEPTEMBER 23-24, 1985

TABLE OF CONTENTS

Introduction

- 1 - Realization of the boring
- 2 - Self-Boring Logs
- 3 - Pressuremeter results

Conclusions

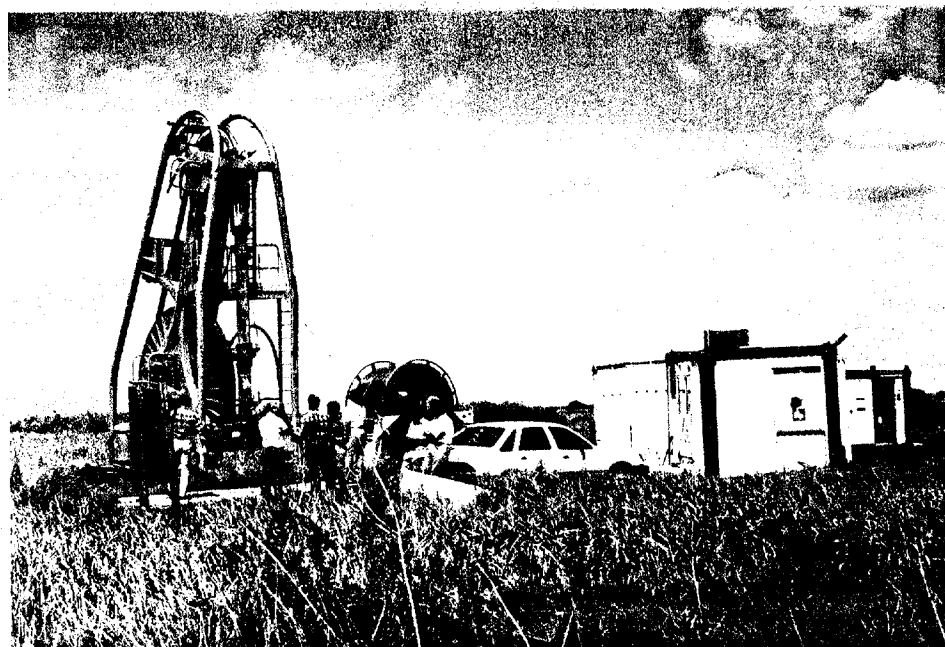
- Appendix 1 - General location MAP
 - Boring position

- Appendix 2 - Daily report

- Appendix 3 - Self-Boring Logs

- Appendix 4 - Pressuremeter curves

- Appendix 5 - Pressuremeter Logs



PAM demonstrated on Sabine test site



PAM demonstration participants

The PAM Demonstration at the Sabine Site
September 23-24, 1985

Introduction

The PAM (Offshore Self-Boring Pressuremeter) developed by the Institut Français du Pétrole was demonstrated on September 23-24, 1985, for The Earth Technology Corporation at the onshore Sabine test site near the mouth of the Sabine River, 15 miles south of Port Arthur, Texas (Appendix 1). After the pressuremeter tests on the WD 58 area, this demonstration had the goal of showing representatives from U.S. oil companies what the PAM was capable of doing. Representatives from ten oil companies attended this demonstration.

The Earth Technology Corporation chose this site because of the experiments it was doing with piles in the vicinity. The data obtained on the area at a short distance from the PAM demonstration site showed a succession of clayey and sandy layers with shell fragments, in particular at depths of 20 to 30 feet (depending on the boring). In addition to the actual demonstration of the PAM on September 23, 1985, the boring had the goal of performing standard and special pressuremeter tests between depths of 13 and 18 meters (40 and 55 feet).

1. Realization of the boring

To a depth of 10 meters (33 ft) the probe proceeded normally, with the performing of standard pressuremeter tests at different levels. The presence of gravels and shells several centimeters in size at a depth of about 10 meters prevented the self-boring probe to penetrate normally. The realization of the borehole between the depths of 10 and 11.5 meters created great difficulties including the blocking off of the outlets for evacuating cuttings inside the probe. At the same time, the caving in of the formations made any further penetration of the probe impossible. Appendix 2 includes the daily report of the Sabine borehole operation.

2. Self-Boring Logs.

During the penetration of the probe, self-boring logs were recorded normally. These logs included:

- the driving force of the probe in the ground,
- the pressure inside the undilated pressuremeter cell,
- the rate of penetration.

It can be seen that, starting at the depth of 10 meters, the driving force was greater than the weight of the probe (Appendix 3)

3. Pressuremeter Results

The standard pressuremeter tests were of very good quality, except for the test at a depth of 10 meters where the formation was already disturbed by the penetration conditions of the probe (Appendix 4). The pressuremeter

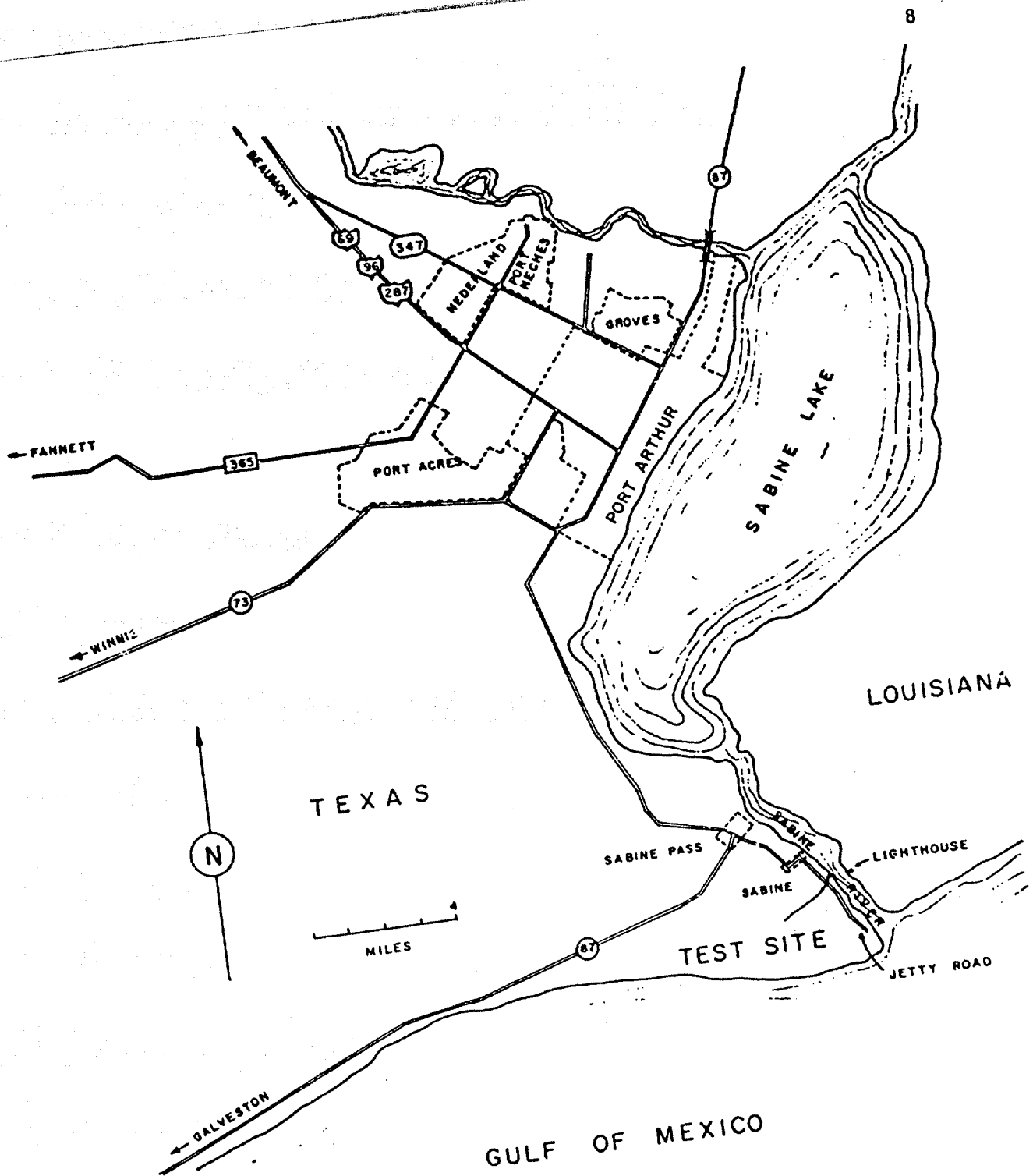
curves clearly indicate a clayey formation (shape coefficient $\beta \approx 25$ to 30%). Parameters p_0 , p_2 , p_5 and p_{20} increase steadily with depth, indicating a normally consolidated soil (Fig. A5-1). Likewise, the moduli increase steadily with depth, except for the tangent modulus G_0 which shows greater dispersion (Fig. A5-1). Shear strength τ deduced from the pressuremeter curves increases fairly steadily from 20 to 40 kPa (Fig. A5-2).

Conclusions

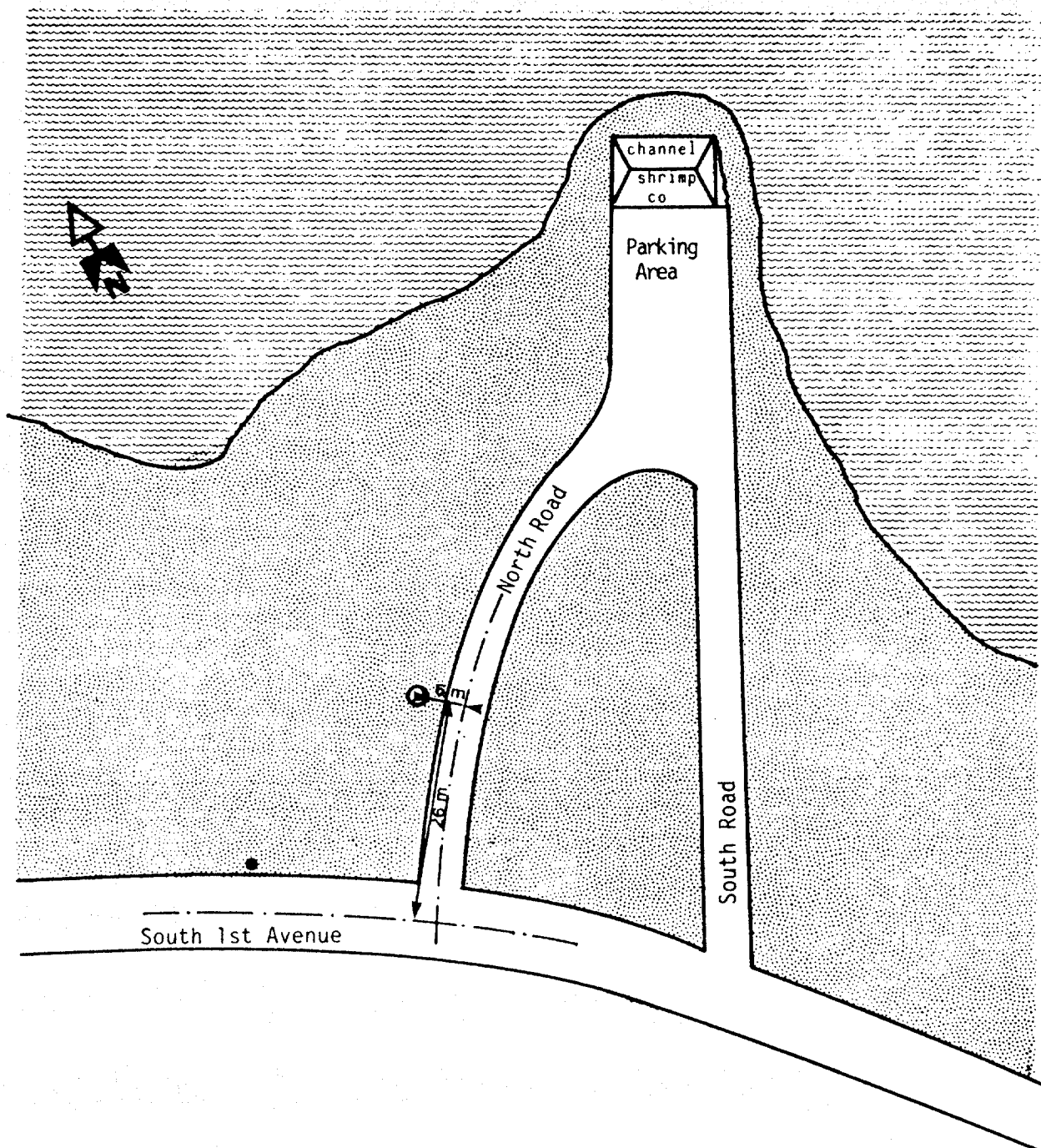
- 1.) The PAM demonstration on the Sabine site illustrated the effectiveness of self-boring in normally consolidated clayey formations.
- 2.) The probe was stopped at the depth of 11.5 meters because of the presence of shells and gravels incompatible with the self-boring process which is especially well suited for reconnaissance in fine clayey and sandy soils.
- 3.) The demonstration clearly showed the excellent quality of the pressuremeter tests performed with data acquisition and processing.
- 4.) The PAM has the advantage of being able to perform standard and special pressuremeter tests (relaxation and creep tests, cyclic tests) to provide a full description of the behavior of fine soils as done on the WD58 area.

APPENDIX 1

- GENERAL LOCATION MAP
- BORING POSITION



GENERAL LOCATION MAP



BORING POSITION

APPENDIX 2

- DAILY REPORT

THE PAM TESTINGS AT SABINE SITE

DAILY REPORT

September 21-22-1985

PAM mobilized on Sabine test site

September 23

9h - PAM presentation to visitors from ten american oil companies

10h - PAM commenced boring and three standard pressuremeter test
are runned

test	test depth (m)	cutting shoe depth (m)
0101	1,5	2,5
0102	3	4
0103	4,5	5,5

16h - Probe penetration is 5.5 metres.

Pressuremeter curves 0102 and 0103 are plotted with pressure
and volume calibrations corrections.

September 24

8h - Probe penetration start from 5.5 metres

9h - Probe penetration is 7 meters.

Start standard pressuremeter test 0104 at 6 metres depth.

10h30 - Probe penetration is 9 metres.

Start standard pressuremeter test 0105 at 8 metres depth

- 10h45 - Self boring start from 9 metres interrupted at 10.7 metres :
maximum penetration force reached and abnormal pressure on
water circulation
- 12h - Maximum probe penetration reached is 11.5 metres using alterna-
tive up and down probe motion effect.
Water circulation plugged into the probe
Test 0106 at 10 metres depth
- 13h - Probe recovered and inspected.
Exhaust sediments circulation 100 % obstructed by shells, sand
and gravels.
- 14h30 - Boring attempted after the probe has been cleared.
But previous 11.5 metres penetration was never reached again
due to shells and sand filling the down hole.
- 18h - Boring ended while probe water circulation nozzles were
obstructed.

September 25-26

PAM demobilized.

APPENDIX 3

- SELF-BORING LOGS

SELF BORING PROBE

MEASURED PARAMETERS

SITE: SABINE PASS No3

DATE: 23/09/85

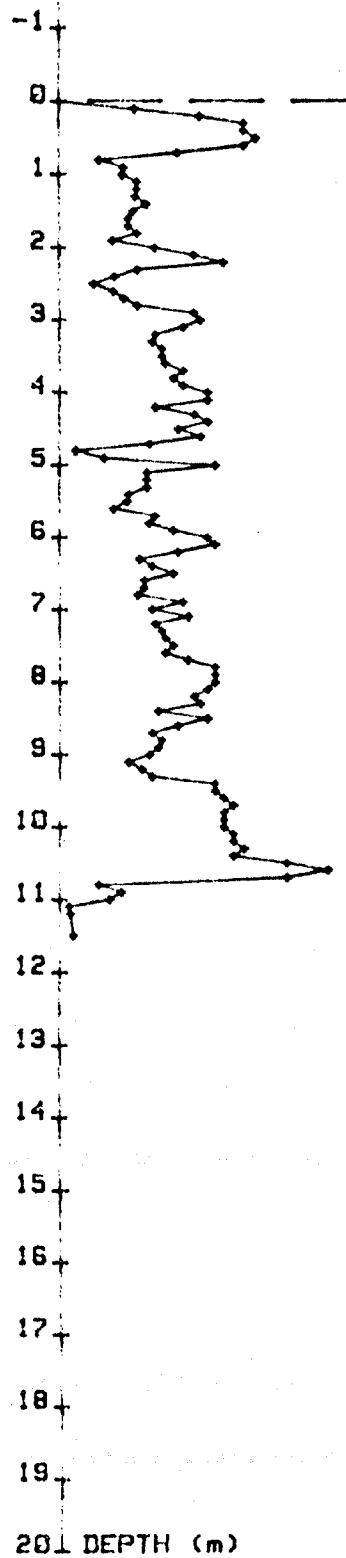
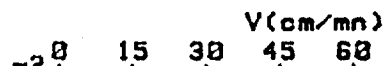
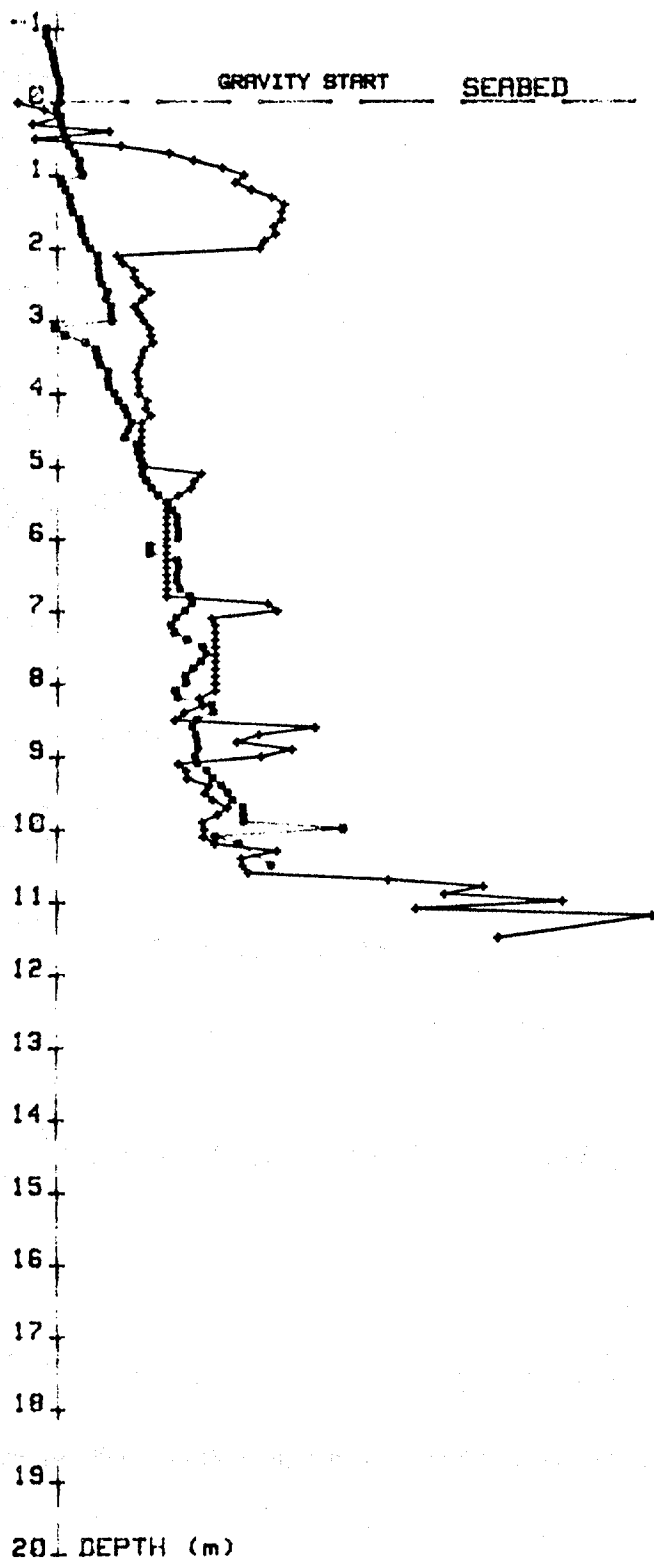
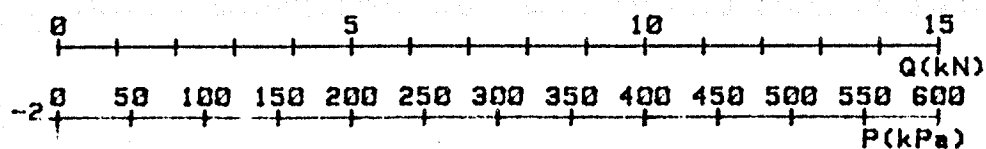
No BORING: 001

Q -> '+' Force of soil reaction

Pi -> '*' CELL pressure at depth (m)

Vi -> '+' boring speed (cm/mn)

FRAME immersion at: 0.00 m



NOTA: mean torque = 8.71 (m*daN) mean Pw = 9.07 (Bars)

SELF BORING PROBE

MEASURED PARAMETERS

SITE: SABINE PASS No3

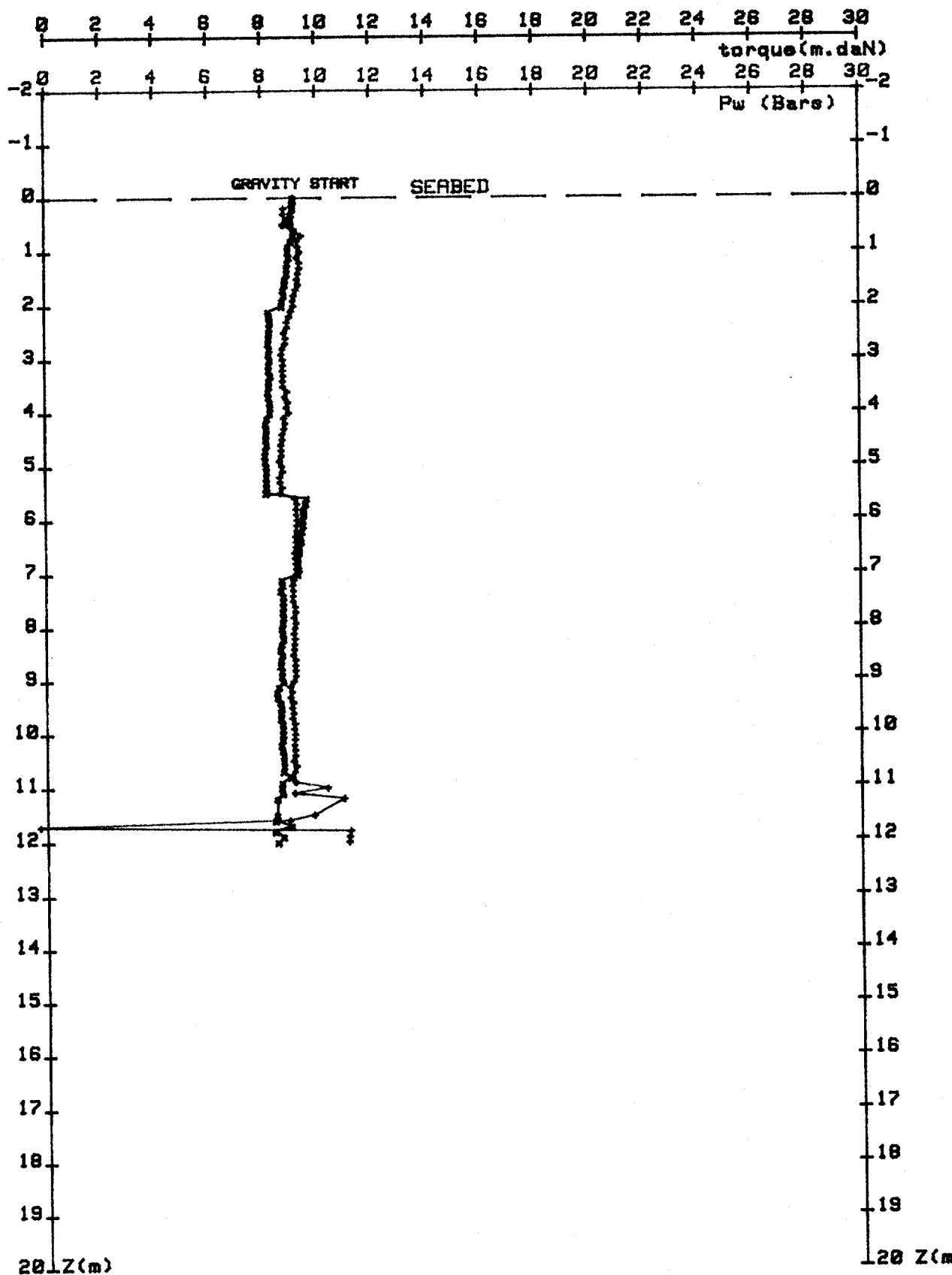
DATE: 23-09-85

No BORING: 001

Cr -> 'x' tool torque

Pw -> '+' water pressure probe

FRAME immersion at: 0.00 m



OBSERVATIONS:

- PRESSUREMETER CURVES

APPENDIX 4

No TEST :0102
 DATE :09/23/85
 SITE :SABINE PASS No3
 SENSORS :C8B1s

No BORING :001
 CODE :A C1%
 DEPTH :3(m)
 WATER DEPTH: 0.00(m)

RESULTS:

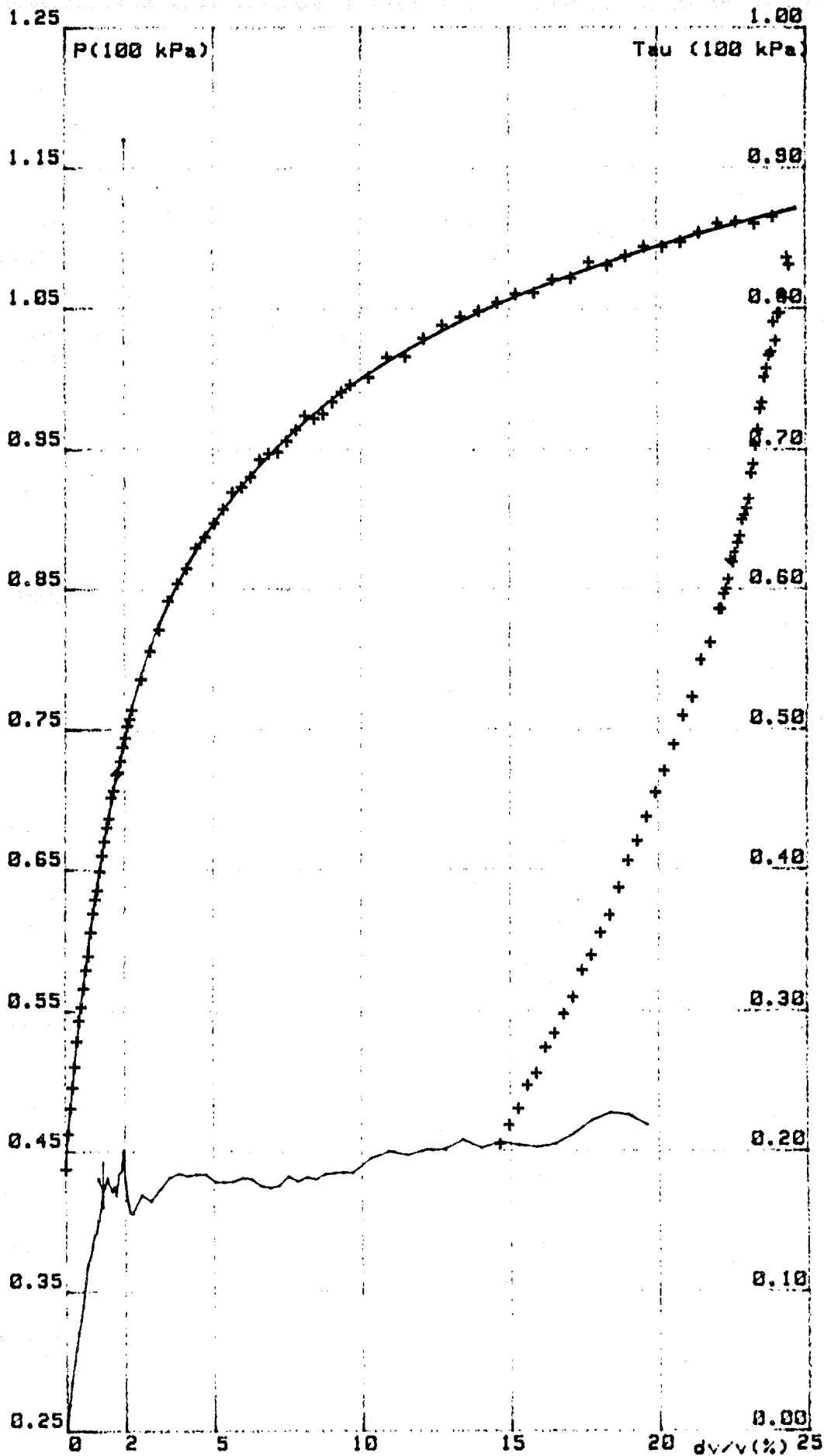
Vo (cm3) : 15
 P1 (100 kPa): 0.378
 dt (s): 15
 Pa (100 kPa): 0.437
 P2 (-): 0.744
 P5 (-): 0.887
 P20 (-): 1.094
 Beta (%) : 29.994
 Go (100 kPa): 32.783
 Gp2 (-): 15.354
 Gp5 (-): 8.188
 af (%) : 1.230
 Tau(f)(100 kPa): 0.178
 Tau(20)(-): 0.000
 Pf (-): 0.660
 Gf (-): 14.305
 G2 (-): 0.851

Derivative with: 7 points

a1 (%) : 3
 a2 (%) : 24
 b (100 kPa)/(%) : -0.000
 Tau a1(100 kPa): 0.198
 Tau(20)(-): 0.181
 P20 (-): 1.094
 P100 (-): 1.295
 Beta (%) : 30.846

Relaxation:

T(e) P(100 kPa)
 0 0.378



No TEST :0103
 DATE :09/23/85
 SITE :SABINE PASS No3
 SENSORS :C8B1s

No BORING :001
 CODE :A C1X
 DEPTH :4.5(m)
 WATER DEPTH: 0.00(m)

RESULTS:

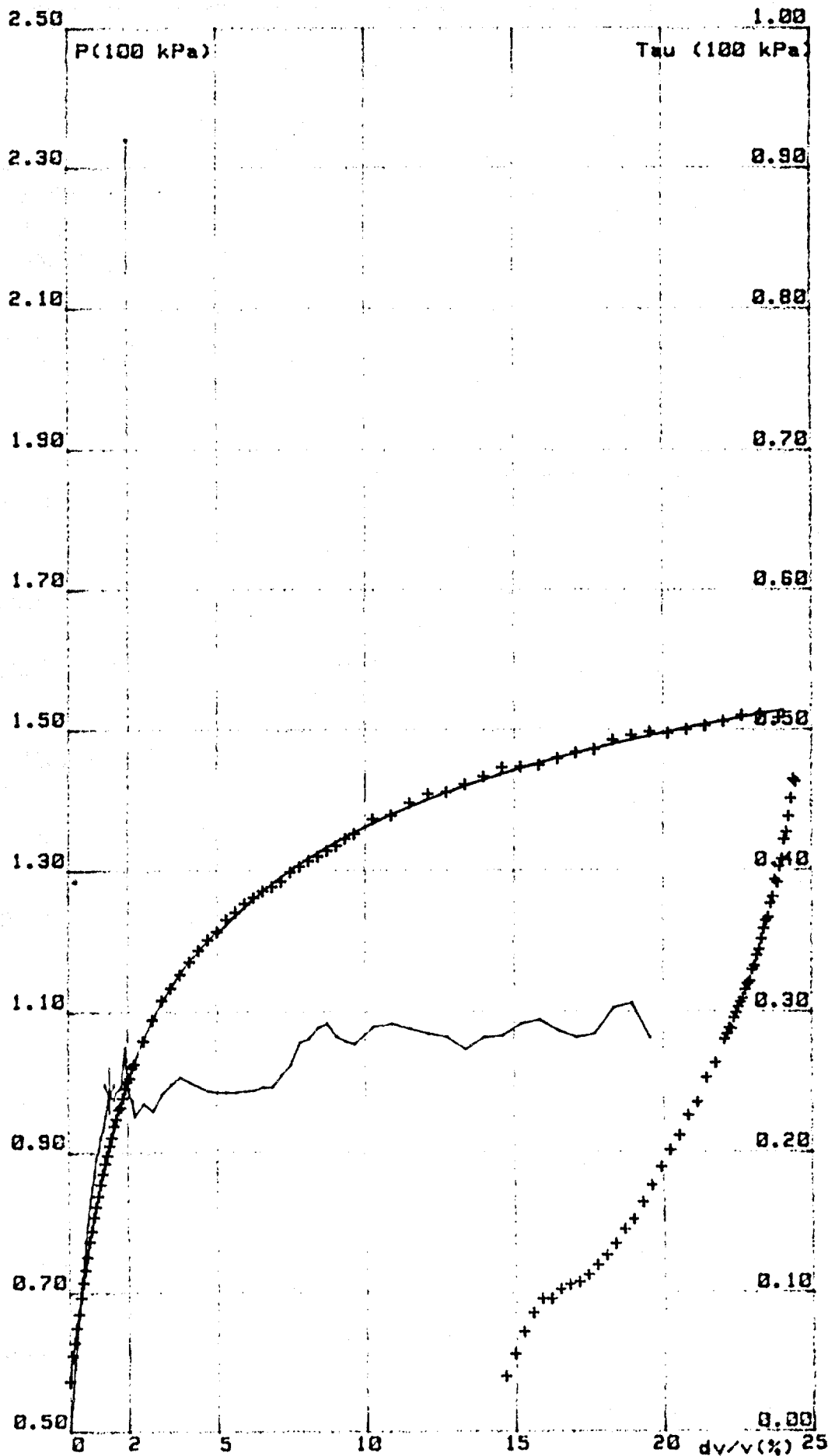
Vo (cm3) : 14
 P1 (100 kPa): 0.488
 dt (s): 15
 Po (100 kPa): 0.573
 P2 (-): 1.001
 P5 (-): 1.213
 P20 (-): 1.486
 Beta (%) : 30.800
 Co (100 kPa): 48.701
 Gp2 (-): 21.431
 Gp5 (-): 12.818
 af (%) : 1.381
 Tau(f)(100 kPa): 0.244
 Tau(20)(-): 0.000
 Pf (-): 0.908
 Gf (-): 17.781
 G2 (-): 12.462

Derivative with: 7 points

a1 (%) : 5
 a2 (%) : 24
 b (100 kPa)/(%) : -0.001
 Tau a1(100 kPa): 0.312
 Tau(20)(-): 0.291
 P20 (-): 1.486
 P100 (-): 1.747
 Beta (%) : 30.819

Relaxation:

T(e)	P(100 kPa)
0	0.478
15	0.479
30	0.478
45	0.478
60	0.478
75	0.479
90	0.478
105	0.478
120	0.478
135	0.000



No TEST :0104
 DATE :23/09/85
 SITE :SABINE PASS No3
 SENSORS :CBB1s

No BORING :001
 CODE :A C1%
 DEPTH :6(m)
 WATER DEPTH: .0.00(m)

RESULTS:

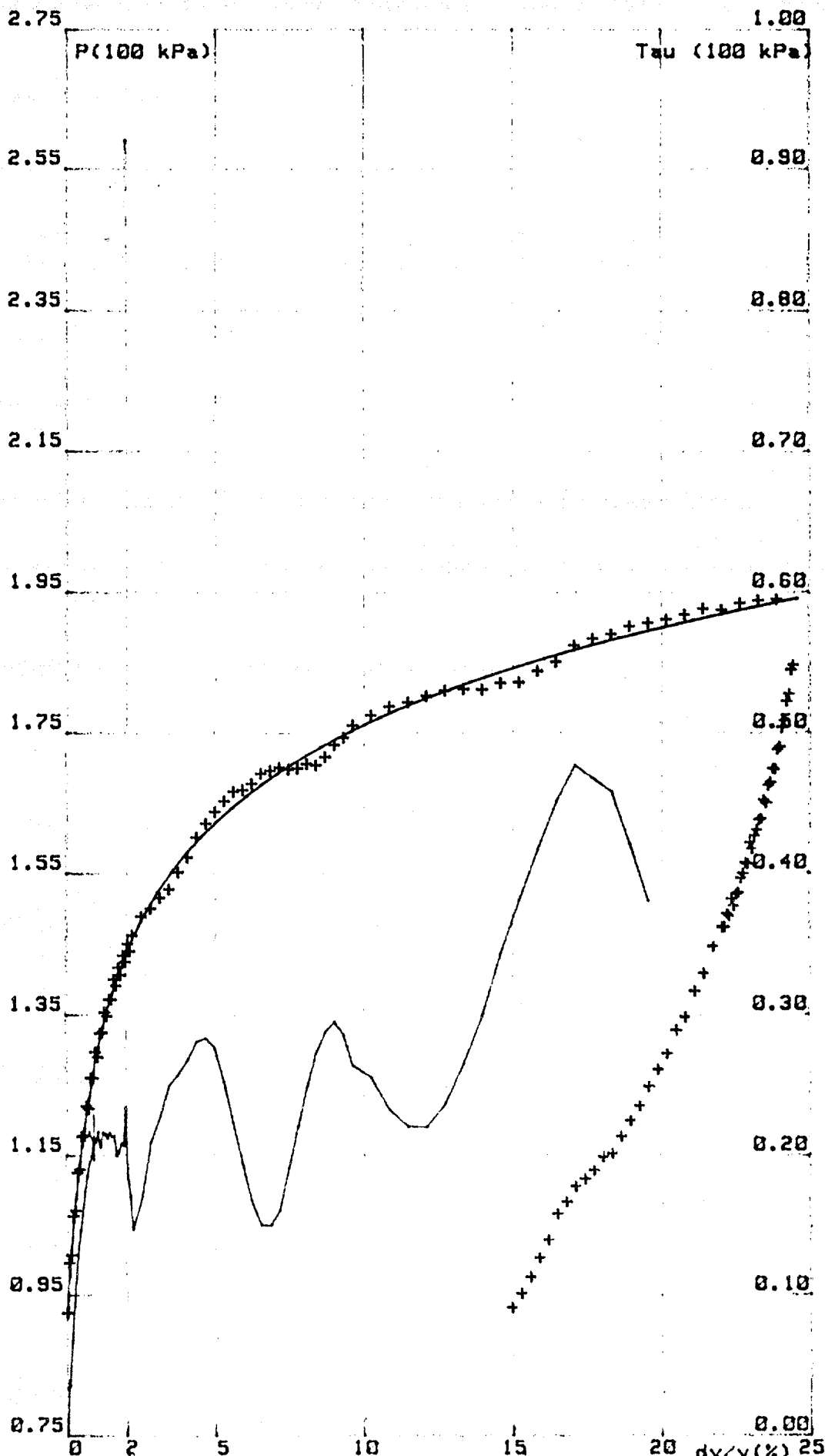
V_o (cm³) : 15
 P_1 (100 kPa): 0.020
 d_t (m): 15
 P_o (100 kPa): 0.924
 P_2 (-): 1.426
 P_5 (-): 1.637
 P_{20} (-): 1.989
 $Beta$ (%) : 27.642
 G_o (100 kPa): 95.140
 G_{p2} (-): 25.092
 G_{p5} (-): 14.252
 a_f (%) : 0.817
 $Tau(f)$ (100 kPa): 0.213
 $Tau(20)$ (-): 0.000
 P_f (-): 1.260
 G_f (-): 23.220
 G_2 (-): 11.576
 Derivative with 7 points

a_1 (%) : 2
 a_2 (%) : 20
 b (100 kPa)/(%) : 0.001
 $Tau a_1$ (100 kPa): 0.236
 $Tau(20)$ (-): 0.247

P_{20} (-): 1.899
 P_{100} (-): 2.249
 $Beta$ (%) : 26.053

Relaxation:

T(e)	P(100 kPa)
0	0.816
15	0.811
30	0.804
45	0.802
60	0.789
75	0.785
90	0.784
105	0.789
120	0.785
135	0.800



No TEST :0105
 DATE :23/09/85
 SITE :SABINE PASS No3
 SENSORS :C8B1a

No BORING :001
 CODE :A C1%
 DEPTH :8(m)
 WATER DEPTH: 0.00(m)

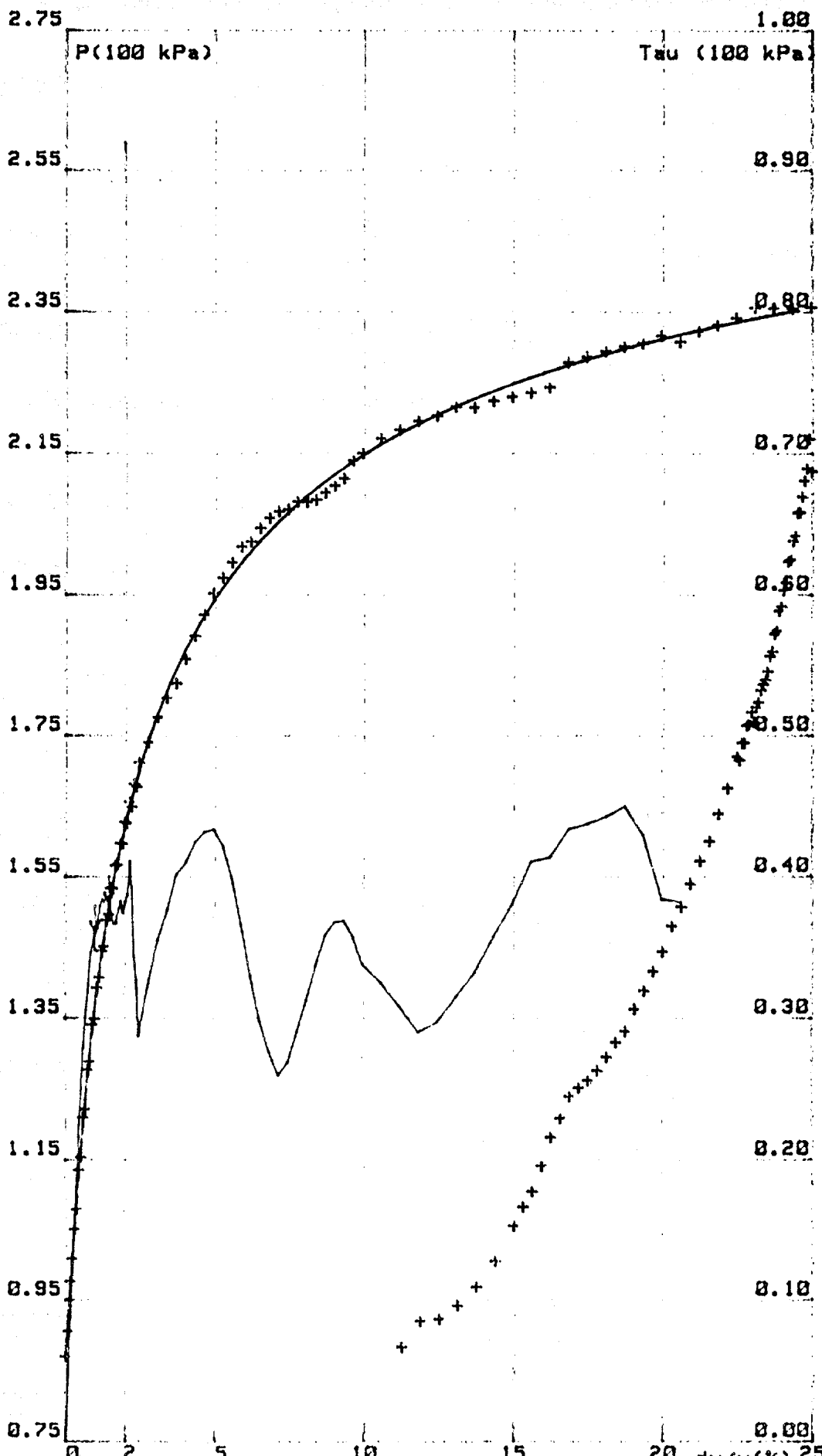
RESULTS:

Vo (cm3) : 0
 P1 (100 kPa): 0.070
 dt (s): 15
 Po (100 kPa): 0.070
 P2 (-): 1.026
 P5 (-): 1.054
 P20 (-): 2.315
 Beta (%) : 25.045
 Go (100 kPa): 45.835
 Gp2 (-): 37.778
 Gp5 (-): 21.665
 af (%) : 1.462
 Tau(f)(100 kPa): 0.384
 Tau(20)(-): 0.000
 P4 (-): 1.487
 G4 (-): 28.257
 G2 (-): 19.075
 Derivative with: 7 points

a1 (%) : 2
 a2 (%) : 25
 b (100 kPa)/(%): -0.003
 Tau a1(100 kPa): 0.454
 Tau(20)(-): 0.380
 P20 (-): 2.311
 P100 (-): 2.580
 Beta (%) : 24.832

Relaxation:

T(s)	P(100 kPa)
0	0.073
15	0.073
30	0.070
45	0.075
60	0.071
75	0.073
90	0.073
105	0.075
120	0.073
135	0.000



No TEST :0106
 DATE :23/09/85
 SITE :SABINE PASS No3
 SENSORS :CBB1s

No BORING :001
 CODE :A C1%
 DEPTH :10(m)
 WATER DEPTH: 0.00(m)

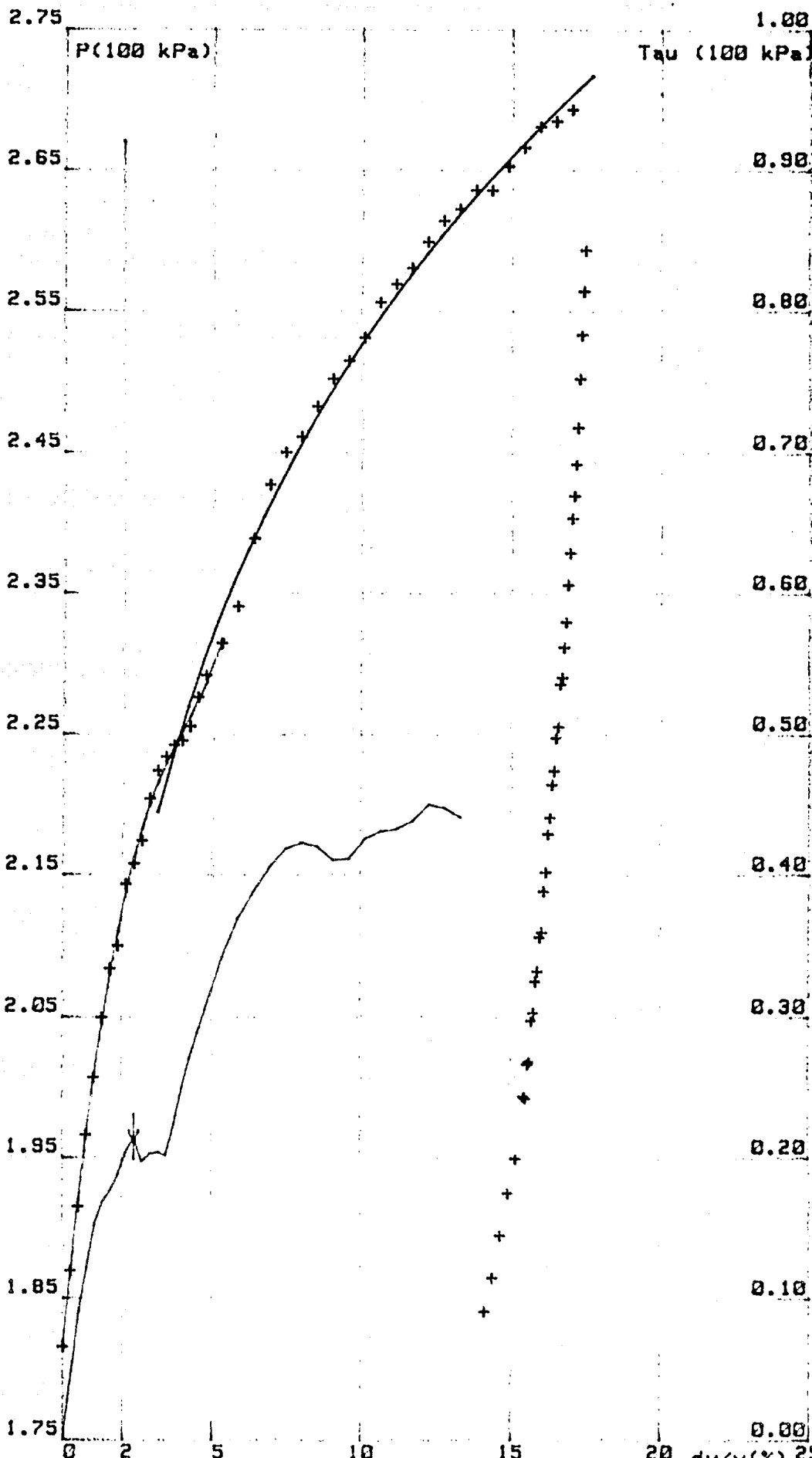
RESULTS:

Vo (cm3) : 280
 P1 (100 kPa): 1.940
 dt (s): 15
 Po (100 kPa): 1.816
 P2 (-): 2.123
 P5 (-): 2.301
 P20 (-): 0.000
 Beta (%) : 0.000
 Go (100 kPa): 20.337
 Gp2 (-): 15.379
 Gp5 (-): 9.701
 af (%) : 2.387
 Tau(f)(100 kPa): 0.215
 Tau(20)(-): 0.000
 Pf (-): 2.158
 Gf (-): 0.985
 G2 (-): 0.828
 Derivative with: 7 points

a1 (%) : 3
 a2 (%) : 17
 b (100 kPa)/(%) : 0.004
 Tau a1(100 kPa): 0.287
 Tau(20)(-): 0.347
 P20 (-): 2.761
 P100 (-): 3.482
 Beta (%) : 40.683

Relaxation:

T(s)	P(100 kPa)
0	1.800
15	1.738
30	1.725
45	1.705
60	1.688
75	1.686
90	1.653
105	1.650
120	1.638
135	0.000

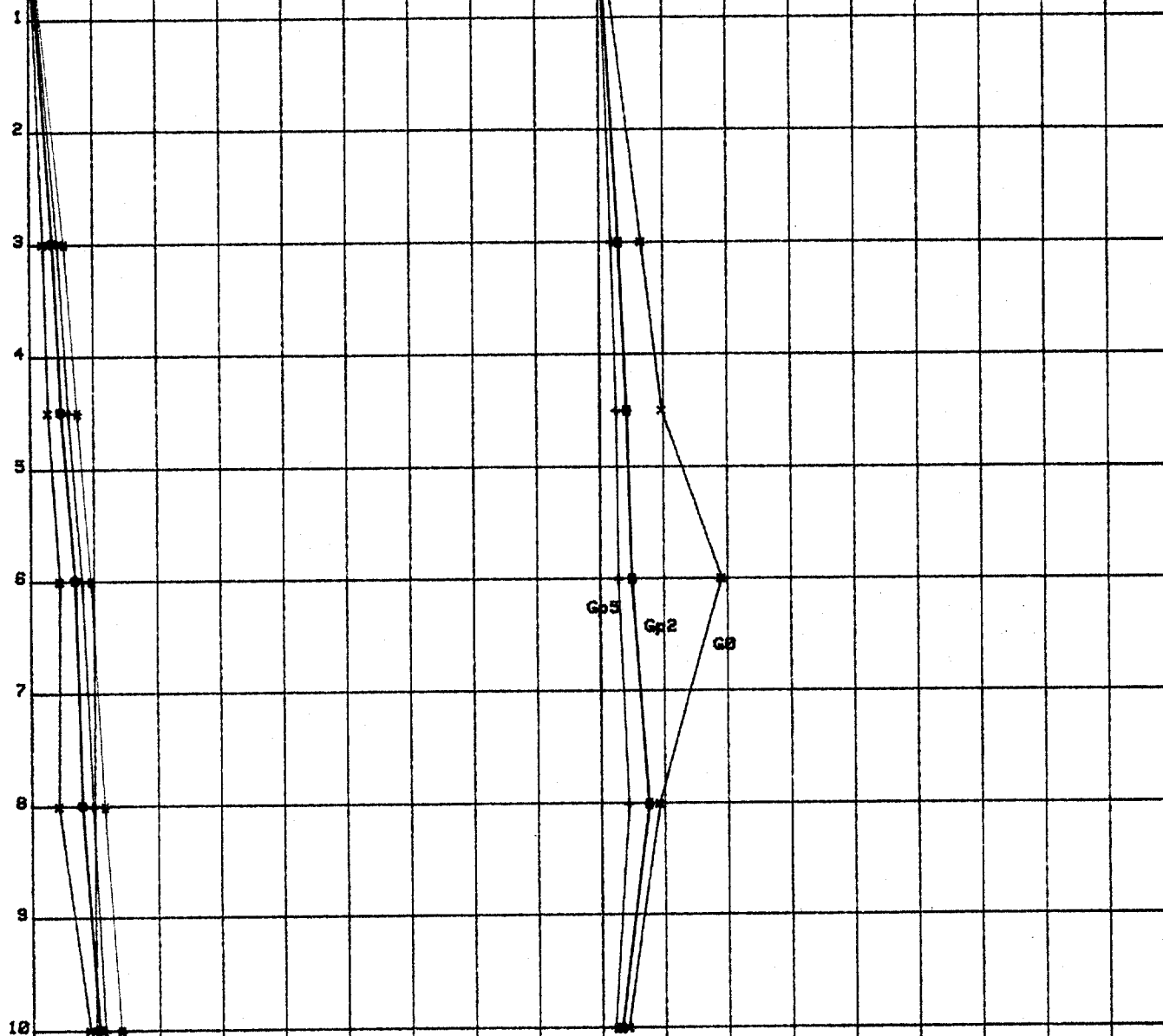


APPENDIX 5

- PRESSUREMETER LOGS

DATE:23/09/85 SONDAGE No:001 SITE:SABINE PASS No3

0 2 4 6 8 10 12 14 16 0 50 100 150 200 250 300 350 400
P(100 kPa) P(100 kPa)

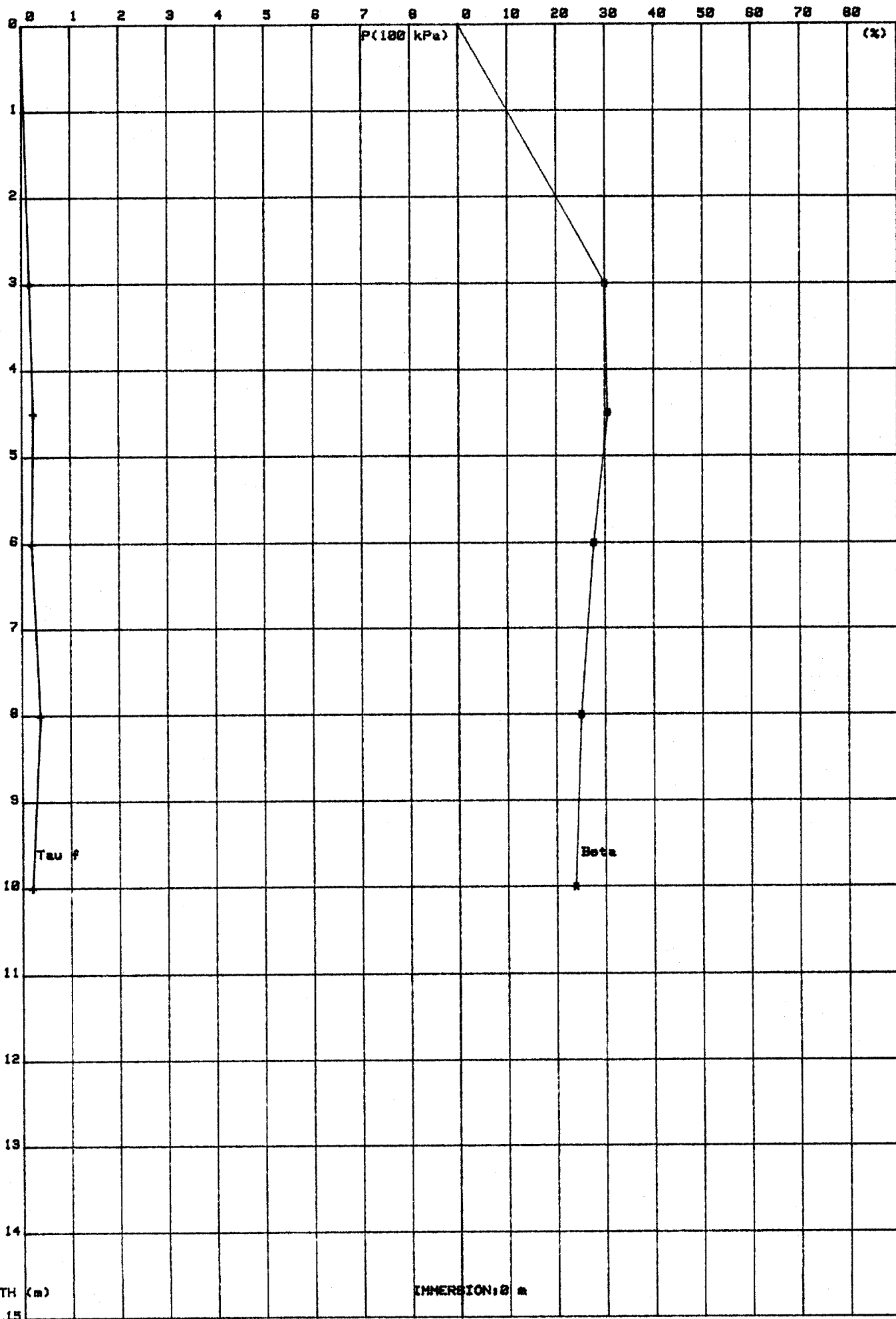


GREEN CURVE → P20
BLUE CURVE → P5
RED CURVE → P2
BLACK CURVE → P0

DEPTH (m)

IMMERSION: 0 m

DATE: 23/09/85 SONDRAGE No: 001 SITE: SABINE PASS No3



INSTITUT FRANCAIS DU PETROLE

B.P. 311

92506 Rueil-Malmaison Cedex - France

Tél. : national (1) 47-49-02-14

international + 33 1 47-49-02-14

Télex : IFP A 203050 F